Exploring New Applications of Group 7 Complexes for Catalytic and CO_2 Reduction Using Photons or Electrochemistry

by

Ahlam G. Alghamdi

A thesis submitted to the
Faculty of Graduate and Postdoctoral Studies
In partial fulfillment of the requirements
For the degree of

Master of Science in chemistry

In the department of Chemistry and Bimolecular Science

University of Ottawa

uOttawa

L'Université canadienne
Canada's university

To my strength, my mother.

Abstract

This thesis focuses on the synthesis, characterization and reactivity of group VII transition metal complexes. It begins with exploring a new pincer geometry of Re(I) compounds and then examining both Re(I) and Mn(I) compound as homogenous catalysts for photocatalytic and electrocatalytic reduction of CO_2. In the first chapter, I focus on some recently reported approaches to photocatalytic and electrocatalytic reduction of CO_2 using homogenous catalysts of transition metal.

The second chapter presents efforts to capture Re(I) in a neutral N,N,N pincer scaffold and the resulting enhanced absorption of visible light. Most of these results have appeared in a publication. In this thesis, I only present my work on rhenium compounds that are supported by the bis(imino)pyridine ligand and an examination of the differences in properties between the bidentate and tridentate ligand geometries. Later I examine both tridentate and bidentate complexes for the photocatalytic and electrocatalytic reduction of CO_2 to CO.

The failure of tridentate Re^1 bis(imino)pyridine compounds to reduce CO_2 to CO prompted a change in direction to rhenium compounds that are supported with diimine ligands. Thus, I choose 4,5-diazafluoren-9-one as supporting ligand for rhenium and manganese. This chapter explained the reasons behind choosing these particular ligand and metal combinations. Re^I and Mn^1 compounds of 4,5-diazafluoren-9-one have shown activity for the photocatalytic and electrocatalytic reduction of CO_2 to CO.

In the fourth chapter, as rhenium and manganese compounds of 4,5-diazafluoren-9-one have shown the great ability of CO_2 reduction to CO, the focus here was to modify the ligand by attaching a photosensitizer to the ligand in order to prepare supramolecular

complexes that may increase the efficiency and yield of reduction products. In this chapter, I examined two types of the photosensitizer; tris(bipyridine)ruthenium(II)chloride and osmium dichloro bis(4,4'-dimethyl-2,2'-bipyridine).

Acknowledgements

In this thesis, I had to take the guideline and support of some wonderful people who gave a hand to me to reach this successful works. I would like to show my gratitude first to the Ministry of Education in Saudi Arabia and Saudi cultural bureau in Canada for their supporting and securing funds for University of Ottawa and ESL schools during my studies in Canada. I am also grateful for professor Richeson who had inspired me to work hard and love what I am doing. During working in the lab we developed a strong relationship: he was more than a supervisor for me and I was more than lucky to be under his supervision in one of the best universes in Canada. For the wonderful team in Richeson's lab, thank you for being my second family and thanks for all the great moments we shared together. Many thanks for all the professors who taught me and the labs who allowed me to use their instruments to succeed with this thesis research; Gambarotta, Brusso, Murugesu and Scaiano.

I would also send my warm greets to my mother who cried a lot for being so far away from her for a long time. I have never forgotten her face, smile and her strong personality that inspired me to be exactly like her. For my siblings, I am very grateful for having them beside me: their support would be never forgotten. I would like also to thanks Basim for being an amazing husband and without his support I would not be here today. Finally, my sincere love to our daughters Retal & Tala who joined me in this long journey from the first day in Canada.

Table of Contents

Chapter 2

Chapter 3

List of Figures

List of Scheme

List of Table

Chapter 1

Introduction

The main human activities that emit CO_2 are the combustion of fossil fuels through industrial processes, transportation and generation of electricity. These activities have resulted in a relentless rise of carbon dioxide, which is the main greenhouse gases, that is directly contributing to climate change. Thus, there is an increasing interest in reducing the consequences of the rising atmospheric CO_2 while also interest in the chemical utilization of CO_2 to produce more valuable products and solar fuels.[1] However, a critical challenge to these efforts is the fact that CO_2 has a low thermodynamically energy value which means a lot of energy input is required to transform CO_2 to other valuable materials and this would lead to a high cost of production. Part of the way to address this challenge is the development of innovative new catalysis systems, which could be employed to increase the potential of transforming CO_2. Though there are many challenges involved in transforming of CO_2, there are some potential means to overcome these challenges such as the photocatalytic or electrocatalytic reduction of CO_2 and CO_2 hydrogenation.

1.1 CO_2 Utilization in The Chemical Industries

The transformation of CO_2 into valuable products is an excellent opportunity to address and reduce the impact of carbon dioxide emission. Success in this regard will help to reduce the negative impacts of the combustion of fossil fuels. However, the development of reliable catalysts that promote such transformations is the main problem that must be addressed.[2] With regard of many applications in chemical

industries to address the emission of CO_2 in the atmosphere such as CO_2 capture and storage and CO_2 hydrogenation,[3,4] this area still needs much exploration and improvements. However, converting CO_2 to more valuable products using transition metal complexes by using solar or electrical energy has attracted a lot of attention in the last few decades. In the follow sections I will provide an an overview of these two approaches by explaining the common terms that are used in photo/electrocatalytic systems and clarifying the mechanism and the requirements of each system. However the main goal in this thesis is exploring new complexes of group 7 that may be efficient catalysts then examining the ability of these catalysts for CO_2 reduction.

1.1.1 Common Terms in The Electro- and Photo Catalytic Reduction

Before getting more specific on the chemical transformations associated with homogeneous electro- and photo catalytic CO_2 reduction, it is important to clearly define the terminology that is frequently used to characterize these reactions.

- **Catalytic Selectivity (CS)**

This term is used to help to define the selectivity for the formation of a specific product of CO_2 reduction relative to other products that can arise from the catalyst system. In the case of CO_2 reduction, a common byproduct is H_2. This product is commonly the result of reduction of protons in the catalyst system (e.g. from H_2O). By reporting the CS value, not only has information on product selectivity but also relates to the overall efficiency of the system for CO_2 reduction. This term is defined as the ratio of the moles of products that are formed from CO_2 reduction to the moles of H_2 formed from the reaction. The reason behind choosing the moles of H_2 is that any catalyst able to

reduce CO_2 to other feedstock as CO and HCOOH is able also to reduce protons to H_2.

$$\mathbf{CS} = \frac{\text{Moles of of products from } CO_2}{\text{Moles of } H_2 \text{ produced}}$$

The Photochemical Quantum Yield (ϕ)

The photochemical quantum yield is the molar ratio of the products of CO_2 reduction to the moles of incident photons

$$\boldsymbol{\phi} = \frac{\text{products of } CO_2 \text{ reduction}}{\text{Incident photons}}$$

This parameter is clearly a key performance measurement for a photocatalytic system because it provides the efficiency of the catalytic system.

- **The Turnover Number (TN)**

Turnover number (TN) is used as a metric for how many times a catalyst can yield product. It is usually calculated as the molar ratio of the products of CO_2 reduction to the catalyst.

$$\mathbf{TN} = \frac{\text{moles of products of } CO_2 \text{ reduction}}{\text{moles of catalyst}}$$

From the turnover number we can know how many reductions occur during the lifetime of catalyst.

- **The Turnover Frequency (TOF)**

It is defined as the specific activity of the catalyst under special reaction conditions by the catalytic cycles that occurring per unit time. The equation of the turnover frequency is the molar ratio of the products of CO_2 reduction to the catalyst per unit time which is usually an hour.

$$\mathbf{TOF} = \frac{\text{moles of products of } CO_2 \text{ reduction}}{\text{moles of catalyst} * \text{unit time}}$$

1.1.2 The Electrocatalytic Reduction of CO_2

In order to attain the environmental stability of a global carbon cycle, the amount of CO_2 that is produced due to the human activities should be balanced with the CO_2 absorbed by plants in nature. However, since the advent of the "Industrial Revolution", an increase in CO_2 emission has disrupted the balance of global carbon cycle. In addition to CCS and CO_2 hydrogenation as means to counteract the increase of CO_2, photocatalytic and electrocatalytic reduction processes have received substantial attention.[5-8] Recently, transforming CO_2 using electrochemical catalysis methods has been widely investigated due to the unique advantages provided by the ability to control the potential of electrodes and the temperature of the reaction. Also in the electrocatalytic reduction, the electricity that drives a reaction can be obtained from natural sources such as solar, the wind and hydroelectric and that means no need to generate other CO_2 sources. The supporting electrolytes in electrocatalytic reaction can be recycled allowing the minimization of the cost of chemical consumption. Unfortunately, with all these advantages there are many challenges with electroreduction, these include the slow kinetic reduction of CO_2 even in the presence of catalysts and high reduction potentials.

There are a number of electrocatalytic reductions that can be envisioned. The reduction can follow pathways that require between two and eight electrons and the reactions could be done in aqueous, gaseous or non-aqueous phases. In general, the main products that have been obtained from electrocatalytic reduction are carbon monoxide, formic acid, oxalate, formaldehyde, methanol and methane. The first challenge in electrocatalytic CO_2 reduction is that reducing CO_2 by one-electron to form a radical anion of CO_2. This requires a large negative (unfavorable) reduction potential of -2.14 V vs. SCE.[9,10] Furthermore the overpotential required for the reduction by one-electron ranges from 0.1 to 0.6 V. A kinetic barrier to this reduction is attributed to the large structural difference between linear CO_2 and bent $CO_2^{\bullet -}$. As a result, reducing CO_2 though proton-assisted multiple electron transfer (MET) provides an alternative pathway to get the level of rapid reduction as shown in Table 1.1.[9]

Table 1.1: The Potential Reductions of CO_2 through proton-assisted-multiple electron transfer.

Reaction	E^O **(V) vs. SCE**[a]
$CO_2 + 2H^+ + 2e^- \longrightarrow HCO_2H$	-0.85
$CO_2 + 2H^+ + 2e^- \longrightarrow CO + H_2O$	-0.77
$CO_2 + 4H^+ + 4e^- \longrightarrow C + 2H_2O$	-0.44
$CO_2 + 4H^+ + 4e^- \longrightarrow HCHO + H_2O$	-0.72
$CO_2 + 6H^+ + 6e^- \longrightarrow CH_3OH + H_2O$	-0.62
$CO_2 + 8H^+ + 8e^- \longrightarrow CH_4 + 2H_2O$	-0.48

a E°′ potentials are reported at pH 7.

The development of catalysts for these reactions continues to play a crucial role in achieving satisfactory electroreduction, and indeed more exploration to increase the catalytic selectivity and stability is still required. In general, most the catalysts in electroreduction can work fewer than a hundred hours and that means it is difficult to commercialize for practical uses. [10-12] Transition metal complexes, which consist of a central metal surrounded by organic ligands, have been demonstrated to be homogenous catalysts for the electrocatalytic reduction of CO_2. The following is a brief survey of the best studies in electrocatalytic reduction of homogeneous catalysis only classified by different ligands types. The most common ligands used in this field have been macrocyclic ligands and bipyridine ligands.

1.1.2.1 Metal catalysts with macrocyclic ligands

Tetraazamacrocyclic compounds of cobalt^{II} and nickel^{II} were the first complexes shown to possess the ability of reducing CO_2 with high current efficiencies in aqueous media (Scheme 1.1). In these systems, the main products of CO_2 reduction are CO and mixture of CO and H_2 at potentials -1.3 to -1.6 V vs. SCE. Although cobalt and nickel macrocyclic complexes have shown high current efficiencies, the turnover frequencies for these catalysts are very low (e.g. 9 cycles per hour).[13] In order to increase the selectivity of CO_2 reduction, Sauvage *et al*, reported $[Ni^{II}(cyclam)]^{2+}$ as a selective electrocatalyst for CO_2 reduction to produce only CO. $[Ni^{II}(cyclam)]^{2+}$ has shown great current efficiencies around 96% with higher turnover frequencies than other macrocyclic complexes, 32 turnover per hour at potentials -1.05V vs. NHE in the presence of water.[14]

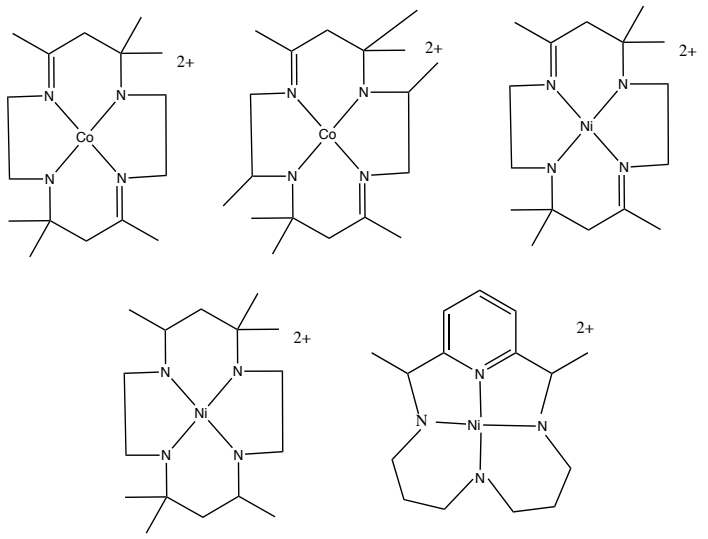

Scheme 1.1: The structures of tetraazamacrocyclic complexes of cobalt and nickel.

Later, Fujita and co-workers synthesized complexes that have high oxidation states of the metal center. These so-called cobalt^{III} and iron^{IV} corroles are shown in Scheme 1.2. Initially these complexes were used as homogeneous catalysts in photocatalytic reduction, but in the presence of acetonitrile (MeCN) as solvent and glassy carbon as a working electrode these complexes have shown the ability for electrocatalytic reduction of CO_2 to CO at around -1.7V vs. SCE.[15,16]

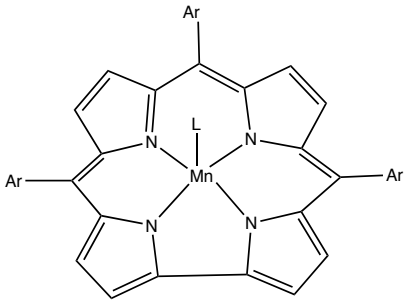

M	n	Ar	L	Abbreviation
Co	III	C_6F_6	Ph_3P	$Ph_3PCo(tpfc)$
Fe	IV	C_6F_6	Cl	ClFe(tpfc)
Fe	IV	2,6-$C_6H_3Cl_2$	Cl	ClFe(tdcc)

Scheme 1.2: structure of Co and Fe corroles complexes.

1.1.2.2 Metal catalysts with bipyridine ligands

The first bipyridine supported metal complexes for reduction of CO_2 to CO were reported by Lehn, Ziessel and Hawecker *et.al*. These species had the formula $[Re^{I}(bipy)(CO)_3Cl]$ (bipy = 2,2'-bipyridine) were shown to have a good selectivity for CO_2 reduction to CO. Using a ratio of 9:1 DMF-H_2O as solvent, $[Re^{I}(bipy)(CO)_3Cl]$ reduced CO_2 to CO at potential -1.49V vs. SCE with high current efficiencies and turnover (98% and TOF of 21 per hour respectively).[17] In the same group of Re, Mn^{I} has shown the ability of reduction CO_2 to CO with lower over potential and cost than Re due the abundance of manganese metal in Earth's crust. Complexes $[Mn(L)(CO)_3Br]$ (L = bipyridine, 4.4'-dimethyl-2,2'-bipyridine(dmby)) have shown good efficiencies in MeCN solvent and at potentials -1.80V vs. SCE both complexes reduced CO_2 to CO with turnover frequencies of 4 per hour.[18.19]

There are studies reporting bipyridine complexes of ruthenium, rhodium and iridium, however; the selectivity of reductions CO_2 to CO is very low due to the formation $HCOO^-$ and H_2. The current efficiencies and turnover are also lower than those with Re or Mn, with TON= 6.8 to 12.3 and the current efficiencies 64% for $HCOO^-$ and 12 % for H_2 .[20,21]

1.2 **The Photocatalytic Reduction of CO_2 Using Homogeneous Transition Metals**

Converting CO_2 to more valuable products by using the energy of sunlight and homogeneous catalysts has been intensively investigated from the standpoint of fundamental chemistry as a way to help to address the environmental issues of carbon dioxide emissions. These reactions are normally carried out in the presence of water as a proton source. Some key products of photocatalytic reduction using homogenous catalysts are CO, H_2 and HCOOH.

The current methods used for homogenous photocatalytic reduction of CO_2 rely on two components: a photosensitizer and a catalyst. The photosensitizer is responsible for absorbing the light and using this energy to address the thermodynamic barriers to reduction by exciting electrons and transferring the absorbed energy to a catalyst. The catalyst takes the energy provided by the photosensitizer and uses it to overcome the kinetic barriers for the reduction. Interestingly, there are a number of studies that have shown the ability of some catalysts can act both as the photosensitizer and the catalyst.

In the photocatalytic reduction of CO_2, the homogeneous catalysis systems can be further categorized as two types: Type I, and Type II. Generally, in Type I systems the photosensitizer and catalyst consist of two separate components that are mixed in solution

to make a photoreduction system. In Type II the two components are combined into a single molecular unit that is constructed of both a light absorber and a catalyst.[22]

The photocatalytic process of CO_2 reduction begins when a photosensitizer absorbs a particular light energy, which excites this species from its ground state to the excited state. In most homogenous CO_2 photocatalytic reduction systems, ruthenium (II) polypyridyl and bipyridyl complexes work as a photosensitizer due to the unique photophysical properties for such compounds. The light absorption leads to a singlet metal-to-ligand charge transfer (^{1}MLCT). Essentially this means that an electron that was originally localized on Ru is now localized in the π orbital system on the bipy ligand. This singlet state then converts to a triplet-excited state (^{3}MLCT) by intersystem crossing (Figure 1.1). The redox properties of this (^{3}MLCT) are responsible for the interaction with the catalyst, which can then interact with CO_2 and carry out the reduction.[23]

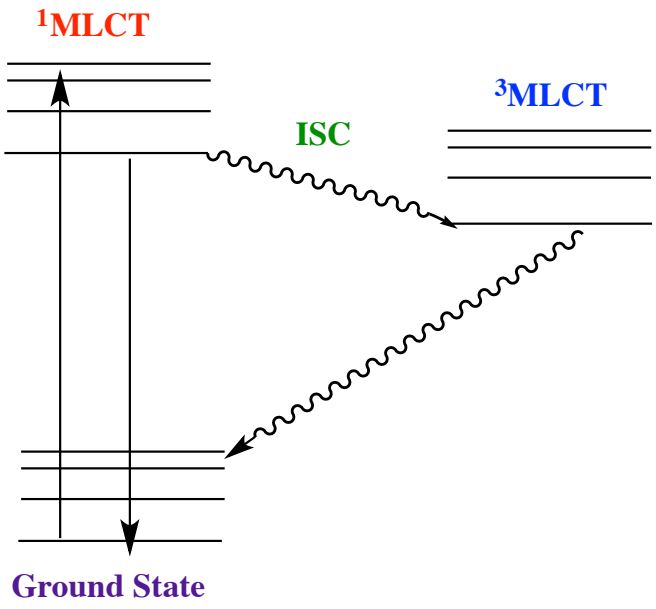

Figure 1.1: The singlet and triplet states that formed after photon absorption

1.2.1 Type I Photocatalyst System

As previously stated, Type I photocatalyst systems are two component systems that consist of a photosensitizer unit (PS) and a catalyst component (CAT). When the PS absorbs the particular energy of light, it is promoted to an excited electronic state PS^* (eq1). One possible route taken by this excited state is to undergo reductive quenching by reaction with a sacrificial donor (D) to form a reduced photosensitizer, PS^-, and the oxidized sacrificial donor $D^{\cdot+}$ (eq2). This reduced photosensitizer can then transfer an electron to the catalyst to yield a reduced catalyst, CAT^-, which is then responsible to react with CO_2 to form reduction products (eq 3,4).[22]

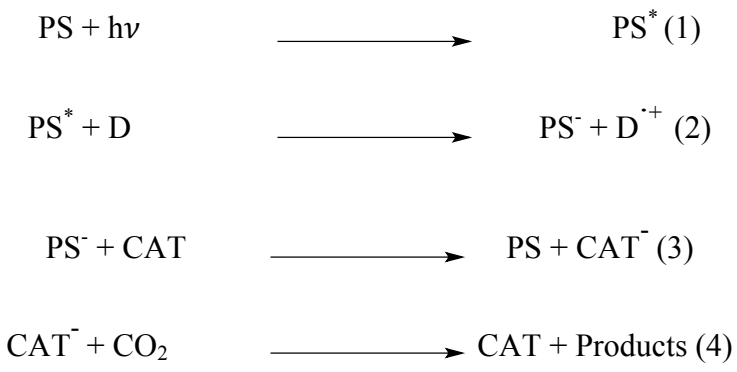

Ruthenium (II) polypyridine complexes are among the most intensively studied photosensitizers for the homogeneous photocatalytic reduction of CO_2. One of the most important features in the photosensitizer unit is the lifetime of an excited state which is an atom, ion or molecule with an electron that in a higher than normal energy level than the energy of ground state. The lifetime of a system is usually very short because the system is returning to a lower energy state (the ground state or a less excited state). The excited lifetime of Ru^{II} complexes is one of the critical features behind their application. The lifetime of the excited state tris(bipyridyl)ruthenium(II) chloride has been measured to be 800 ns in water at room temperature.[23] Recently, a number of studies have focused on efforts to extend the lifetime of Ru^{II} polypyridine complexes. Some examples of this effort are presented in Scheme1.3.[24]

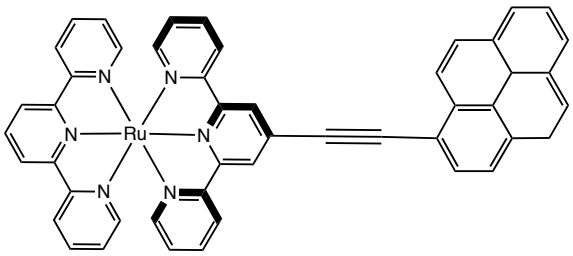

λ_{em}=698nm.

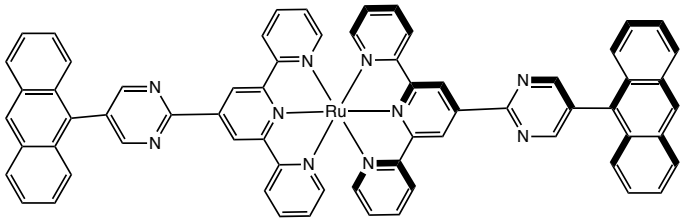

λ_{em}=675nm.

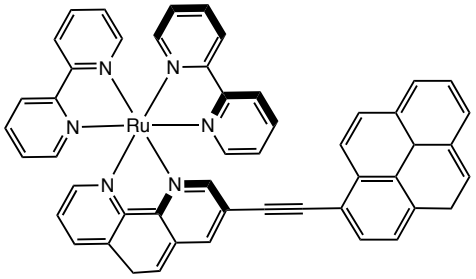

λ_{em}=667nm.

Scheme1.3: Representation of some Ru^{II} bipyridine and terpyridine complexes that have extended lifetimes.

In a Type I system, a transition metal complex is used as the catalyst and coupled with the photosensitizer. Among the first transition metal complexes that were investigated as homogeneous catalysts for CO_2 reduction, are cobalt and nickel

complexes of the tetraaza-macrocylic ligands show in Scheme 1.5. In 1984, Tinnemans *et al.* used $Ru(bpy)_3^{-2+}$ as a photosensitizer with Co and Ni tetraaza-macrocylic complexes as a catalyst. The main products from photocatalyzed reduction of CO_2 were CO and HCOOH. Subsequent studies were carried out in an effort to suggest proposed mechanisms for the formation of these products [25-27].

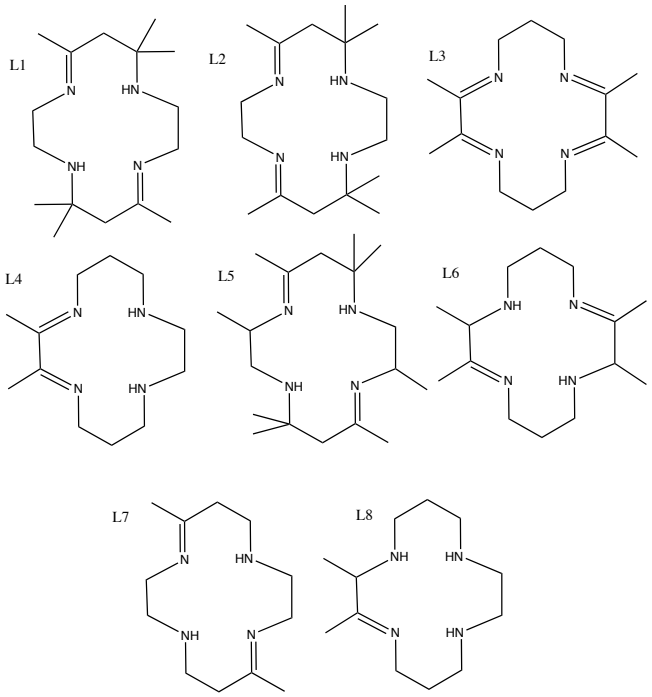

Scheme 1.4: The base macrocycle ligands of Co(II)

1.2.2 **Supramolecular Complexes**

Several studies have reported Type I catalysis for CO_2 reduction with the main goal of increasing the efficiency of the reactions by increasing both the turnover number of the products as well as the selectivity. One possible route to increase the efficiency may be to

covalently attach a photosensitizer to a catalyst to form a supramolecular complex. The idea here is that the covalent attachment between a photosensitizer and the catalyst can more efficiently transfer the electron faster between the photoactive component and a catalyst acceptor during the excited state of the photosensitizer.

Supramolecular complexes are defined as the covalent attachment of a redox photosensitizer to a transition metal catalyst center. Such complexes are members of the Type I class of catalysts for the reduction of CO_2. To date, two classes of compounds have been investigated as supramolecular complexes for CO_2 reduction. These two classes of compounds have employed attachment of ruthenium polypyridine complexes, as photosensitizer, to modified Ni and Re catalysts. Representations of these efforts are shown in Scheme 1.6. In one case the Ni cyclam system was linked to the PS and in the other a $Re(bpy)(CO)_3X$ was used. [28-31]

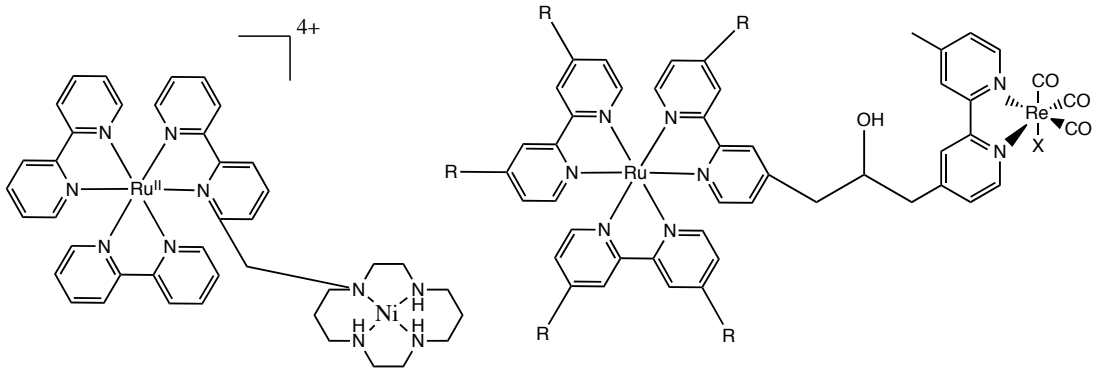

Scheme1.5: Some supramolecular complexes that were used in Ishitani and Kimura studies.

These supramolecular complex systems have shown success in increasing the efficiency of CO_2 reduction compared to more conventional Type I systems employing separate components. For example, Ishitani *et al*. have prepared supramolecular complexes shown in Scheme 1.6 that gave increased efficiency of CO_2 reduction as shown in (Table 1.2) .[31]

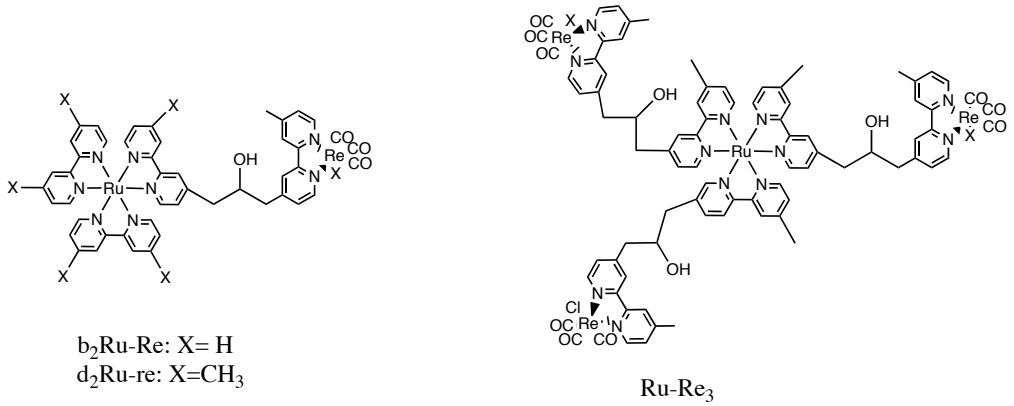

Scheme 1.6: Some supramolecular complexes that were utilized by Ishitani

Table 1.2: The turnover number of CO product that formed from different types of supramolecular complexes

Compound	TN_{CO}
separate molecules of Ru and Re	101
d_2Ru-Re	170
$RuRe_3$	240

To conclude, Type I catalysts systems and their modified supramolecular complex systems have demonstrated the ability to reduce CO_2 in homogeneous reactions. However, the main challenge of this approach is a low stability of the catalyst and this

would be a main obstacle of transfer of these catalysts from the laboratory scale to the practical applications. Although supramolecular complexes have shown increased activity, the synthesis of these complicated complexes is not easy.

1.2.3 Type II Photocatalytic System

In contrast with Type I, Type II catalyst systems have a single transition metal complex that is able to absorb the light and catalyze the reduction of CO_2. This single complex functions as both photosensitizer and catalyst and is therefore represented as PSCAT. The general photocatalytic process can be represented by equations 5-7. First the complex absorbs light to achieve the excited state. The excited state catalyst is reduced by reductive quenching to yield the reduced catalyst species which reacts with CO_2 to yield reduction products.[22]

$$PSCAT + h\nu \longrightarrow PSCAT^{*} \quad (5)$$

$$PSCAT^{*} + D \longrightarrow PSCAT^{-} + D^{\cdot +} \quad (6)$$

$$PSCAT^{-} + CO_2 \longrightarrow PSCAT + Product \quad (7)$$

Type II catalysis derived from rhenium complexes were investigated for the first time by Hawecker, Lehn and Ziessel *et al*. in 1983, when they discovered that $Re^{I}(CO)_3(bipy)X$ can act as both a redox photosensitizer and a catalyst. Firstly, they used $Re^{I}(CO)_3(bipy)X$, (X= Cl^- or Br^-) as only a photosensitizer in place of $Ru^{II}(bipy)$ with $Co(bipy)_3^{2+}$ as a catalyst. During the control experiments, they found rhenium complexes

have the ability to produce CO in the absence of $Co(bipy)_3^{2+}$.[17,33] Closely related $Re^I(CO)_3(L)X$-based complexes have been investigated as Type II catalysis where L=4,4′-R_2-2,2′-bipyridine (R=H or CH_3) or 1,10-phenanthroline, and X=Cl^-or Br^-.

The accepted mechanism for these complexes begins when the Re^I complexes absorb light and are promoted to an MLCT excited state with a Re^{II} as a metal center with one electron that located on a bipy ligand during MLCT period. The sacrificial reductant (D) (usually triethanolamine, TEOA) then reductively quenched the excited state to form $[Re^I(L^{\bullet})(CO)_3X]^-$ as shown in Scheme 1.7.[22]

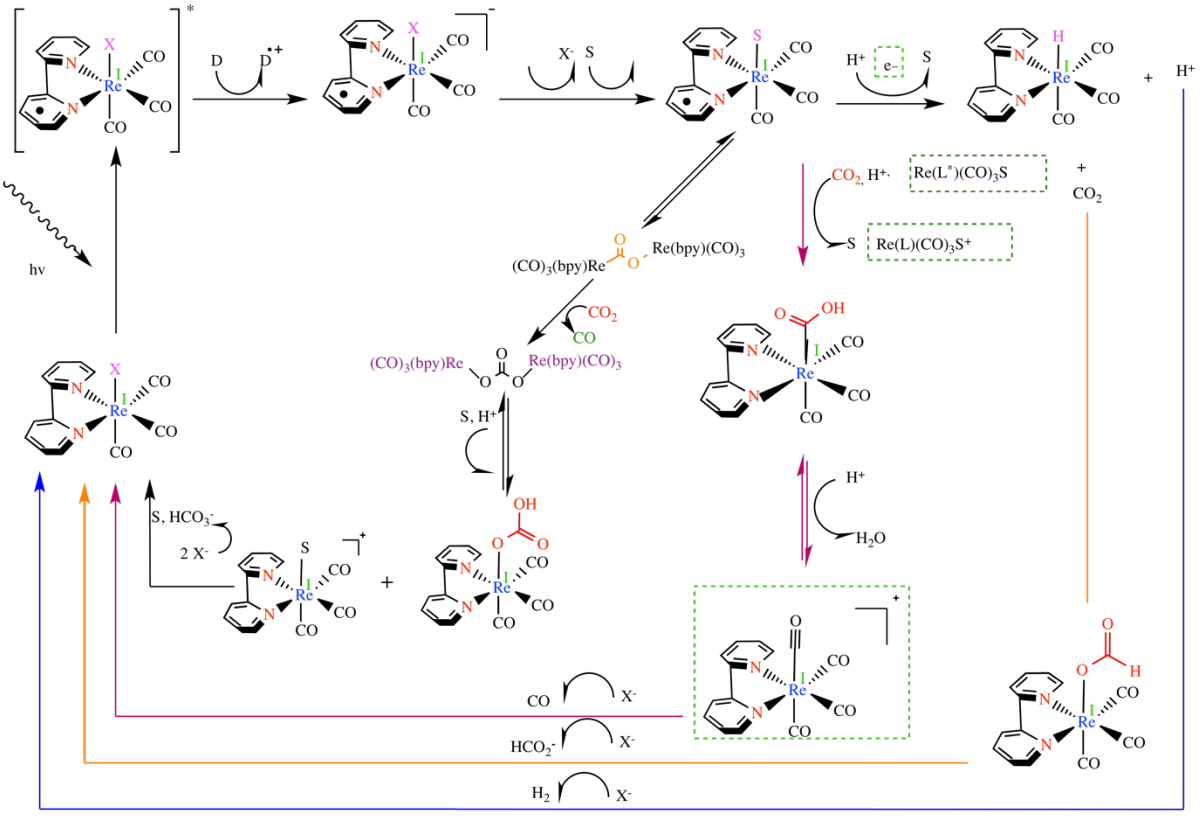

Scheme 1.7: The proposed mechanism of $Re^I(CO)_3(bpy)X$-based complexes

Later, Fujita *et al.* proposed that a solvent (S) can replace the halide ligand (X) in [Re(CO)3LX]- to form $[Re^{I}(CO)_3(L^{\bullet})S]$.[36] Protonation of $[Re^{I}(CO)_3(L^{\bullet})S]$ is proposed to form a rhenium-hydride complex, $[Re^{I}(CO)_3(L)H]$ that can be protonated to yield H_2 as the main product and react with X^- to regenerate the initial $Re^{I}(CO)_3(L)X$. Another proposed route for the reaction with $[Re^{I}(CO)_3(L)X]$ also goes through the solvent substituted compound, $[Re^{I}(CO)_3(L^{\bullet})S]^+$ followed by protonation and CO_2 insertion to form a metal carboxylate which in the presence of H^+ (acid acting as a catalyst) can hydrolyze to from CO as the main product and H_2O.[33,34] Another suggested mechanism is proton-promoted dehydroxylation of $[Re(L)(CO)_3(COOH)]$ to form $Re(L)(CO)_4^+$ (Scheme 1.8). A new formation $[Re(L)(CO)_4^+]$ in the addition of X^- and under irradiation can form CO.[35]

$$Re(L)(CO)_3(COOH) \rightleftharpoons Re(L)(CO)_4^+ + OH^-$$

Scheme 1.8: The elimination reaction of Re^{I} complex which yields $Re(L)(CO)_4^+$

Ishitani *et al*. have discussed the last route of the proposed mechanism when they suggested the possibility of a binuclear complex of Re^{I}. In the presence of CO_2, the CO_2-bridged dimer can slowly react with CO_2 to release CO and form $Re(L)(CO)_3OCO_2Re(L)(CO)_3$. Protonation of $Re(L)(CO)_3OCO_2Re(L)(CO)_3$ in the addition of X^- can form HCO_3^-.[31]

Since the first paper on the catalytic ability of $Re^{I}(CO)_3(bpy)X$ was published by Hawecker and Lehn, there are many studies focused to increase the selectivity and the efficiency of Re^{1} complexes to form CO as the main product. One possible way to increase the efficiency of photoreduction is by substituting halo ligand X^- with other ligands such as Br, PPh_3, $\{P(OEt)_3\}$, CN^- (Scheme 1.9).[17,36] The highest turnover number for CO production was obtained by substituting Cl^- with CN^-, which also showed the longest lifetime of ^{3}MLCT than other ligands.

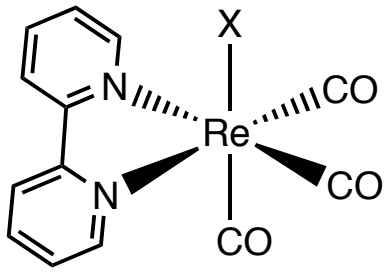

Scheme 1.9: Representing the structure of *fac*-$Re^{I}(CO)_3(bpy)Cl$

Another approach to increasing the efficiency of CO_2 reduction to yield CO as the main product was explored through substitution on the pyridyl ligands. Several studies have shown the effect of substituting bipyridine with substituted bipyridine derivatives such as Re(bpy-R)$(CO)_3$Cl (R = -H or $-CH_3$ or -COOH or -CN) (Scheme1.10).[37] $-CH_3$ is an electron-donating group, which is in contrast with -COOH and CN^- as an electron-withdrawing group. The effect of these ligand substitutions on the photocatalytic reduction as correlated with absorption properties as summarized in Table 1.3.

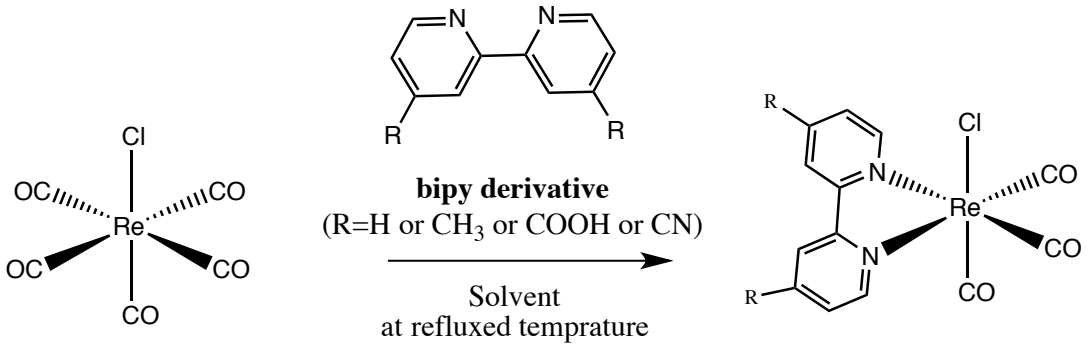

$Re(CO)_5Cl$ Re (bipy-R)

Scheme1.10: The base structure of $Re(bpy\text{-}R)(CO)_3Cl$

Compound	MLCT transitions	Absorbance at 365nm
Re(bpy-H)	370nm	0.2
Re(bpy-CH_3)	375nm	0.19
Re(bpy-COOH)	400nm	0.25
Re(bpy-CN)	450nm	0.15

Table 1.3: The UV-Vis absorption spectra of $Re(bipy\text{-}R)(CO)_3Cl$ complexes.[37]

In general, there are two absorption bands in the UV-Vis spectra: the first absorption bands were around 300-350 nm corresponded to $\pi - \pi^*$ transitions, the second absorption bands were around 350 to 400 nm corresponded to MLCT transitions. This spectrum has shown different adsorption coefficient (ε) due to the unique photophysical properties of each group on pyridine. The maximum (ε) was observed for CN and COOH respectively, and no significance changes in H and CH_3.[37]

When the CO_2 reduction ability of these compound was examined, the amount of CO after 120 min of irradiation in typical run was largest for Re(bpy-COOH) (TON= 6)

while Re(bpy-CN) did not form any CO. However, in both, substituting the halide X^- and pyridine derivatives with CN^-, the studies have approved that CN^- group yielded the maximum amount of CO comparing with other groups

As already discussed in this chapter, the approaches of utilization CO_2 started from last few decades, but until now the scientists and investigators are trying to overcome the challenges of transforming CO_2 to more valuable products as CO and CH_4. In this thesis, the research objective are highlighted to explore new catalysts of group VII for photocatalytic and electrocatalytic reduction of CO_2 to produce CO as the main product. Thus in this thesis, there are different approaches, many reaction parameter, different ligand geometries and photosensitizer units have been under investigation.

References

1. Ampelli, C.; Perathoner, S.; Centi, G. *Phil. Trans. R. Soc*. A*,* **2014**, *373*.
2. Appel, A. M.; Bercaw, J. E.; Bocarsly, A. B.; Dobbek, H.; DuBois, D. L.; Dupuis, M.; Ferry, J. G.; Fujita, E.; Hille, R.; Kenis, P. J.; Kerfeld,C. A.; Morris, R. H.; Peden, C. H.; Portis, A. R.; Ragsdale, S. W.; Rauchfuss, T. B.; Reek, J.N.; Seefeldt, L. C.; Thauer, R. K.; Waldrop, G. L. *Chem. Rev.* **2013**, *113*, 6621−6658.
3. Metz, B.; Davidson, O.; Coninck, H.; Loos, M.; Meyer, L. Eds.; *Cambridge, U.K*. **2005**, 442.
4. Wang, W.; Wang, S. P.; Ma, X. B.; Gong, J. L. *Chem. Soc. Rev.* **2011**, *40*, 3703−3727.

5. Meyer, T. J. *Acc. Chem. Res.* **1989**, *22*, 163–170.
6. Leitner,W. *Coord. Chem. Rev.* **1996**, *153*, 257–284.
7. Alstrum-Acevedo, J. H.; Brennaman, M.K.; T. J. Meyer, T. J. *Inorg. Chem.* **2005**, *44*, 6802–6827.
8. Aresta, M.; Dibenedetto,A. *Dalton Trans*. **2007**, 2975–2992.
9. Fujita, E. *Coord.Chem. Rev.* **1999**, 185-186, 373–384.
10. Schwarz, H. A.; Dodson, R. W. *J. Phys. Chem*. **1989**, *93*, 409–414.
11. Lexa, D.; Momenteau, M.; Saveant, J. M. *J. Am. Chem. Soc*. **1991**, *113*, 8455–8466.
12. Bhugun, I.; Lexa, D.; Saveant, J. M. *J. Phys. Chem.,* **1996**, *100*, 19981–19985.
13. Wong, K. Y.; Chung, W. H.; Lau, C. P. *J. Electroanal. Chem.* **1998**, *453*, 161–169.
14. Fisher, B.; Eisenberg, R. *J. Am. Chem. Soc.,* **1980**, *102*, 7361.
15. Beley, M.; Collin, J. P.; Ruppert, R.; Sauvage, J. P. *J. Chem Soc., Chem. Commun*. 1**984**, 1315.
16. Grodkowski, J.; Neta, N.; Fujita, E.; Mahammed, M.; Simkhovich, L.; Gross, Z. *J. Phys. Chem*. A, **2002**, *106*, 4772.
17. Hawecker,J.; Lehn, J. M.; Ziessel, R. *Helv. Chim. Acta,* **1986**, *69*, 1990–2012.
18. Takeda, H.; Koizumi, H.; Okamoto, K.; Ishitani, O. *Chem. Commun.,* 2014, *50*, 1491.
19. Bourrez, M.; Molton, F.; Chardon-Noblat, S.; Deronzier, A. *Angew. Chem., Int. Ed.,* **2011**, *50*, 9903–9906.

20. Kimura, E.; Wada, S.; Shionoya, M.; Takahashi, T.; Iitaka, Y. *J. Chem. Soc., Chem. Commun.,* **1990**.

21. Bolinger, C. M.; Story, N.; Sullivan, B. P.; Meyer, T. J. *Inorg.Chem.,* **1988**, *27*, 4582.

22. Morris, A.; Meyer, G.; Fujita, E. *Acc. Chem. Res,* **2009**.

23. Reithmeier, R.; Bruckmeier, C.; Rieger, B. *Catalysts.* **2012**, *2*, 544-571.

24. Kalyanasundaram, K. *Coord. Chem. Rev*. **1982**, *46*, 159–244.

25. Tinnemans, A. H. A.; Koster, T. P. M.; Thewissen, D.; Mackor, A. *Recl. Trav.Chim. Pays-Bas* **1984**, *103*, 288–295.

26. Matsuoka, S.; Yamamoto, K.; Ogata, T.; Kusaba, M.; Nakashima, N.; Fujita, E.; Yanagida, S. *J. Am. Chem. Soc*. **1993**, *115*, 601–609.

27. Ogata, T.; Yamamoto, Y.; Wada, Y.; Murakoshi, K.; Kusaba, M.; Nakashima, N.;Ishida, A.; Takamuku, S.; Yanagida, S. *J. Phys. Chem*. **1995,** *99*, 11916–11922.

28. Kimura, E.; Bu, X.; Shionoya, M.; Wada, S.; Maruyama, S. *Inorg. Chem*. **1992**, *31*, 4542–4546.

29. Kimura, E.; Wada, S.; Shionoya, M.; Okazaki, Y. *Inorg. Chem.* **1994**, *33*, 770–778.

30. Gholamkhass, B.; Mametsuka, H.; Koike, K.; Tanabe, T.; Furue, M.; Ishitani, O. *Inorg. Chem*. **2005**, *44*, 2326–2336.

31. Sato, S.; Koike, K.; Inoue, H.; Ishitani, O. *Photochem. Photobiol. Sci.* **2007**, *6*, 454–461.

32. Hawecker, J.; Lehn, J. M.; Ziessel, R. J. Chem. Soc., *Chem. Commun.* **1984,** 328–330.

33. Hawecker, J.; Lehn, J.; Ziessel, R. ***Chem. Commun.*** **1983**, 536-538.

34. Sullivan, B. P.; Meyer, T. J. *Organometallics* **1986**, *5*, 1500–1502.

35. Gibson, D. H.; Yin, X. L. *J. Am. Chem. Soc.* **1998**, *120*, 11200–11201.

36. Hayashi, Y.; Kita, S.; Brunschwig, B. S.; Fujita, E. *J. Am. Chem. Soc*. **2003**, *125*, 11976–11987.

37. Hori, H.; Johnson, P. A.; Koike, K.; Ishitani, O.; Ibusuki. T. *J. Photochem. Photobiol. A: Chem*., **1996**, *96*, 171–174.

Chapter 2

Capturing Re(I) in an Neutral N,N,N Pincer Scaffold and Resulting Enhanced Absorption of Visible Light.

The work in this chapter formed a significant component of the publication:

(Bulsink, P.; Al-Ghamdi, A.; Joshi, P.; Korobkov, I.; Woo, T.; Richeson, D. *Dalton Trans.* **2016**, *45* (21), 8885–8896.)

This manuscript reported on a family of Re(I) complexes with a unique tridentate neutral pincer coordination geometry and addressed a major deficiency in the chemistry of imine-coordinated Re(I) carbonyl chemistry. The supporting ligands used in this manuscript were bis(imino)pyridine and terpyridine. The manuscript reports sixteen Re(I) complexes, four employed terpyridine chemistry and are a contribution from P. Bulsink and that chemistry appears in his MSc thesis. I made the major contribution to the synthesis and characterization of the remaining species. P. Joshi initiated the synthesis of many of these species and his contribution is appreciated. The crystallography was carried out by I. Korobkov. Bulsink and T. Woo carried out the computational analysis of these complexes. In addition to elaborating on the new coordination geometry, an additional goal was to explore the photocatalysis and electrocatalytic ability of the compounds.

2.1 Introduction

The photophysical properties of pseudo-octahedral Re(I) complexes with a *fac*-$Re^{I}(CO)_3$ core and α-diimine ligation have been a field of interest since the mid-1970's.

They are readily prepared by the direct addition of chelating diimine ligands to $[Re(CO)_5X]$ resulting in quantitative replacement of two *cis* carbonyls in the Re(I) starting material.[1–12] A significant limitation of these high yielding reactions is that only bidentate coordinated ligands with pseudo-octahedral *fac*-$[L_2Re(CO)_3X]$ and *fac*-$[L_2(L')Re(CO)_3]^+$ isomers are formed as products even when a potentially tridentate σ–donor, such as bis(imino)pyridine or 2,2':6',2"-terpyridine (terpy) are employed (Scheme 2.1).[13–15]

These robust α-diimine species have been examined for a remarkable range of applications in catalysis,[16–18] as potential radiopharmaceuticals,[12,19,20] for applications in organic light-emitting diodes (OLEDs),[21,22] as chemosensors and biotechnology probes,[4,23–31] and for the photochemical reduction of CO_2 to CO.[32–37] A key photophysical feature of these α–diimine Re(I) compounds is the electron transfer relationship between the Re center and the well-known non-innocent redox-activity of the ligands.[38,39]

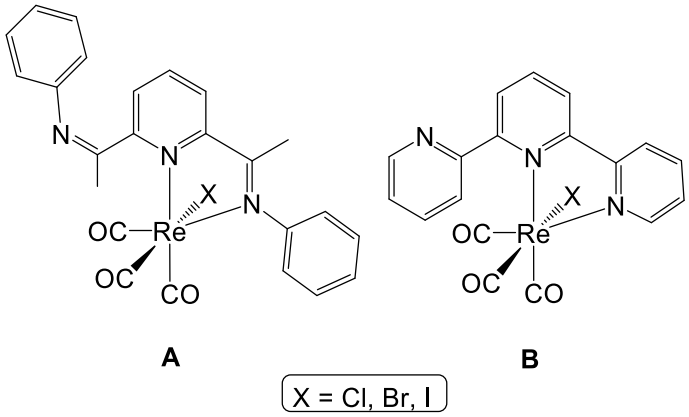

Scheme 2.1: The general structures of reported bidenate compounds of terpy and bis-aminopyridine.

In order to discover new attributes and applications for this chemistry we are developing routes to add new coordination environments to Re(I). Studies detailing the coordination chemistry of the meridionally-coordinated tridentate triimine Re(I) dicarbonyl core are quite limited. Our group recently reported the conversion of bidentate bis(imino)pyridine complexes 2,6-{2,6-$Me_2C_6H_3N$=CPh}$_2$(NC_5H_3)$Re(CO)_3X$ (X = Cl, Br) into tridentate pincer ligand compounds, 2,6-{2,6-$Me_2C_6H_3N$=CPh}$_2$(NC_5H_3)$Re(CO)_2X$ (X = Cl, Br).[40] This established a high yield synthetic method and, through structural characterization, Re(I) carbonyl complexes supported by a planar, tridentate bis(imino)pyridine ligand. However, this was demonstrated for only a single ligand, 2,6-{2,6-$Me_2C_6H_3N$=CPh}$_2$(NC_5H_3). Similarly, a claim for (κ^3-(terpy)$Re(CO)_2Cl$) was reported in 1988, but closer analysis of the reported analytical data indicate that this compound is more likely (κ^2-(terpy)$Re(CO)_3Cl$).[41] The ^{1}H NMR data for what is described as (κ^3-(terpy)$Re(CO)_2Br$) has been reported.[15] More recent reports regarding this compound provide spectroscopic details of this species as well as the report for the generation of [(κ^3-(terpy)$Re(CO)_2L'$]$^+$ cations (L = PPh_3, PEt_3, NC_5H_5, and $NCCH_3$).[42,43] None of these compounds was crystallographically characterized. Very recently, the first crystallographic characterization of a tridentate terpy ligand was reported for [(κ^3-4-pytpy)$Re(CO)_2$py]$^+PF_6^-$ (4-pytpy = 4-(4-pyridyl)-2,2':6',2"-terpyridine).[44]

The goal of the chemistry reported in this chapter is to significantly expands on the accessible synthesis of tridentate pincer complexes and the analysis of their visible electronic transitions. The synthesis and characterization six new κ^3-bis(imino)pyridine complexes, [κ^3-2,6-{2,6-$R_2C_6H_3N$=CMe}$_2$(NC_5H_3)]$Re(CO)_2X$ (R = H, Me, ^{i}Pr; X = Cl,

Br) is described. This contribution broadens the availability of such compounds to further enhance the versatile chemistry of Re(I) and promote new venues for exploration.

2.2 Results and Discussion

The initial incorporation of ligand, *en route* to our target species, proceeded smoothly by the direct reaction of the bis(imino)pyridine ligands **I-III** with 1 equivalent of $Re(CO)_5X$ (X = Cl or Br) and mild heating (e.g. 100°C) within 1 hour as summarized in Scheme 2.2. The resulting bright yellow/orange powders **1-6** were isolated in yields of 60% to 85% respectively. Spectroscopic (^1H and ^{13}C NMR, IR) and elemental analysis was consistent with the formulation and suggested structural features.

While complex **2** has been structurally characterized,[14] the definitive confirmation of the detailed metrical parameters for compounds **1** and **3-5** was obtained from single crystal X-ray analyses. The five products, 2,6-$\{ArN{=}CMe\}_2(NC_5H_3)Re(CO)_3X$ (X = Cl, Br) (**1-5**) exhibited analogous ligand dispositions with the Re(I) center in a pseudo-octahedral geometry as represented in Scheme 1 and shown in Figures 2.1-2.5.

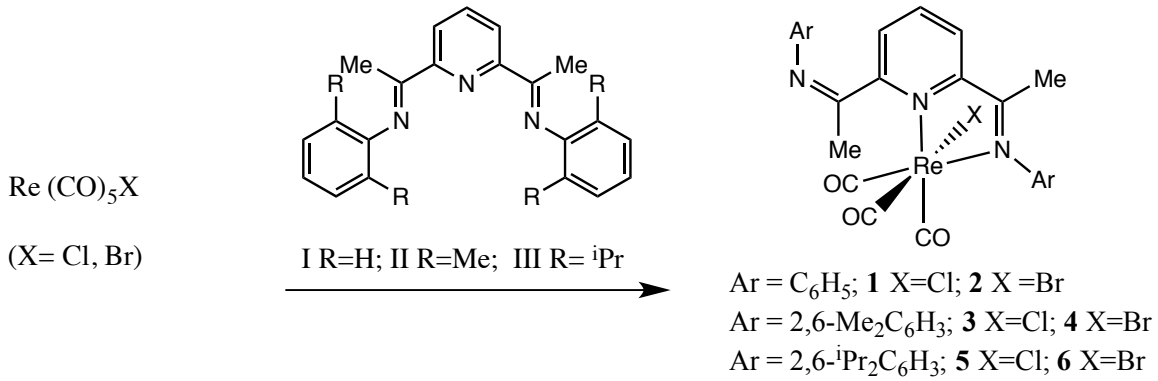

Scheme 2.2: Synthesize of bidentate compounds with different substitute groups on the ligand

In addition to displaying a bidentate bis(imino)pyridine ligand, the coordination geometries of these six compounds are completed by a facial array of three carbonyl groups and the respective chloro or bromo groups that are *trans* to a carbonyl ligand and on an axis perpendicular to the plane of the coordinated nitrogen ligand.

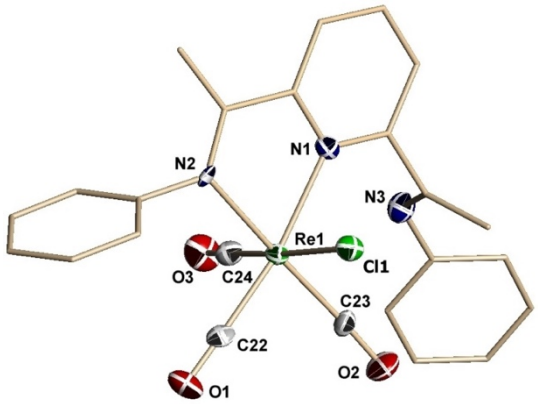

Figure 2.1. X-ray structure derived representation of compound (**1**) κ^2-2,6-$\{C_6H_5N{=}CMe\}_2(NC_5H_3)Re(CO)_3Cl$**.** Hydrogen atoms and thermal ellipsoids of the ligand carbon atoms are omitted for clarity.

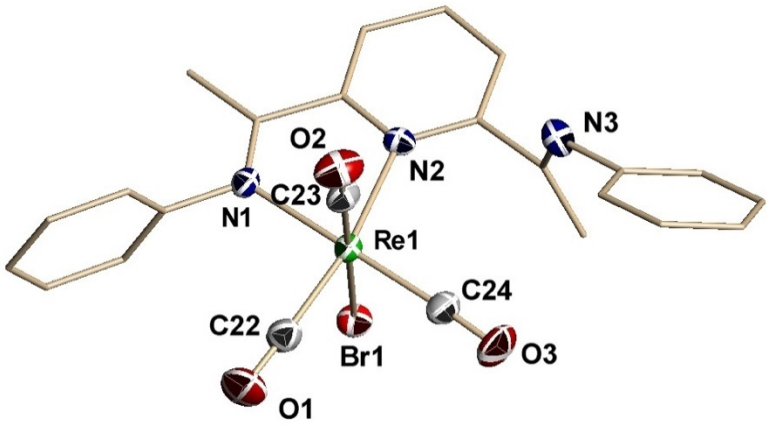

Figure 2.2. X-ray structure derived representation of compound (**2**) κ^2-2,6-$\{C_6H_5N{=}CMe\}_2(NC_5H_3)Re(CO)_3Br$**.** Hydrogen atoms and thermal ellipsoids of the ligand carbon atoms are omitted for clarity.

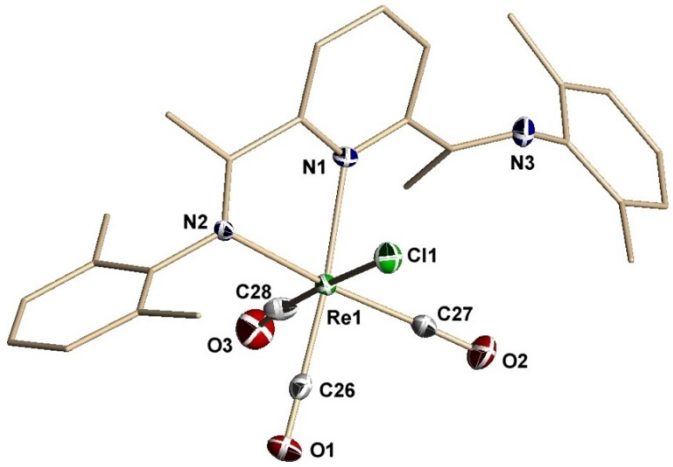

Figure 2.3. X-ray structure derived representation of compound **(3)** κ^2**-2,6-**$\{Me_2C_6H_3N{=}CMe\}_2(NC_5H_3)Re(CO)_3Cl$**.** Hydrogen atoms and thermal ellipsoids of the ligand carbon atoms are omitted for clarity.

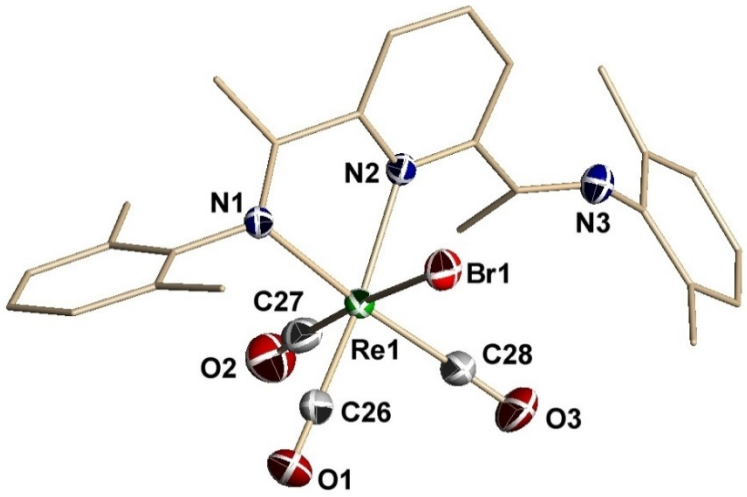

Figure 2.4. X-ray structure derived representation of compound **4** κ^2-2,6-$\{Me_2C_6H_3N{=}CMe\}_2(NC_5H_3)Re(CO)_3Br$**.** Hydrogen atoms and thermal ellipsoids of the ligand carbon atoms are omitted for clarity.

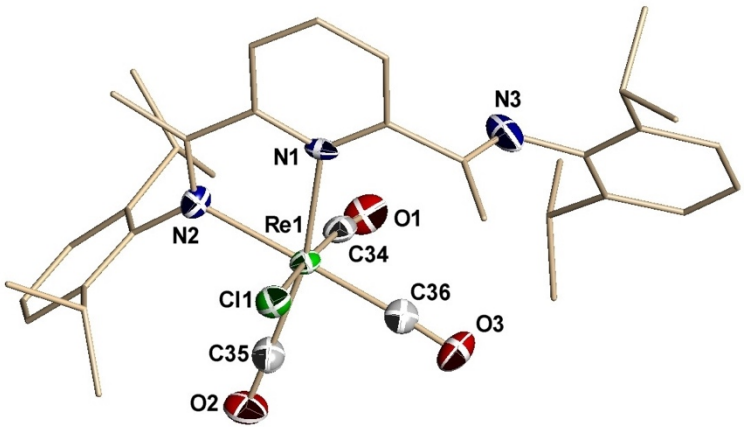

Figure 2.5. X-ray structure derived representation of compound **(5)** κ^2-2,6-{$iPr_2C_6H_3N{=}CMe$}$_2(NC_5H_3)Re(CO)_3Cl$**.** Hydrogen atoms and thermal ellipsoids of the ligand carbon atoms are omitted for clarity.

The bidentate complexes (**1-6)** provide intermediates for our goal to transform these species into tridentate pincer ligand compounds through release of CO and coordination of the pendant imine or pyridyl group. This entropy driven reaction was carried out by heating powders of (**1-6)** in a tube furnace under a dynamic flow of nitrogen[48–50] Heating these compounds to 250°C, for one hour gave new compounds (**7**-**12)** in good to excellent yields (Scheme 2.3). Other than the very apparent changes to darker colored species, further indication that tridentate species were formed was provided by the simplification of the ^{1}H and ^{13} C NMR spectra due to the increased amount of molecular symmetry for these species. As well for the tridentate complexes, the CO stretch is generally lower in energy (lower cm^{-1}) than the bidentate which have shown only two CO stretches in the IR spectra.

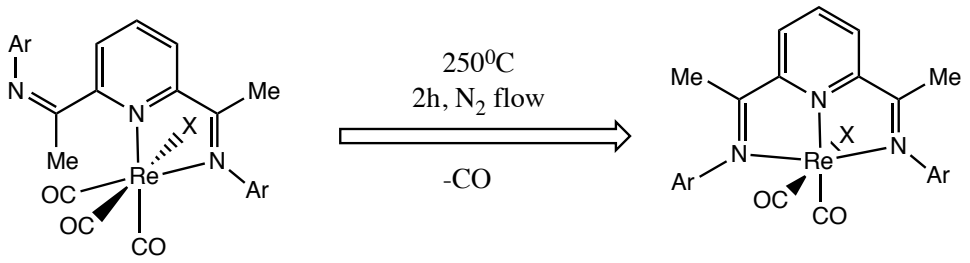

Ar = C_6H_5; **1** X=Cl; **2** X =Br
Ar = 2,6-$Me_2C_6H_3$; **3** X=Cl; **4** X=Br
Ar = 2,6-$^i Pr_2C_6H_3$; **5** X=Cl; **6** X=Br

Ar = C_6H_5; **7** X=Cl; **8** X =Br
Ar = 2,6-$Me_2C_6H_3$; **9** X=Cl; **10** X=Br
Ar = 2,6-$^i Pr_2C_6H_3$; **11** X=Cl; **12** X=Br

Scheme 2.3: Transforming bidentate compounds to tridentate under flow of N_2 at high temperature.

The structural details of the κ^3-bis(imino)pyridine species (**7**, **9**, and **10)** were examined by single crystal X-ray analysis. In addition to the structural representation in Figures 2.6-2.8, selected bond distances and angles for these species are presented in Table 2.1. All three of these species display a Re(I) center in a pseudo-octahedral environment supported by a planar, tricoordinate bis(imino)pyridine ligand.

The results for the structural analysis of complexes(**7**, **9**, and **10)** confirm a Re geometry defined by meridional coordination of the pyridine (Npy) and imine (Nim) nitrogen centers of the ligand with *cis* oriented carbonyl groups. One of the carbonyl groups lies in the same plane as the bis(imino)pyridine ligand and *trans* to the pyridyl group, while the remaining CO and halo ligands are perpendicular to this plane and define the pseudo-axial sites. In general, the Re-Npy distances are slightly shorter than the Re-Nim distances and these three bond lengths are significantly shorter than those observed for the respective bidentate precursors thus indicating a stronger L-M interaction. The remaining metal ligand distances are similar to those observed in the bidentate precursors (**1-6)**.

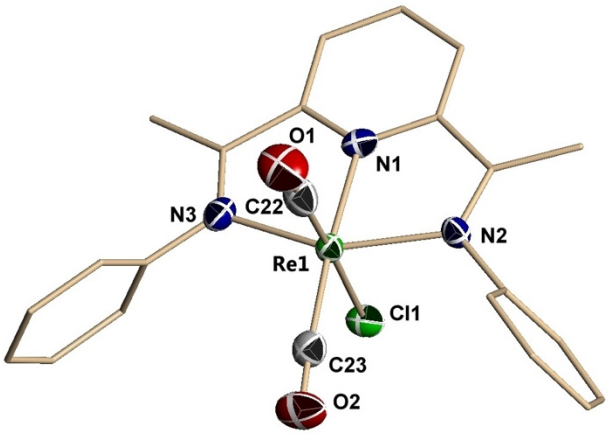

Figure 2.6. A structural representation of $[\kappa^3\text{-}2,6\text{-}\{C_6H_5N{=}CMe\}_2(NC_5H_3)]Re(CO)_2Cl$ (**7**). Co-crystallized chloroform, hydrogen atoms and thermal ellipsoids of the ligand carbon atoms are omitted for clarity.

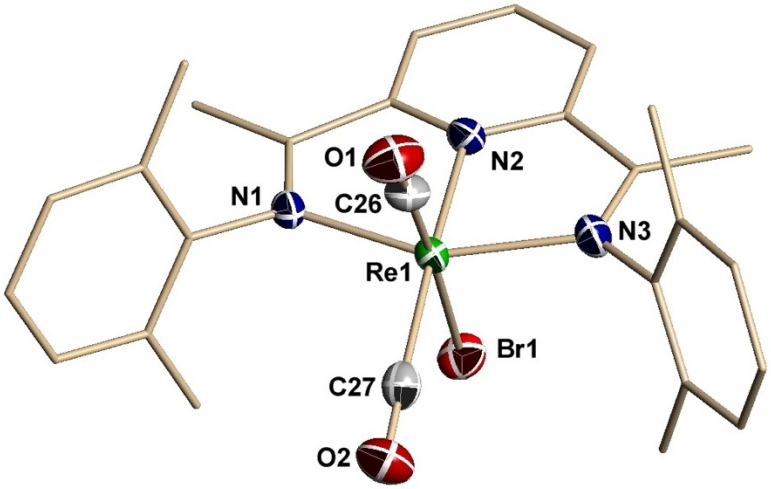

Figure 2.7. A structural representation of $[\kappa^3\text{-}2,6\text{-}\{2,6\ Me_2C_6H_3N{=}CMe\}_2(NC_5H_3)]Re(CO)_2Br$ (**10**). Hydrogen atoms and thermal ellipsoids of the ligand carbon atoms are omitted for clarity.

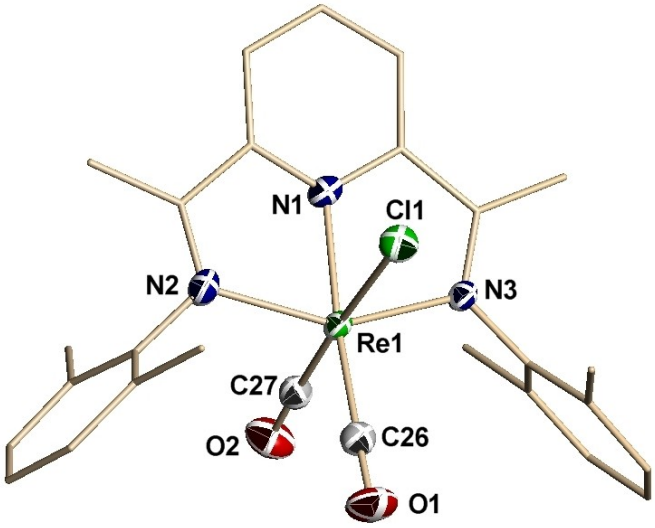

Figure 2.8. A structural representation of [κ^3-2,6-{2,6-$Me_2C_6H_3N$=CMe}$_2$(NC_5H_3)]Re(CO)$_2$Cl (**9**). Co-crystallized chloroform, hydrogen atoms and thermal ellipsoids of the ligand carbon atoms are omitted for clarity.

Table 2.1. Selected bond lengths [Å] and angles [deg] for (**7**, **9** and **10)**.

Compound **7**			
Re(1)-C(22)	1.888(3)	Re(1)-N(2)	2.104(2)
Re(1)-C(23)	1.902(3)	Re(1)-N(3)	2.126(2)
Re(1)-N(1)	2.071(2)	Re(1)-Cl(1)	2.4960(7)
C(22)-Re(1)-C(23)	86.40(13)	N(2)-Re(1)-N(3)	150.31(8)
C(22)-Re(1)-N(1)	97.67(11)	C(22)-Re(1)-Cl(1)	177.92(9)
C(22)-Re(1)-N(2)	93.13(10)	C(23)-Re(1)-Cl(1)	91.62(8)
C(23)-Re(1)-N(1)	174.94(10)	N(1)-Re(1)-Cl(1)	84.34(6)
C(22)-Re(1)-N(3)	94.53(11)	N(2)-Re(1)-Cl(1)	87.88(6)
C(23)-Re(1)-N(2)	101.49(10)	N(3)-Re(1)-Cl(1)	85.46(6)
C(23)-Re(1)-N(3)	107.58(11)	O(1)-C(22)-Re(1)	177.5(3)
N(1)-Re(1)-N(2)	75.36(9)	O(2)-C(23)-Re(1)	176.2(3)
N(1)-Re(1)-N(3)	75.20(9)		
Compound **9**			
Re(1)-C(27)	1.878(3)	Re(1)-N(3)	2.111(2)
Re(1)-C(26)	1.918(3)	Re(1)-N(2)	2.124(2)
Re(1)-N(1)	2.070(2)	Re(1)-Cl(1)	2.5069(7)
C(27)-Re(1)-C(26)	87.40(11)	N(3)-Re(1)-N(2)	150.74(8)
C(27)-Re(1)-N(3)	92.69(10)	C(27)-Re(1)-Cl(1)	176.66(8)
C(27)-Re(1)-N(1)	104.48(10)	C(26)-Re(1)-Cl(1)	89.47(8)
C(27)-Re(1)-N(2)	92.39(11)	N(1)-Re(1)-Cl(1)	78.66(6)
C(26)-Re(1)-N(3)	104.46(10)	N(3)-Re(1)-Cl(1)	86.96(6)
C(26)-Re(1)-N(1)	168.12(9)	N(2)-Re(1)-Cl(1)	89.52(6)
C(26)-Re(1)-N(2)	104.55(10)	O(2)-C(27)-Re(1)	177.0(2)
N(1)-Re(1)-N(3)	75.63(8)	O(1)-C(26)-Re(1)	177.1(2)
N(1)-Re(1)-N(2)	75.19(9)		
Compound **10**			
Re(1)-C(26)	1.877(3)	Re(1)-N(1)	2.110(2)
Re(1)-C(27)	1.944(3)	Re(1)-N(3)	2.126(2)
Re(1)-N(2)	2.069(2)	Re(1)-Br(1)	2.6429(3)
C(26)-Re(1)-C(27)	87.14(12)	N(1)-Re(1)-N(3)	151.03(9)
C(26)-Re(1)-N(2)	105.39(11)	C(26)-Re(1)-Br(1)	175.72(9)
C(26)-Re(1)-N(1)	93.06(11)	C(27)-Re(1)-Br(1)	88.59(8)
C(26)-Re(1)-N(3)	92.55(11)	N(2)-Re(1)-Br(1)	78.86(7)
C(27)-Re(1)-N(2)	167.42(10)	N(1)-Re(1)-Br(1)	87.59(6)
C(27)-Re(1)-N(1)	103.18(10)	N(3)-Re(1)-Br(1)	88.90(7)
C(27)-Re(1)-N(3)	105.48(10)	O(1)-C(26)-Re(1)	175.9(3)
N(2)-Re(1)-N(3)	75.45(9)	O(2)-C(27)-Re(1)	177.0(3)
N(2)-Re(1)-N(1)	75.65(9)		

Perhaps the most prominent observation with the conversion of the bidentate species into the tridentate complexes is that these new compounds are substantially darker in color than the starting complexes. Given the richly developed photophysical features and documented photocatalytic activity of Re(I) complexes, this significant optical absorbance change that occurs upon formation of the pincer complexes (**7**-**12**) was investigated using a combination of UV-visible spectroscopy and electronic structure modeling. [51,52,53]

The stronger absorbance for the tridentate complexes (**7**-**12**) compared to bidentate precursor species (**1**-**6**) is evident in the UV-Vis spectra of these species and presented in the Figure 2.9. The upper part of the figure provides the spectra for the six bidentate, κ²-bis(imino)pyridine species and these can be compared with their respective tridentate products in the lower part of the figure. From examination of this figure it is evident that the tridentate complexes have more intense absorbance across the UV-vis spectral region.

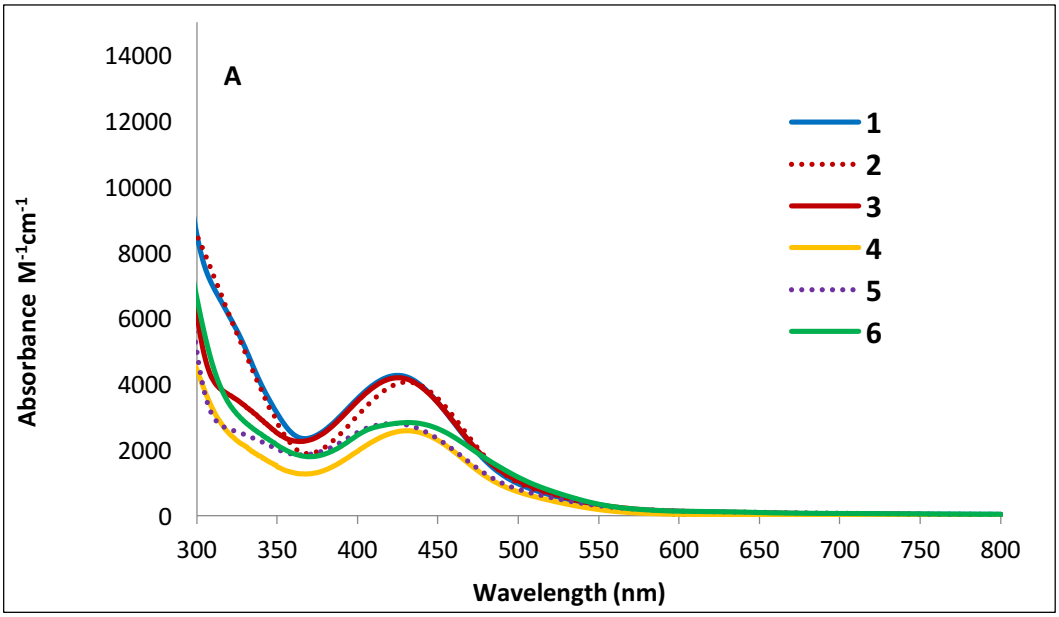

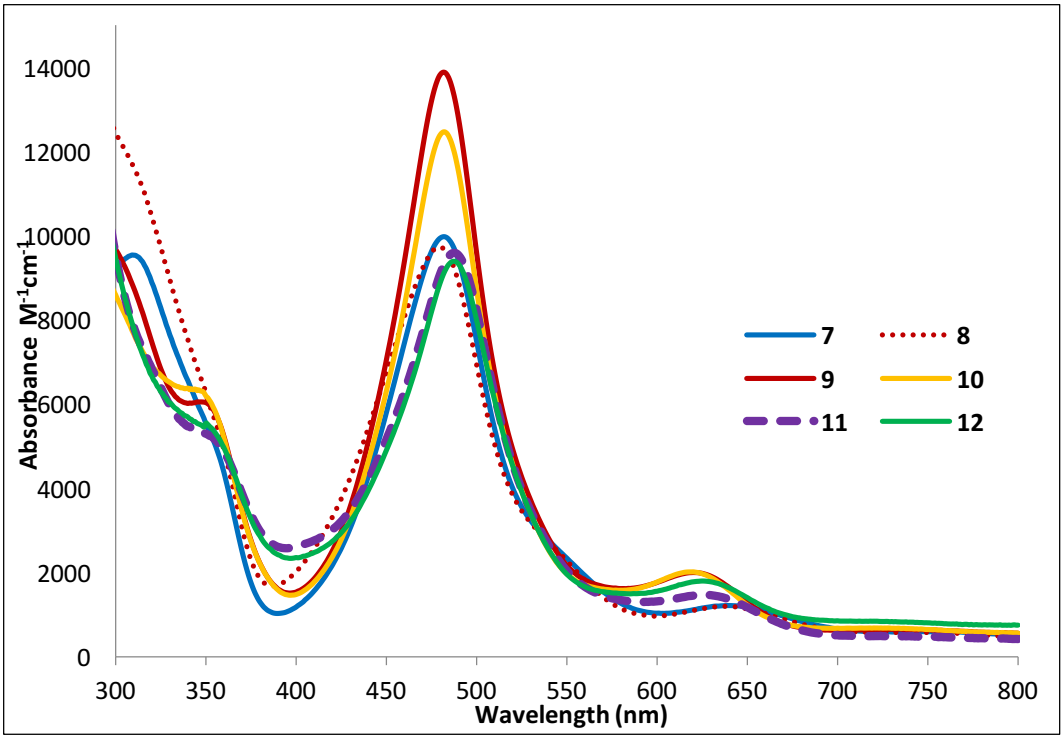

Figure 2.9. UV-Visible spectra (300-800nm) in DMSO of the bidentate complexes κ^2-2,6-{ArN=CMe}$_2$(NC_5H_3)Re(CO)$_3$X **(1-5)** (upper, **A**) and the tridentate analogues κ^3-2,6-{ArN=CMe}$_2$(NC_5H_3)Re(CO)$_2$X (**7-12)** (lower, **B**).

These UV-Vis spectra of compounds (**1-12)** were modeled by P. Bulsink using time-dependent DFT (TD-DFT) computations with the Gaussian 09 program, the B3LYP functional[54,55] and the integral equation formalism variant of the PCM solvation model with DMSO as the solvent.[56,57] The LanL2DZ basis set/effective core potentials[58] were utilized for Re while the all-electron TZVP basis set[59] was used for all lighter atoms. The resulting computed spectra were excellent matches to the experimental spectra. The similarity of the spectra between the six bidentate compounds (**1-6**) as well as among the six tridentate analogues (**7-12**) indicates that corresponding electronic transitions occur

within these two groups and I have chosen to focus on the chloro compounds, (**1** and **7**), for the discussion of the specific transitions. The ideas presented for these complexes are readily extended to the analogues.

The plots of experimental and computational data for the bi- and tridentate complexes, (**1** and **7**), are presented in Figures 2.10 and 2.11, respectively.[60] Common to all of the experimental spectra for the bidentate bis(imino)pyridine compounds were peaks at wavelengths between 315-325 nm corresponding to excitation from ligand-based π to the LUMO orbitals which is predominantly ligand centered π* in nature. A second, longer wavelength absorbance in the range 425-430 (computational maximum 470 nm) was assigned as Re-*d* to a π* LUMO.

In general, as seen in Figure 2.9. the six $\kappa^3\{ArN{=}CMe\}_2(NC_5H_3)Re(CO)_2X$ species have higher absorbance coefficients than their bidentate analogues, and all contain long trailing absorptions across the visible region. All of these compounds show similar analogous strong absorption bands centered at approximately 325, and 460 as well as two less intense bands centered at 640 and 740nm. Examples of the experimental and computed spectra for complex (**7**) are shown in Figure2.11. The two higher energy bands are assigned to transitions from ligand based orbitals to π* orbitals on the phenyl and pyridine moieties. The band at 459 nm was constituted from two approximately equal contributions arising from Re-*d* to pyridine-base π* transitions. The two less intense and lower energy bands at 640 and 740 nm also corresponded to MLCT (e.g. d-π*) transitions. The analysis of the electronic transitions for (**7**) are easily generalized to the experimental and computed transitions that were observed for all six

κ^3-{ArN=CMe}$_2$(NC_5H_3)Re(CO)$_2$X compounds, and thus confirm the fundamental photophysical features of this new family of compounds.

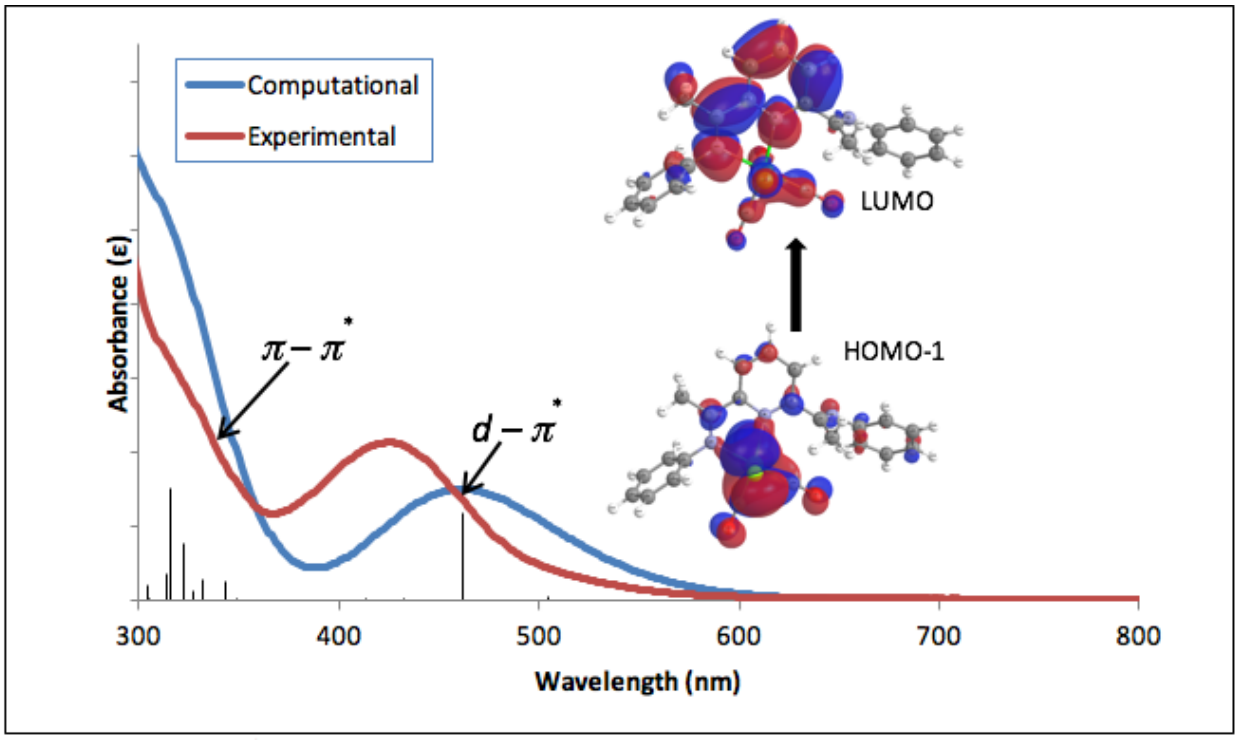

Figure 2.10. Plots of the experimental and computed UV-Vis spectra for compound **1** κ^2-2,6-{PhN=CMe}$_2$(NC_5H_3)Re(CO)$_3$Cl. The vertical lines show the calculated transitions and relative intensities from the TDDFT calculations. Key orbitals associated with the observed transitions are shown. Further analysis of the electronic transitions is described in the text.

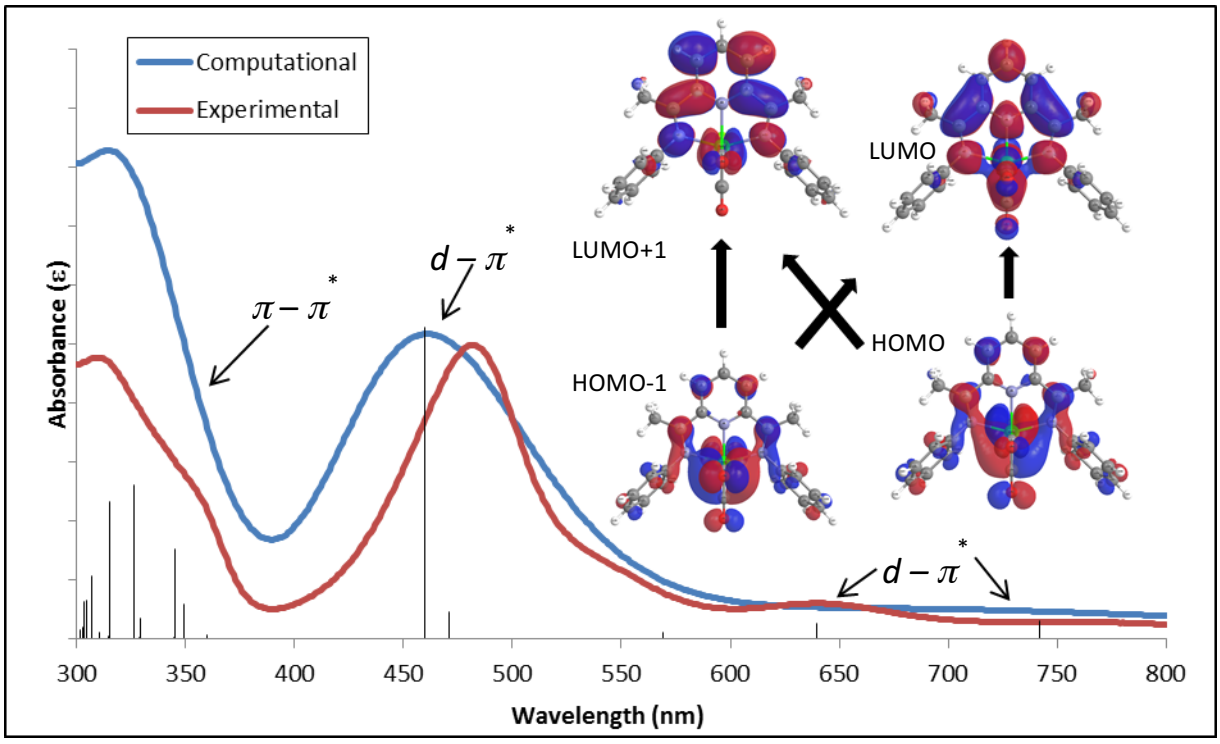

Figure 2.11. Plots of the experimental and computed UV-Vis spectra for compound **7** κ^3-2,6-{ArN=CMe}$_2$(NC_5H_3)Re$(CO)_2$Cl. The vertical lines show the calculated transitions and relative intensities from the TDDFT calculations. Key orbitals associated with the observed transitions are shown. Bold arrows indicate electronic transitions discussed in text. Further analysis of the electronic transitions is described in the text.

2.3 Examining the ability of κ^3(bis(imino)pyridine)Re$(CO)_2$X) complexes for the photocatalytic reduction of CO_2.

Given the prominence of α-diimine Re(I) tricarbonyl complexes in the field of photochemical CO_2 reduction and the enhanced UV-visible absorption features for the κ^3 species, I examined the ability of complexes (**1-12**) for their ability to reduce CO_2 under

the so-called "Strasbourg conditions" which is a mixture of dimethylformamide (DMF) and triethanolamine (TEOA. Photochemical reactions were carried out in DMF solution in a quartz cell. The solution was bubbled with CO_2 for 20 minutes and sealed with a silicon- teflon septum. The photochemical CO_2 reduction was studied in the presence of sacrificial reductants such as triethanolamine (TEOA), 1-benzyl-1,4-dihydronictinamide (BNAH) or ascorbic acid. As well as in the presence of a small amount of H_2O as a source of proton. Reactions were carried out at ambient temperature using a mercury lamp as the light source. The volatiles of these reactions were analyzed after 1, 12, 24 and 48h of irradiation by gas chromatography. Unfortunately, in all cases neither formation of CO nor H_2 was observed and no change in the color. This indicated that, at least under these conditions, these compounds did not catalyze the reduction of CO_2.

2.4 Examining the ability of κ^3(bis(imino)pyridine)Re(CO)$_2$X) complexes for the electrocatalytic reduction of CO_2.

While the failure to photochemically reduce CO_2 was disappointing, I also considered that these species might have the ability to reduce CO_2 electrochemically. Before attempting CO_2 reduction, the electrochemical behavior of compounds (**8, 9&12)** was examined. Since we were primarily interested in reduction, the focus of these experiments was on the reduction behavior of the complexes. The tridentate complexes exhibited redox behavior under nitrogen environment at negative potential versus Fc/Fc^+. Under a saturated atmosphere of nitrogen, the cyclic voltammograms of κ^3-2,6-$\{Me_2C_6H_3N{=}CMe\}_2(NC_5H_3)Re(CO)_2Cl$ **(9)** (100 mV/sec scan rate) showed a quasireversible reduction at -1.4 V vs. Fc/Fc^+ as the difference between cathodic and

anodic peak found to be 48 mV. This peak may be attributed to reduction of Re^{I} to Re^{0} .[66] Two quasireversible reductions waves were observed at -2.42 and -2.76 V vs. Fc/Fc^{+}. The third reduction wave at -2.76 V vs.Fc/Fc^{+} is one-electron transfer and ascribed to ligand localized reduction.[67] Under an atmosphere of CO_2, the cyclic voltammogram reveals that the first reduction has negatively shifted to -1.46 V vs. Fc/Fc^{+}. The two later reduction had dissappeared. It would appear that the product of the first reduction has reacted with the added CO_2 Figure 2.12.

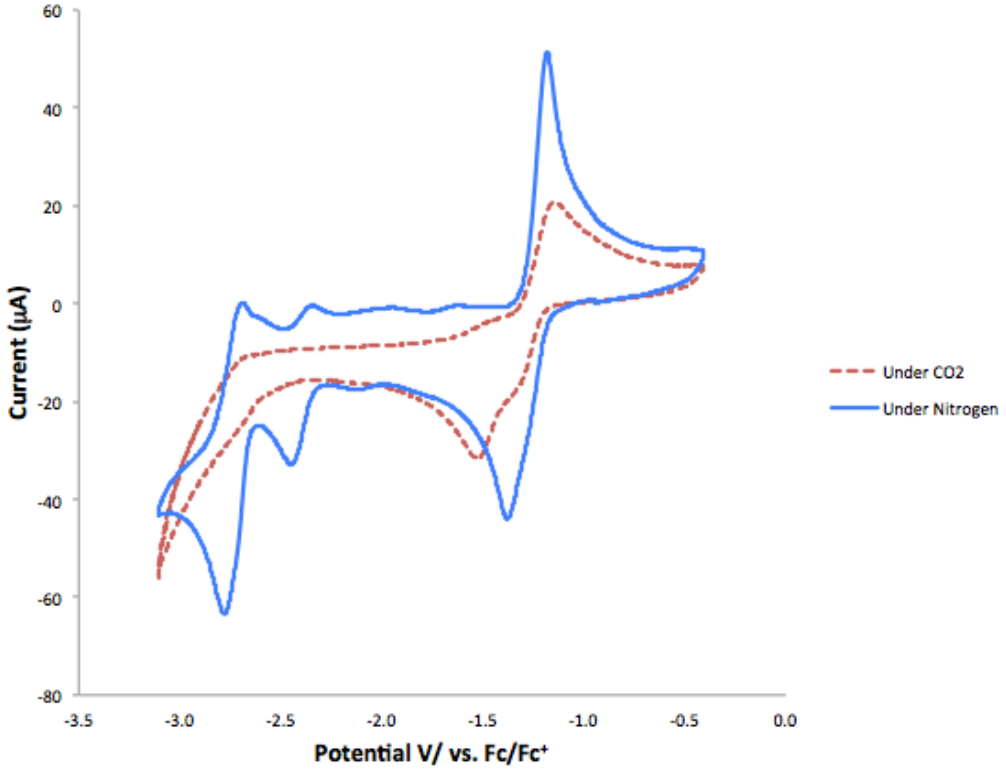

Figure 2.12: Cyclic voltammogram of 0.01 M κ^3-2,6-$\{Me_2C_6H_3N{=}CMe\}_2$ $(NC_5H_3)Re(CO)_2Cl$ (**9**) in dry MeCN, 0.1 M ($TBAPF_6$) under N_2 and CO_2.

Comparing the cyclic voltammogram of κ^3-2,6-{C_6H_5N=CMe}$_2$(NC_5H_3)Re(CO)$_2$Br (**8**) to the previous compound, I found there is no significant changes. Under N_2 atmosphere, the first reversible reduction waves was at -1.38 V vs. Fc/Fc^+ and is attributed to one-electron transfer that could refer to the reduction $Re^1$to $Re^{0.66}$. The different between cathodic and anodic peak found to be for the first redcution is 57 mV. The second reduction wave at -2.8 V vs. Fc/Fc^+, is a also reversible reduction with different between cathodic and anodic 85 mV and this reduction is ascribed to a ligand localized reduction. Under CO_2 atmosphere, similar changes in the reduction behavior were observed as shown for compound **(9)**. The first reduction wave has positively shifted to -1.28 V vs. Fc/Fc^+ with one electron transfer. The second reduction wave had disappeared and that revels that compound **(8)** has reacted with CO_2 under this condition.

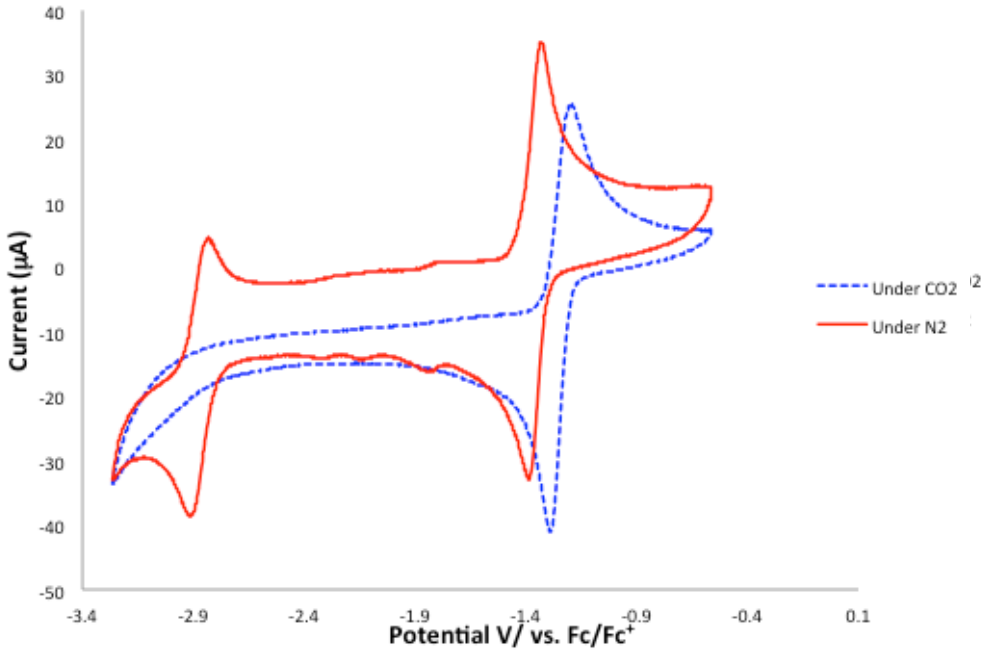

Figure 2.13: Cyclic voltammogram of 0.01 M κ^3-2,6-{C_6H_5N=CMe}$_2$ (NC_5H_3)Re(CO)$_2$Br (**12**) in dry MeCN, 0.1 M (($TBAPF_6$) (a) under N_2 and CO_2.

The last cyclic voltammogram presented is for the reduction behavior of κ^3-2,6-{C_6H_3N=CMe}$_2$(NC_5H_3)Re(CO)$_2$**Br** 8**.** The first reduction wave was a reversible reduction at -1.31 V vs. Fc/Fc^+ with 70 mV as the difference between cathodic and anodic peak and this reduction attributed to one-electron transfer of reduction Re^1 to Re^0. The second irreversible reduction wave was at -2.63 V/ vs. Fc/Fc^+ refers to the ligand localized. Again, similar changes in redox behavior were noticed when the analysis was carried out under an atmosphere of CO_2. The first reduction slightly shifted to -1.37 V vs. Fc/Fc^+ and the second reduction also has disappeared Figure 2.14.

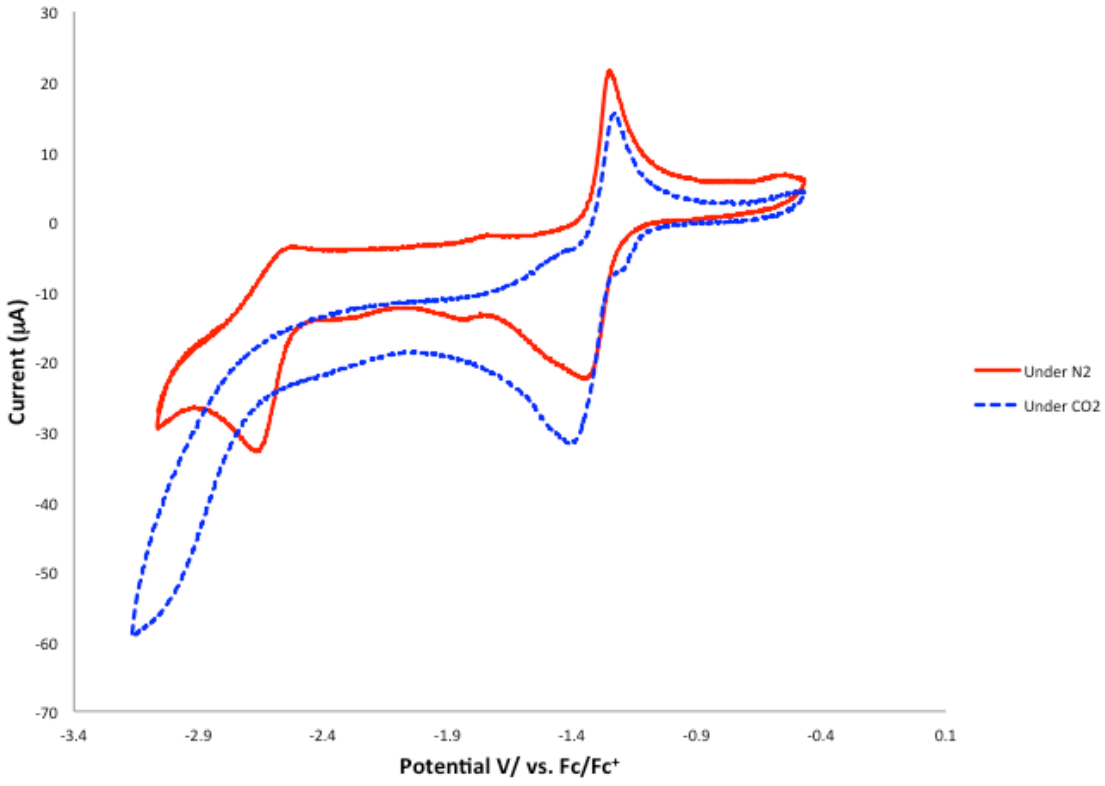

Figure 2.14: Cyclic voltammogram of 0.01 M κ^3-2,6-{C_6H_3N=CMe}$_2$(NC_5H_3)Re(CO)$_2$Br **(8)** in drey MeCN, 0.1 M (($TBAPF_6$) under N_2 and CO_2.

The electrochemical characterization of compounds (**8**, **9**&**12)** appears to indicate that the reduced compounds do react with CO_2 but did not provide indications of electocatalytic behaviour. Examining the ability of tridentate complexes **8, 9** and **12** for the electrocatalytic reduction of CO_2 failed to produce CO. All sample are analysed in both gas chromatography and gas-liquid chromatography to ensure there is no other valuable products may be in the solvent.

2.5 Conclusions

This chapter reported on a family of Re(I) complexes with a unique coordination geometry which adds significantly to authenticated low-valent Re(I) tridentate pincer complexes, and thus addresses a major deficiency in the chemistry of imine-coordinated Re(I) carbonyl chemistry. The efficient solid-state thermolysis synthetic route was demonstrated to be applicable to variation of the ligand framework. A general physical feature for these new pincer complexes are enhanced metal-to-ligand d-π* electronic transitions which were characterized through DFT analysis. The tridentate compounds do not show the ability of photochemically reducing CO_2 to CO as well as bidentate complexes. This was the case with changing light source, solvents and sacrificial reductants. Addition of a small amount of water on the process system has failed too to reduce CO_2 to CO. In addition, the electrocatalytic reductions have failed for reducing CO_2. There are a number of reasons that may explain the failure for the CO_2 reduction with these compounds. One potential reason may refer to the framework of bis-imino

pyridine ligand especially after I found that not only the tridentate complexes have failed to reduce CO_2 but also the bidentate complexes. It seems that the third arm in bis-imino pyridine have affected on both tridentate and bidentate complexes. Moreover, Alberto *et al.* has shown that only the diimine ligand of Re(I) complexes that show fluorescence are catalytic activity for CO_2 reduction. However, the lifetime of bis-imino pyridine of tridentate is very short, less than 0.7 ns, which means that these compounds do not exhibit fluorescence and sequences of that these complexes failed to reduce CO_2 under "Strasbourg condition". From this point, I slightly changed the direction of the thesis to diimine ligand that can enhance the light harvesting ability and the efficiency of the photocatalytic reductions by ligand modifications.

Experimental Section

General Methods. Reactions were performed in a glovebox under a nitrogen atmosphere. Solvents were sparged with nitrogen and then dried by passage through a column of activated alumina using an apparatus purchased from Anhydrous Engineering. Deuterated chloroform and deuterated acetonitrile was dried using activated molecular sieves. Rhenium starting materials were purchased from Strem Chemicals and used as received. All other chemicals were purchased from Aldrich and used without further purification. NMR spectra were run on Bruker Avance 400MHz spectrometers with CD_3CN or $CDCl_3$ as solvent and internal standard. Elemental analyses were performed by Midwest Microlab LLC, Indianapolis IN. Solid state reactions were carried out in a

Lindberg Blue M Mini-Mite Tube Furnace (model TF55035A-1). Infrared spectra were collected using an Agilent Technologies Cary FT-IR spectrometer using a diamond ATR attachment. UV-Vis spectra were collected using a Agilent Technologies Cary 5000 UV-Vis spectrometer.

Computational Methods: The structures of all species were optimized using Gaussian 09[61] employing the B3LYP exchange-correlation (XC) functional with a mixed basis set (LanL2DZ on Re and TZVP on all other atoms). Frequency analysis of all structures was used to confirm the nature of the stationary points. Solvent effects were computed using the integral equation formalism variant of the PCM solvation model within Gaussian 09 for both the ground state and excited state TD-DFT calculations with DMSO as the solvent. The UV-Vis absorption spectra were simulated using the Chemissian software.[60] In these calculations, a pseudo-Voigt band shape was employed with a default average band width at half-height of 2000cm^{-1}. The resultant computed spectra are shown, with comparison to experimental spectra in Figures S11 to S18.

κ^2-2,6-{C_6H_5N=CMe}$_2$(NC_5H_3)Re(CO)$_3$Cl (1)

In a glove box, 100mg (0.319mmol) of ligand **A** and 120mg (0.332mmol) $Re(CO)_5Cl$ were suspended in 50mL of dry toluene. The mixture was stirred with a magnetic stir bar until the solution became a yellow in color. The flask was sealed with a stopper and removed from the glove box. The reaction mixture was heated to reflux under nitrogen for 4 hours. During the first 30 min. the reaction mixture changed color from yellow to a dark/black red. The reaction mixture was cooled to room temperature and allowed to stir overnight to yield an opaque orange reaction mixture with reddish-orange precipitate.

The mixture was stored in a refrigerator for 2 days to allow complete precipitation of a bright red-orange solid which was removed by suction filtration. The solid was washed with diethyl ether then dissolved in chloroform to obtain a bright red solution. Filtration and removal of solvent with a rotary evaporator yielded a yellow precipitate of **1**. Total yield: 120mg (0.194mmol) (60.8%). Crystals were grown for X-ray crystallography from a saturated chloroform solution with hexanes diffusion.

^{1}H NMR (CD_2Cl_2, 400 MHz) δ 8.25(t, J = 7.9 Hz, 1H py), 8.10(d, J = 7.9 Hz, 1H, py), 7.80(d, J = 7.8Hz, 1H, py), 7.55(t, J 7.3Hz, 2H, phenyl), 7.44-7.05 (m, 8H, phenyl), 2.50 (s, 3H, Me), 2.45 (s, 3H, Me). $^{13}C\{^{1}H\}$ NMR (CD_2Cl_2). δ 195.7(CO), 194.9(CO), 185.3(CO), 177.9 (C=N), 163.9(C=N), 163.0, 157.9, 148.5, 147.1, 133.3, 131.3, 129.2, 128.7, 128.3, 128.1, 126.1, 123.9, 122.5, 19.6(CH_3), 18.8(CH_3). FTIR: 2019, 1926, 1900 cm-1 (ν CO). Elemental analysis calcd (%) for $C_{24}H_{19}ClN_3O_3Re$: C, 46.56; H, 3.09; N, 6.79 found C 46.19, H 3.09, N 6.75.

κ^2-2,6-{C_6 H_5N=CMe}$_2$(NC_5H_3)Re(CO)$_3$Br (2)

A similar procedure as for the synthesis of **1** was used with 95mg (0.303mmol) of ligand **A** and 130mg (0.320mmol) of $Re(CO)_5Br$. During the reflux step, the reaction mixture changed from clear yellow to a red solution. After cooling and stirring overnight, an opaque orange-red reaction mixture was obtained. Suction filtration gave a yellow precipitate. The filtrate was kept in a refrigerator for over 3-4 days and filtered to yield additional solid. The combined solids were dissolved in chloroform, filtered and evaporated to obtain a yellow solid. Total yield: 92mg (0.139 mmol), 45.8%). Crystals

were grown for X-ray crystallography from a saturated chloroform solution with hexanes diffusion.

^{1}H NMR (CD_2Cl_2, 400 MHz): δ 8.24 (t, J = 7.7 Hz, 1H, py), 8.10 (dd, J = 8.0, 1.2 Hz, 1H, py), 7.79 (dd, J = 8.5, 1.3Hz, 1H, py), 7.55 (t, J = 8.3 Hz, 2H, phenyl), 7.44-7.06 (m, 8H, phenyl), 2.51(s, 3H, Me), 2.46(s, 3H, Me). $^{13}C\{^{1}H\}$ NMR (CD_2Cl_2). δ 195.3(CO), 194.1(CO), 188.0(CO), 178.5 (C=N), 165.9(C=N), 152.7, 146.3, 139.2, 133.6, 131.2, 131.0, 130.5, 130.0, 128.2, 127.8, 126.2, 123.4, 122.8, 19.6(CH_3), 17.9(CH_3). FTIR: 2017, 1918, 1880 cm-1 (ν CO). Elemental analysis calcd (%) for $C_{24}H_{19}BrN_3O_3Re$•0.5($CHCl_3$) C, 40.69; H, 2.72; N, 5.81, found C 40.34, H 2.65, N 5.70.

κ^2-2,6-{$Me_2C_6H_3N$=CMe}$_2$(NC_5H_3)$Re(CO)_3Cl$ (3)

In a glove box, 150mg (0.41mmol) of ligand **B** and 110mg (0.30mmol) $Re(CO)_5Cl$ were suspended in 50mL of dry toluene. The mixture was stirred with a magnetic stir bar until the solution became a clear yellow color. The flask was sealed with a stopper and removed from the glove box. The reaction mixture was heated to reflux under nitrogen for 4 hours. During the first 30 min. the reaction mixture changed color from yellow to clear red to an opaque orange. The reaction mixture was cooled to room temperature and allowed to stir overnight. The opaque yellow-orange reaction mixture was filtered in air to yield a bright yellow precipitate which was washed three times with diethyl ether. The precipitate was dissolved in chloroform to obtain a bright red solution which was filtered followed by solvent removal using a rotary evaporator to yield a yellow precipitate of **3**. Total yield: 120mg (0.178mmol, 60%).Crystals were grown for X-ray crystallography using a saturated chloroform solution with hexanes diffusion.

^{1}H NMR (CD_2Cl_2, 400 MHz): δ 8.20 (t, J = 7.4 Hz, 1H, py), 8.09 (d, J = 7.7 Hz, 1H, py), 7.85 (d, J = 7.3 Hz, 1H, py), 7.2-6.98 (m, 6H, aromatic), 2.55(s, 3H, Me), 2.46(s, 3H, Me), 2.37(s, 6H, Me), 2.25 (br s, 3H, Me), 2.15 (s, 3H, Me). ^{13}C{^{1}H} NMR (CD_2Cl_2). δ 196.3(CO), 195.1(CO), 186.0(CO), 178.1 (C=N), 163.9(C=N), 157.7, 148.3, 139.2, 133.4, 131.1, 130.9, 130.5, 128.8, 128.4, 128.2, 128.1, 127.7, 126.9, 123.9, 122.8, 22.0(Ar-Me, CH_3), 20.3(Ar-Me, CH_3), 18.7(br, Ar-Me, CH_3), 17.3(CH_3), 16.4(CH_3).). FTIR: 2013, 1916, 1880 cm-1 (ν CO). Elemental analysis calcd (%) for $C_{28}H_{27}ClN_3O_3Re$ C, 49.81; H, 4.03; N, 6.22. found C 49.83, H 4.38, N 6.60.

κ^2-2,6-{$Me_2C_6H_3N$=CMe}$_2$(NC_5H_3)$Re(CO)_3Br$ (4)

A similar procedure was used as for the synthesis of **3** using 150mg (0.278mmol) of ligand **B** and 133mg (0.327 mmol) of $Re(CO)_5Br$ in 50mL of dry toluene. During the reflux step, the reaction mixture changed color from yellow to clear orange, to a dark red. After reflux and stirring overnight, a dull yellow precipitate was isolated by and washing with diethyl ether. The precipitate was dissolved in chloroform to obtain a bright red solution which was filtered followed by solvent removal using a rotary evaporator to yield a yellow precipitate of **4**. Total yield: 144mg (0.200mmol) (72%). Crystals were grown for X-ray crystallography using a saturated 1,2-dichloroethane solution, with cyclohexane diffusion.

^{1}H NMR (CD_2Cl_2) δ 8.25 (t, J = 7.9 Hz, 1H, py), 8.15(d, J = 7.4Hz, 1H, py), 7.87(d, J = 7.5Hz, 1H, py), 7.25-6.98 (m, 6H, aromatic), 2.49(br s, 6H, Me), 2.38(s, 3H, Me), 2.28(br s, 6H, Me), 2.16(s, 3H, Me). ^{13}C{^{1}H} NMR (CD_2Cl_2) δ 195.7(CO), 194.9(CO), 185.3(CO), 177.9 (C=N), 163.9(C=N), 163.0, 157.9, 148.5, 147.1, 139.1, 131.3, 131.1,

130.9, 129.2, 128.7, 128.4, 128.1, 127.8, 126.1, 123.9, 122.5, 21.1(Ar-Me, CH_3), 18.7(Ar-Me, CH_3), 18.0(CH_3), 16.5(CH_3). FTIR: 2007, 1927, 1868 cm-1 (ν CO). Elemental analysis calcd (%) for $C_{28}H_{27}BrN_3O_3Re$ C, 46.73; H, 3.78; N, 5.84. Found C 46.41, H 3.80, N 5.49.

κ^2-2,6-{^{i}Pr$_2$C$_6$H$_3$N=CMe}$_2$(NC$_5$H$_3$)Re(CO)$_3$Cl (5)

In a glove box, 38 mg (0.0789 mmol) of ligand **C** and 38 mg (0.11mmol) $Re(CO)_5Cl$ were suspended in 50mL of dry toluene. The mixture was stirred with a magnetic stir bar until the solution became a cloudy yellow color. The flask was sealed with a stopper and removed from the glove box. The reaction mixture was heated to reflux under nitrogen for 4 hours. During the first 15 min. the reaction mixture changed color from yellow to red. The reaction mixture was cooled to room temperature and allowed to stir overnight. The solvent was removed with a rotary evaporator to yield a dark, brown solid Total yield: 61mg (0.0775mmol) of **5** (98.2%). Crystals were grown for X-ray crystallography using a saturated chloroform solution with hexanes diffusion.

^{1}H NMR (CD_2Cl_2) δ 8.29(t, J = 7.5Hz, 1H, py), 8.15(d, J = 8.0 Hz, 1H, py), 7.82(d, J = 7.7Hz, 1H py), 7.39-7.11(m, 6H, aromatic), 3.65(sept, J = 6.9Hz, 1H, CH) 3.17(sept, J = 6.3Hz, 1H, CH), 2.97-2.85 (overlapping sept, J = 6.9Hz 2H, CH), 2.51 (s, 3H, Me), 2.42(s, 3H, Me), 1.38-1.05 (overlapping doublets, 24H, $CH(CH_3)$). $^{13}C\{^1H\}$ NMR (CD_2Cl_2) δ 199.5 (CO), 196.2 (CO), 195.7 (CO), 187.8 (C=N), 176.6 (C=N), 160.7, 156.5, 144.4, 140.4, 140.3, 138.7, 128.1, 128.0, 125.0, 124.8, 124.6, 30.9(iPr-CH), 28.0 (iPr-CH), 27.6 (br, iPr-CH_3), 24.9(br, iPr-CH_3), 24.5(br, iPr-CH_3), 24.2(br, iPr-CH_3), 24.1

(CH_3), 20.4(CH_3). FTIR: 2017, 1916, 1890 cm-1 (ν CO). Elemental analysis calcd (%) for $C_{36}H_{43}ClN_3O_3Re$ C 54.91, H 5.50, N 5.34, found C 54.56, H 5.90, N 5.60.

κ^2-2,6-{^{i}Pr$_2$C$_6$H$_3$N=CMe}$_2$(NC$_5$H$_3$)Re(CO)$_3$Br (6)

A similar procedure was used as for the synthesis of **5** using 116mg (0.241mmol) of ligand **C** and 110mg (0.271 mmol) of $Re(CO)_5Br$ in 50mL of dry toluene. During the reflux step, the reaction mixture changed color from yellow to dark red. After reflux and stirring overnight, a dull yellow precipitate was isolated by filtration and washing with diethyl ether. The precipitate was dissolved in chloroform to obtain a bright red solution which was filtered followed by solvent removal using a rotary evaporator to yield a yellow precipitate of **6**. Total yield: 185mg (0.222 mmol) (92%). Crystals are grown for X-ray crystallography using a saturated solution in chloroform, with hexanes diffusion.

^{1}H NMR (CD_2Cl_2) δ 8.28 (t, J = 7.7Hz, 1H, py), 8.16(dd, J = 8.0, 1.4 Hz, 1H, py), 7.83(dd, J = 7.8, 1.3Hz, 1H, py), 7.39-7.33 (m, 3H, aromatic) 7.2-7.12(m, 3H, aromatic), 3.65(sept, J = 6.8 Hz, 2H, CH), 3.17(sept, J = 7.0 Hz, 1H, CH), 2.94 (sept, J = 7.0 Hz, 1H, CH), 2.88 (sept, J = 6.8 Hz, 1H, CH), 2.53 (s, 3H, Me), 2.44(s, 3H, Me), 1.36 (d, J = 7.0 Hz, 3H, $CH(CH_3)_2$), 1.34 (d, J = 6.8 Hz, 3H, $CH(CH_3)_2$), 1.30 (d, J = 7.0 Hz, 3H, $CH(CH_3)_2$), 1.15 (d, J = 7.0 Hz, 3H, $CH(CH_3)_2$), 1.10 (d, J = 6.9 Hz, 3H, $CH(CH_3)_2$), 1.08-1.03(overlapping d, 9H, $CH(CH_3)_2$). $^{13}C\{^1H\}$ NMR (CD_2Cl_2) δ 196.3(CO), 188.4(CO), 178.6(CO), 165.7(C=N), 163.3(C=N), 157.2, 148.1, 147.6, 139.3, 133.9, 132.2, 131.5, 130.9, 129.3, 128.8, 127.9, 126.7, 30.4(iPr-CH), 28.0 (iPr-CH), 27.8 (iPr-

CH), 23.2(br, iPr-CH_3), 22.8(br, iPr-CH_3), 17.8(br, iPr-CH_3), 17.2(iPr-CH_3), 17.0(CH_3), 16.8(CH_3).). FTIR: 2020, 1925, 1899 cm-1 (ν CO). Elemental analysis calcd (%) for $C_{36}H_{43}BrN_3O_3Re$•0.5($CHCl_3$) C 49.17, H 4.92, N 4.71, Found C 48.77, H 5.24, N 4.62.

κ^3-2,6-{C_6H_5N=CMe}$_2$(NC_5H_3)Re(CO)$_2$Cl (7)

A 50mg (0.0807mmol) sample of **1** was placed in a ceramic crucible and introduced into a tube furnace at 200 to 220ºC under flow of nitrogen for 1 hour. The bright orange starting material became an opaque black powder during this time span. Total yield: 38mg (0.06429mmol) (79.6%). Crystals are grown for X-ray crystallography using a saturated solution in chloroform, with hexanes diffusion.

^{1}H NMR (CD_2Cl_2) δ 7.64(t, J = 8.0 Hz, 1H, py), 7.50(d, J = 8.0Hz, 2H, py); 7.46-7.38 (m, 4H, aromatic); 7.22 (t, J= 7.4 Hz, 2H, aromatic), 7.17-7.02 (br s, 4H, aromatic), 2.24 (s, Me, 6H).

^{13}C NMR (CD_2Cl_2) δ 215.7 (CO), 206.4 (CO), 171.2(C=N), 165.0, 159.7, 153.2, 138.3, 129.6, 126.7, 121.7, 17.3 (CH_3). FTIR: 1889, 1830 (νCO). Elemental analysis calcd (%) for $C_{23}H_{19}ClN_3O_2Re$•0.5($CHCl_3$) C 43.37, H 3.02, N 6.46, found C 43.08, H 3.29, N 6.38.

κ^3-2,6-{C_6H_5N=CMe}$_2$(NC_5H_3)Re(CO)$_2$Br (8)

A 55mg (0.0829 mmol) sample of solid **2** was placed in a ceramic crucible and introduced into a tube furnace at 200 to 220ºC under flow of nitrogen for 1 hour. The bright orange starting material became an opaque black powder during this time span.

Total yield: 49mg (0.0771 mmol) of **2** (93.0%). Crystals are grown for X-ray crystallography using a saturated solution in chloroform, with hexanes diffusion.

^{1}H NMR (CD_2Cl_2) δ .7.63(t, J=8.0 Hz, 1H, py), 7.53(d, J=8.0 Hz, 2H, py), 7.42 (t, J=8.4 Hz, 4H, aromatic), 7.22(t, J=7.6 Hz, 2H, aromatic) 7.10 (br s, 4H, aromatic) 2.43(s, 6H, CH_3).

^{13}C{^{1}H} NMR (CD_2Cl_2) δ 215.0 (CO), 206.0 (CO), 171.1 (C=N), 161.6, 159.8, 153.2, 138.2, 129.1, 126.6, 121.5, 17.3 (CH_3). FTIR: 1886, 1823 cm-1 (ν CO). Elemental analysis calcd (%) for $C_{23}H_{19}BrN_3O_2Re$ C, 43.47; H, 3.01; N, 6.61.found C 43.86, H 3.35, N 6.28.

κ^3-2,6-{$Me_2C_6H_3N$=CMe}$_2$(NC_5H_3)Re(CO)$_2$Cl (9)

A small ceramic boat was charged with 60mg (0.0889mmol) of **3** which was introduced into a tube furnace. The sample was heated to 200- 220ºC under flowing nitrogen for 1 hour. The initially yellow solid turned to an opaque black powder during this time span. Total yield: 55mg (0.0850mmol) of **11** (95.6%). Crystals were grown for X-ray crystallography using a saturated chloroform solution with hexanes diffusion.

^{1}H NMR (CD_2Cl_2) δ 7.61 (t, J=6.4 Hz, 1H), 7.48(d, J=6.4 Hz 2H), 7.1 (t, J=6.3 Hz 4H), 7.03 (m, 2H, aromatic), 2.35 (s, 6H), 2.25(s, 6H), 2.19(s, 6H). 13C{1H} NMR (CD_2Cl_2) δ 221.8 (CO), 172.3 (CO), 170.4 (C=N), 159.5, 150.4, 138.8, 130.5, 129.1, 128.3, 127.6, 126.3, 122.0, 19.4 (CH_3), 17.7(CH_3), 17.1(CH_3). FTIR: 1887, 1835 cm-1 (ν CO). Elemental analysis calcd (%) for $C_{27}H_{27}ClN_3O_2Re$ •0.5($CHCl_3$) C, 46.73; H, 3.92; N, 5.94, found C 46.46, H 4.24, N 5.64

κ^3-2,6-{$Me_2C_6H_3N$=CMe}$_2$(NC_5H_3)Re(CO)$_2$Br (10)

A small ceramic boat was charged with 100mg (0.139 mmol) of **4** which was introduced into a tube furnace. The sample was heated to 200- 220ºC under flowing nitrogen for 1 hour. The initially yellow solid turned to an opaque black powder during this time span. Total yield: 89mg (0.0850mmol) of **12** (92.6%) Crystals were grown for X-ray crystallography using a saturated chloroform solution with hexanes diffusion.

^{1}H NMR (CD_2Cl_2) δ 7.63 (t, J=8 Hz, 1H), 7.56(d, J=8 Hz 2H), 7.09 (t, J=6.5 Hz 4H), 7.03 (m, 2H, aromatic), 2.35 (s, 6H), 2.18(s, 6H), 2.13(s, 6H). ^{13}C{^{1}H}NMR (CD_2Cl_2) δ 221.6 (CO), 172.8 (CO), 167.2 (C=N), 160.5, 151.4, 138.7, 133.5, 130.8, 128.3, 127.4, 126.3, 123.0, 19.3 (CH_3), 17.2(CH_3), 17.0(CH_3). FTIR: 1890, 1840 cm-1 (ν CO). Elemental analysis calcd (%) for $C_{27}H_{27}BrN_3O_2Re$ •0.5($CHCl_3$) C, 43.96; H, 3.69; N, 5.59, found C 43.99, H 3.91, N 5.73.

κ^3-2,6-{^{i}$Pr_2C_6H_3N$=CMe}$_2$(NC_5H_3)Re(CO)$_2$Cl (11)

A 82mg (0.104mmol) sample of **5**, in a ceramic crucible was placed in a tube furnace at 200 to 220ºC under flow of nitrogen for 1 hour. During this period, the brown starting material converted into an opaque black powder. Total yield: 72mg (0.0948mmol) of **13** (91%) Crystals are grown for X-ray crystallography using a saturated solution in chloroform, with hexanes diffusion.

^{1}H NMR (CD_2Cl_2) δ 7.65 (t, J=7.7 Hz, 1H, py), 7.55 (d, J= 7.8 Hz, 2H, py), 7.23(m, 6H, aromatic), 3.91(sept, J=6.7 Hz, 2H, CH), 2.97(sept, J=6.4 Hz, 2H, CH), 2.32(s, 6H, Me), 1.27(d, J=6.7 Hz, 6H, CH(CH=)$_2$), 1.24(d, J=6.4, 6H, CH(CH_3)$_2$), 1.13 (doublet, J=6.7 Hz, 6H, CH(CH_3)$_2$), 0.99 (doublet, J=6.7 Hz, 6H, CH(CH_3)$_2$). ^{13}C{^{1}H} NMR

(CD_2Cl_2) δ 199.5 (CO), 178.8 (CO), 176.6 (C=N), 160.7, 156.6, 144.4, 140.4, 138.8, 128.2, 125.1 124.8, 30.9(iPr-CH), 28.0 (iPr-CH), 24.9 (CH_3), 24.6 (CH_3), 24,3 (CH_3), 24.1 (CH_3), 20.4 (CH_3) . (only 8 aromatic signals, rather than the expected 9 were resolved in this spectrum). FTIR: 1892, 1827 cm-1 (ν CO). Elemental analysis calcd (%) for $C_{35}H_{43}ClN_3O_2Re$•0.5($CHCl_3$) C 46.72, H 4.78, N 4.48, found C 46.45, H 5.08, N 4.71.

κ^3-2,6-{^{i}Pr$_2$C$_6$H$_3$N=CMe}$_2$(NC$_5$H$_3$)Re(CO)$_2$Br (12)

A 70mg (0.0842 mmol) sample of solid **6**, in a ceramic crucible was placed in a tube furnace at 200 to 220ºC under flow of nitrogen for 1 hour. During this period, the dark brown starting material converted into an opaque black powder. Total yield: 56mg (0.0697mmol) of **14** (82.7%) Crystals are grown for X-ray crystallography using a saturated solution in chloroform, with hexanes diffusion.

^{1}H NMR (CD_2Cl_2) δ 7.65 (t, J=6.8 Hz, 1H, py), 7.56 (d, J= 6.8 Hz, 2H, py), 7.28(m, 6H, aromatic), 3.81(sept, J=6.7 Hz, 2H, CH), 2.97(sept, J=6.4 Hz, 2H, CH), 2.32(s, 6H, Me), 1.28(doublet, J=6.7 Hz, 6H, $CH(CH_3)_2$), 1.24(d, J=6.4 Hz, 6H, $CH(CH_3)_2$), 1.13 (d, J=6.7 Hz, 6H, $CH(CH_3)_2$), 0.99 (d, J=6.4 Hz, 6H, $CH(CH_3)_2$). ^{13}C{^{1}H} NMR (CD_2Cl_2) δ 200.6 (CO), 178.4 (CO), 177.2 (C=N), 160.6, 157.0, 145.0, 141.0, 138.2, 127.9, 125.2 125.0, 31.0(iPr-CH), 28.6(iPr-CH) 25.1 (CH_3), 24.8 (CH_3), 24.4 (CH_3), 24.1 (CH_3), 20.4 (CH_3). (only 8 aromatic signals, rather than the expected 9 were resolved in this spectrum). FTIR: 1890, 1860 cm-1 (ν CO). Elemental analysis calcd (%) for $C_{35}H_{43}BrN_3O_2Re$•0.5($CHCl_3$) C, 49.38; H, 5.08; N,4.87, found C 49.10, H 5.09, N 4.57.

X-ray Crystallography: The X-ray data were collected at 200(2) K on Bruker Smart and Kappa Apex II CCD diffractometers with graphite-monochromatised Mo-Kα

radiation (wavelength 0.71073 Å). Raw data collection and processing were performed with APEX II software package from BRUKER AXS.[62] Semi-empirical absorption corrections based on equivalent reflections were applied.[63] Systematic absences in the diffraction data-set and unit-cell parameters were consistent with triclinic **P-1** (№2) for compounds **1** (dr100)**, 2** (dr108), **3** (dr101_5), **4** (dr110), monoclinic $\mathbf{P}2_1/c$ (№14) for compounds **5** (dr137a), **7** (dr104), orthorhombic $\mathbf{P}2_12_12_1$ (№19) for compounds **9** (dr102) and **10** (d105). The structures were solved by direct methods, completed with difference Fourier synthesis, and refined with full-matrix least-squares procedures based on F^2.

On the final model refinement stage for compound **5** thermal motion parameters for coordinated CO (-C(33)=O(3)) and Cl (Cl(2)) moieties as well as presence of unusually strong residual electron density peaks in one of the compound molecules suggested a positional CO / Cl disorder not related by symmetry. Disorder was successfully modeled with refined occupation ratio at one position CO / Cl = 70%:30%. Disorder of the second position was inversed in such way that overall occupancy summed up to one full CO and one full Cl ligands in the first coordination sphere of Re metal center. Set of geometrical (SADI) and thermal motion (SIMU, DELU) restrains were applied to achieve acceptable molecular fragment geometries and thermal motion parameter values.

For all the compounds hydrogen atoms positions were initially assigned from the residual electron density peaks coordinates. However, after initial placement all hydrogen atoms were treated as idealized contributions during the refinement. All scattering factors are contained in several versions of the SHELXTL program library, with the latest version used being v.6.12.[64]

Photochemical Experiments:

The photochemical of CO_2 reduction was done in a quartz cell that sealed with silicon-teflon septum after mix 15 ml of DMF/TEOA volume ratio is 4:1 with 0.01 M of bidentate and tridentate compounds then The solution was bubbled with CO_2 for 20 minutes and sealed with a silicon- teflon septum at room temperature. A mercury lamp (500 W) was used as a source of light and after 24h of irradiation the gas chromatography was used to analyze the reduction products.

Electrochemical Experiments:

In typical run of dry MeCN, 0.01 M of the catalyst, 0.1 M tetrabutylammonium hexafluorophosphate ($TBAPF_6$) as the supporting electrolyte, with a glassy carbon as working electrode, a platinum wire as a counter electrode, a Ag/AgCl as reference and with Fc added in last step as an internal references.

REFERENCES

1 Potgieter, K.; Mayer, P.; Gerber, T.; Yumata, N.; Hosten, E.; Booysen, I.; Betz, R.; Ismail, M.; Van Brecht, B. *Polyhedron*, **2013**, *49*, 67–73.

2 Walters, K. A.; Kim, Y.; Hupp, J. T. *Inorg. Chem.* **2002**, *41*, 2909–2919.

3 Ruiz, G.; Wolcan, E. *J. Photochem. Photobiol.* **1996**, *101*, 119.

4 Lo, K. K.-W.; Louie, M.-W.; Zhang, K. Y. *Coord. Chem. Rev.* **2010**, *254*, 2603–2622.

5 Striplin, D. R.; Crosby, G. A. *Coord. Chem. Rev.* **2001**, *211*, 163–175.

6 Giordano, P. J.; Wrighton, M. S. *J. Am. Chem. Soc.* **1979**, *101*, 2888–2897.

7 Giordano, P. J.; Fredricks, S. M.; Wrighton, M. S.; Morse, D. L. *J. Am. Chem. Soc.* **1978**, *100*, 2257–2259.

8 Wrighton, M.; Morse, D. L. *J. Am. Chem. Soc.* **1974**, *96*, 998–1003.

9 Luong, J. C.; Nadjo, L.; Wrighton, M. S. *J. Am. Chem. Soc.* **1978**, *100*, 5790–5795.

10 Gamelin, D. R.; George, M. W.; Glyn, P.; Grevels, F.; Johnson, F. P. A.; W. Klotzbucher, W.; S. L. Morrison, S. L.; G. Russell, G.; K. Schaffner, K.; J. J. Turner, J. J. *Inorg. Chem.* **1994**, *33*, 3246–3250.

11 Marti, A. A.; Mezei, G.; Maldonado, L.; Paralitici, G.; Raptis, R. G.; Colon, J. L. *Eur. J. Inorg. Chem.* **2005**, 118–124.

12 Coogan, M. P.; Fernández-Moreira, V.; Kariuki, B. M. .; Pope, S. J. A.; Thorp-Greenwood, F. L. *Angew. Chem. Int. Ed. Engl.* **2009**, *48*, 4965–4968.

13 Granifo, J.; Bird, S. J.; Orrell, K. G.; Osborne, A. G.; Šik, V. *Inorganica Chim. Acta*. **1999**, *295*, 56–63.

14 Orrell, K. G.; Osborne, A. G.; Sik, V.; da Silva, M. W.; Hursthouse, M. B.; Hibbs, D. E.; Malik, K. M. A.; Vassilev, N. G. *J. Organomet. Chem.* **1997**, *538*, 171–183.

15 Abel, E. W.; Dimitrov, V. S.; Long, N. J.; Orrell, K. G.; Osborne, A. G.;

Hursthousec, M. P, M. B.; Mazid, M. A. *J. Chem. Soc. Dalton Trans.,* **1993**, 597–603.

16 Dudle, B.; Rajesh, K.; Blacque, O.; Berke, H. *J. Am. Chem. Soc.,* **2011**, *133*, 8168–78.

17 Jain, K. R.; Herrmann, W. A.; Kühn, F. E. *Coord. Chem. Rev.,* **2008**, *252*, 556–568.

18 Kuninobu, Y.; Takai, K. *Chem. Rev.,* **2011**, *111*, 1938–1953.

19 Bartholomä, M.; Valliant, J.; Maresca, K. P., Babich, J.; Zubieta, J. *Chem. Commun.*, **2009,** *7345*, 493–512.

20 Schibli, R.; Schubiger, P. A. *Eur. J. Nucl. Med. Mol. Imaging*, **2002**, *29*, 1529–42.

21 Gong, X.; Ng, P. K.; Chan, W. K. *Adv. Mater.*, **1998**, *10*, 1337–1340.

22 Yu, T. ; Tsang, D. P. K.; Au, V. K. M.; Lam, W. H.; Chan, M. Y.; Yam, V. W. W. *Chem. Eur. J.*, **2013**, *19*, 13418–13427.

23 Lin, T.-P.; Chen, C.-Y.; Wen, Y.-S.; Sun, S.-S. *Inorg. Chem.*, **2007**, *46*, 9201–12.

24 Slone, R. V.; Yoon, D. I.; Calhoun, R. M.; Hupp, J. T. *J. Am. Chem. Soc.*, **1995**, *117*, 11813–11814.

25 Beer, P. D.; Timoshenko, V.; Maestri, M.; Passaniti, P.; Balzani, V. *Chem. Commun.*, **1999**, 1755–1756.

26 Beer, P. D.; Hayes, E. J. *Coord. Chem. Rev.*, **2003**, *240*, 167–189.

27 Amoroso, A. J.; Arthur, R. J.; Coogan, M. P.; Court, J. B.; Fernández-Moreira, V.; Hayes, A. J.; Lloyd, D.; Millet, C.; Pope, S. J. A. *New J. Chem.*, **2008**, *32*, 1097.

28 Amoroso, A. J.; Coogan, M. P.; Dunne, J. E.; Fernández-Moreira, V.; Hess, J. B.; Hayes, A. J.; Lloyd, D.; Millet, C.; Pope, S. J. A.; Williams, C. *Chem. Commun. (Camb).*, **2007**, 3066–8.

29 Fernández-Moreira, V.; Marzo, I.; Gimeno, M. C.. *Chem. Sci.*, **2014**, *3*, 4434–4446.

30 Bertrand, H. C.; Clède, S.; Guillot, R.; Lambert, F.; Policar, C. *Inorg. Chem.*, **2014**, *53,* 6204–6223.

31 Clède, S.; Policar, C. *Chem. Eur. J.*, 2015, *21*, 942–958.

32 Hawecker, J.; Lehn, J.; Ziessel, R. *Helv. Chim. Acta*, **1986**, *69*, 1990–2012.

33 Hawecker, J.; Lehn, J.; Ziessel, R. *J. Chem. Soc. Chem. Commun.*, **1983**, 536–538.

34 Takeda, H.; Ishitani, O. *Coord. Chem. Rev.*, **2010**, *254*, 346–354.

35 Christensen, P.; Hamnett, A.; Muir, S. A. V. G.; Timneyb, J. A.; Section, S.; College, N. T.; Ne, W. *J. Chem. Soc. Dalt. Trans.*, **1992**, 1455–1463.

36 Sullivan, B. P.; Bolinger, C. M.; Conrad, D.; Vining, W. J.; Meyer, T. J. *J. Chem. Soc. Chem. Commun.*, **1985**, 1414–1416.

37 Vollmer, M. V.; Machan, C. W.; Clark, M. L.; Antholine, W. E.; Agarwal, J.; III, H. F. S.; Kubiak, P.; Walensky, J. R. *Organometallics*, **2015**, *34*, 3–12.

38 Caulton, K. G. *Eur. J. Inorg. Chem.*, **2012**, 435–443.

39 Lyaskovskyy, V.; De Bruin, B. *ACS Catal.*, **2012**, *2*, 270–279.

40 Jurca, T.; Chen, W.-C.; Michel, S.; Korobkov, I.; Ong, T.-G.; Richeson, D.S

Chem. Eur. J., **2013**, *19*, 4278–4286.

41 Juris, A.; Campagna, S.; Bidd, I.; Lehn, J.-M.; Ziessel, R. *Inorg. Chem.*, **1988**, 4007–4011.

42 Black, D. R.; Hightower, S. E. *Inorg. Chem. Commun.*, **2012**, *24*, 16–19.

43 Frenzel, B. A.; Schumaker, J. E.; Black, D. R.; Hightower, S. E. *Dalton Trans.*, **2013**, *42,* 12440–51.

44 Laramée-Milette, B.; Lachance-Brais, C.;Hanan, G. S. *Dalton Trans.*, **2015**, *44,* 41–45.

45 Ge, Q.; Corkery, T. C.; Humphrey, M. G.; Samoc, M.; Hor, T. S. A. *Dalton Trans.*, **2009,** *6*, 6192–6200.

46 Anderson, P. A.; Keene, F. R.; Horn, E.; Tiekink, E. R. T. *Appl. Organomet. Chem.*, **1990**, *4*, 523–533.

47 Kurz, P.; Probst, B.; Spingler, B.; Alberto, R. *Eur. J. Inorg. Chem.*, **2006**, 2966–2974.

48 Buckingham, D. A.; Dwyer, F. P.; Goodwin, H. A.; Sargeson, A. M. *Aust J Chem*, 1**964**, *17*, 325–336.

49 Buckingham, D. A.; Dwyer, F. P.; Goodwin, H. A.; Sargeson, A. M. *Aust J Chem*, **1964**, *17*, 315–324.

50 Jurca, T.; Chen, W.-C.; Michel, S.; Korobkov, I.; Ong, T.-G.; Richeson, D.S .*Chem. Eur. J.*, **2013**, *19,* 4278–4286.

51 Yi, X.; Zhao, J.; Sun, J.; Guo, S.; Zhang, H. *Dalton Trans.*, **2013**, 2062–2074.

52 Yi, X.; Zhao, J.; Wu, W.; Huang, D.; Ji, S.; Sun, J. *Dalton Trans.*, **2012**, 8931–8940.

53 Li, H.; Wu, J.; Zhou, X.; Kang, L.; Li, D.; Sui, Y.; Zhou, Y.; Zheng, Y.; Zuo, J.; You, X. *Dalton Trans.*, **2009**, 10563–10569.

54 Becke, A. D. *J. Chem. Phys.*, **1993**, *98*, 5648.

55 Lee, C.; Yang, W.; Parr, R. G. *Phys. Rev. B*, **1988**, *37*, 785.

56 Tomasi, J.; Mennucci, B.; Cammi, R. *Chem. Rev.*, **2005**, *105,* 2999–3093.

57 Scalmani, G.; Frisch, M. J.; Mennucci, B.; Tomasi, J.; Cammi, R.; Barone, V. *J. Chem. Phys.*, **2006,** *124,* 94107.

58 Hay, P. J.; Wadt, W. R. *J. Chem. Phys.*, **1985**, *82*, 299.

59 Schäfer, A.; Huber, C.; Ahlrichs, R. *J. Chem. Phys.*, **1994**, *100,* 5829.

60 Skripnikov, L. Chemissian, a computer program to analyze and visualize quantum-chemical calculations, **2012**

61 Frisch, M. J.; Trucks, G. W.; Schlegel, H. B.; Scuseria, G. E.; Robb, M. A.; Cheeseman, J. R.; Scalmani, G.; Barone, V.; Mennucci, B.; Petersson, G. A.; Nakatsuji, H.; Caricato, M.; Li, X.; Hratchian, H. P.; Izmaylov, A. F.; Bloino, J.; Zheng, G.; Sonnenb, D. J. Gaussian 09, Revision A.02.

62 APEX Software Suite v.2010; Bruker AXS: Madison, WI, 2005.

63 Blessing, B. Y. R. H. . *Acta Crystallogr. Sect. A*, **1995**, 33–38.

64 Sheldrick, G. M. *Acta Crystallogr. Sect. A*, **2008**, 112–122.

65 Paolucci, F.; Marcaccio, M.; Paradisi, C.; Roffia, S.; Bignozzi, C. A.; Amatore, C.

J. Phys. Chem. B **1998**, *102* (24), 4759–4769.

66 Chiericato, G.; Arana, C.; Casado, C.; Cuadrado, I.; Abruña, H. *Inorganica Chimica Acta* **2000**, *300-302*, 32–42.

Chapter 3

New Metal/Ligand Arrays for CO_2 Reduction: Re(I) and Mn(I) Complexes of 4,5-diazafluorene-9-one

3.1 Introduction

In the previous chapter, our investigation of new elusive pincer geometries of Re^I produced compounds with increased light absorption but the system failed to photo- or electrochemically reduce CO_2 to CO under "Strasbourg Conditions". The reasons for the failure of the κ^3-bis(imino)pyridine framework to provide a functioning catalyst are not completely clear. It is generally agreed that an efficient catalyst for CO_2 reduction must overcome the overpotential of transferring a single electron to CO_2 to form the bent radical molecule $CO_2^{\cdot -}$ and that may be addressed through proton-coupled, multi-electron conversion. Moreover, α-diimine complexes of Re^I have shown a unique ability and selectivity to reduce CO_2 to CO comparing with other catalyst.[1-7] With these general features in mind, I present an investigation on the application of a diimine ligand that has not been previously applied to this chemistry and which possessed a functional group that could provide an avenue for ligand modification.

There are number of published manuscripts on modified diimine supported complexes of Re(I) and the unique feature in this chapter is that I selected a diimine framework that has the ability to be more easily modified. This may allow direct attachment/linkage of a photosensitizer to the metal-ligand complex and lead to enhanced absorbance of photons by the catalyst species. Such a modification converts a monometallic catalyst from a Type II catalyst (see Introduction) to a supramolecular reduction system. I focused here

on 4,5-diazafluoren-9-one, as an α-diimine ligand that can be modified through the ketone function by reacting firstly with an amine ligand and then a light-harvesting compound. To begin, I focused in this chapter on studying the ability of 4,5-diazafluoren-9-one compounds of rhenium and manganese for CO_2 reduction before converting to Supramolecular complexes.

Recently, Re[8-16] and Mn[17-29] bipyridine (bipy) complexes have received significant interest for CO_2 reduction. In Chapter 1 of this thesis, the desirability of replacing Re complexes with Mn complexes was justified. Basically, manganese is more abundant in the Earth's crust than rhenium which means a lower cost. Also in electrocatalytic reduction of CO_2, Mn catalysts have lower potential than Re catalysts and that means less energy is needed to drive the reaction. However, it is important to realize that for photochemical reduction, Mn complexes require a photosensitizer such as tris(bipyridine)ruthenium(II) chloride to activate the catalyst for CO_2 reduction.

3.2. Synthesis of Ligand and Catalysts.

4,5-Diazafluoren-9-one is a rigid planar molecule and is displayed in Scheme 3.1. This compound is an α-diimine with two nitrogen atoms that can coordinate in a bidentate fashion to a metal to form the catalyst. The presence of the ketone function was envisioned to provide a site which can be used to connect this ligand, through a bridge to a photosensitizer and increase the efficiency and the selectivity of CO_2 reduction. The synthesis of this ligand is illustrated in Scheme 3.1 and proceeds with a low yield of 37%. After chromatographic purification, the diazafluorenone was employed in a direct reaction with $M(CO)_5X$, (M= Re^I or Mn^I and X= Cl^- or Br^-) to form the potential catalysts $M(CO)_3LX$ with a good yield 85% to 90% (see Scheme 3.2). This approach was used to

prepare three catalysts $Re(CO)_3LCl$ **2**, $Re(CO)_3LBr$ **3**, and $Mn(CO)_3LBr$ **4** (L=4,5-diazafluoren-9-one).

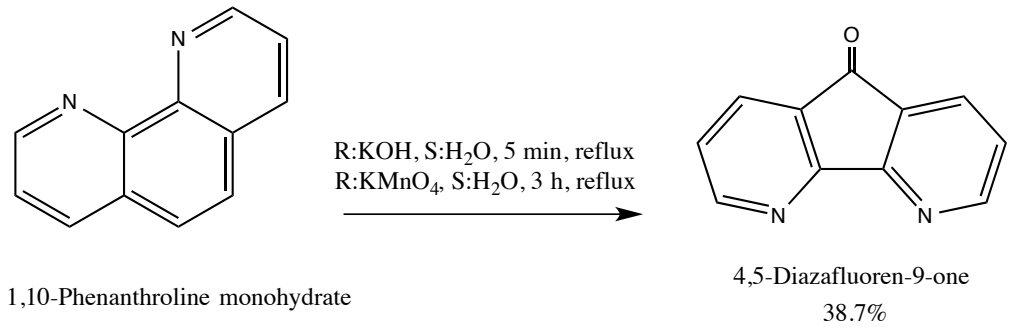

Scheme 3.1: Synthesis of the ligand

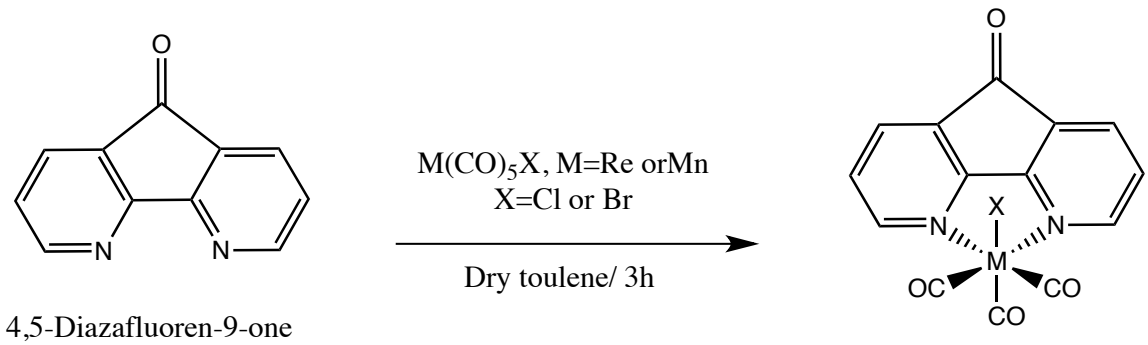

Scheme 3.2: Synthesis of the catalysts **2**, **3** and **4**

3.3 Characterization

Full characterization was performed, including ^{1}H and ^{13}C Nuclear Magnetic Resonance (NMR) analysis, UV-Vis and IR spectroscopy as well as the X-ray crystallography.

3.3.1 NMR analysis

The ^{1}H and ^{13}C NMR spectra of the ligand and the complexes **2**, **3** and **4** were

measured on a on a Bruker AVANCE 400 MHz spectrometer in deuterated dichloromethane (CD_2Cl_2). Detailed peak analysis comparing the complexes **2**, **3** and **4** show a great similarity in aromatic region due the similarity of catalysts structures and are shown in Figure 3.1.

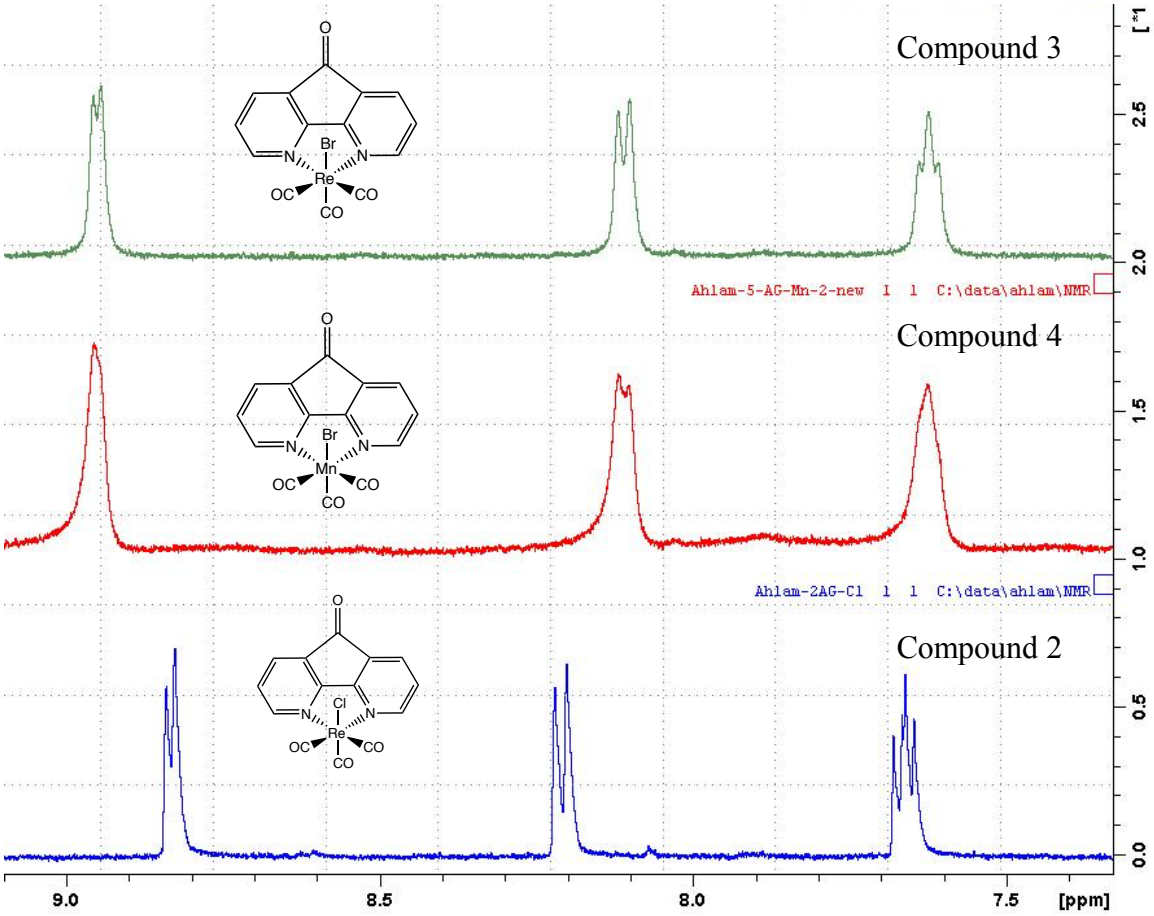

Figure 3.1: The similarity of ^{1}H NMR shift peaks between the catalyst compounds.

3.3.2 Infrared Spectroscopy

The three complexes (**2**, **3** and **4)** were confirmed by using Fourier Transforming Infrared (FTIR) Spectroscopy carried out on the Agilent Cary 630 FTIR spectrometer. Figure 3.2 and 3.3 show the expected three CO stretching peaks for a *fac* complex of $M(L)CO_3X$ at 2100 and 1850 cm^{-1}. Also the absorption peak at 1720 cm^{-1} refers to the carbonyl peak of 4.5-diazafluoren-9-one.[1]

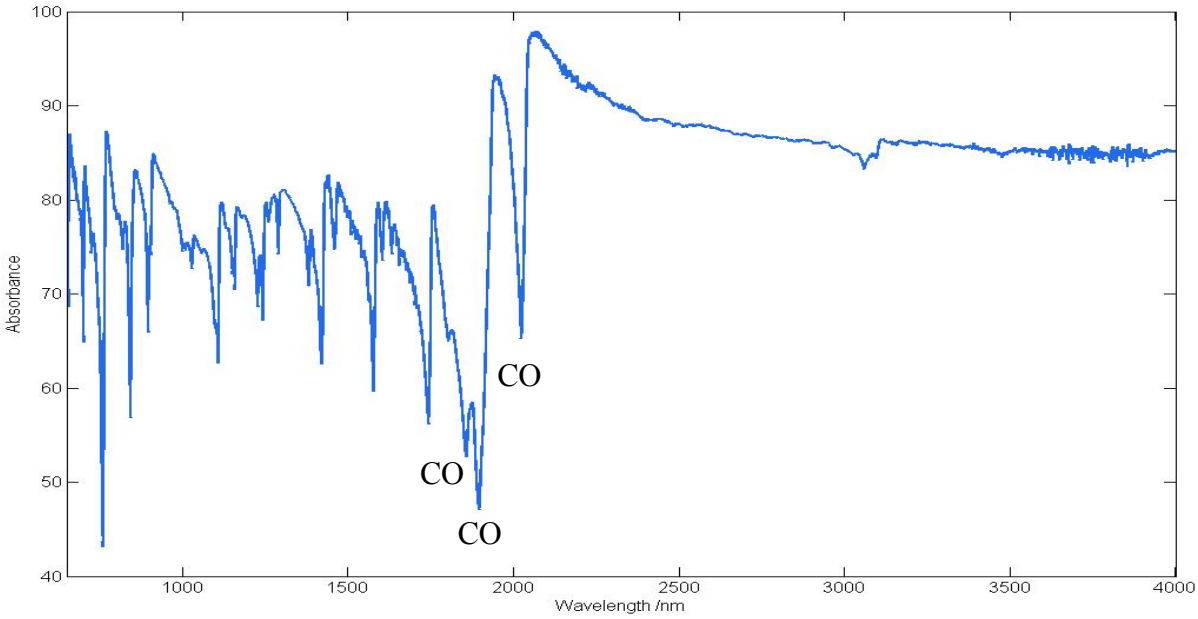

Figure 3.2: FTIR Spectra for $Re^{I}(CO)_3$ L Cl (**2**).

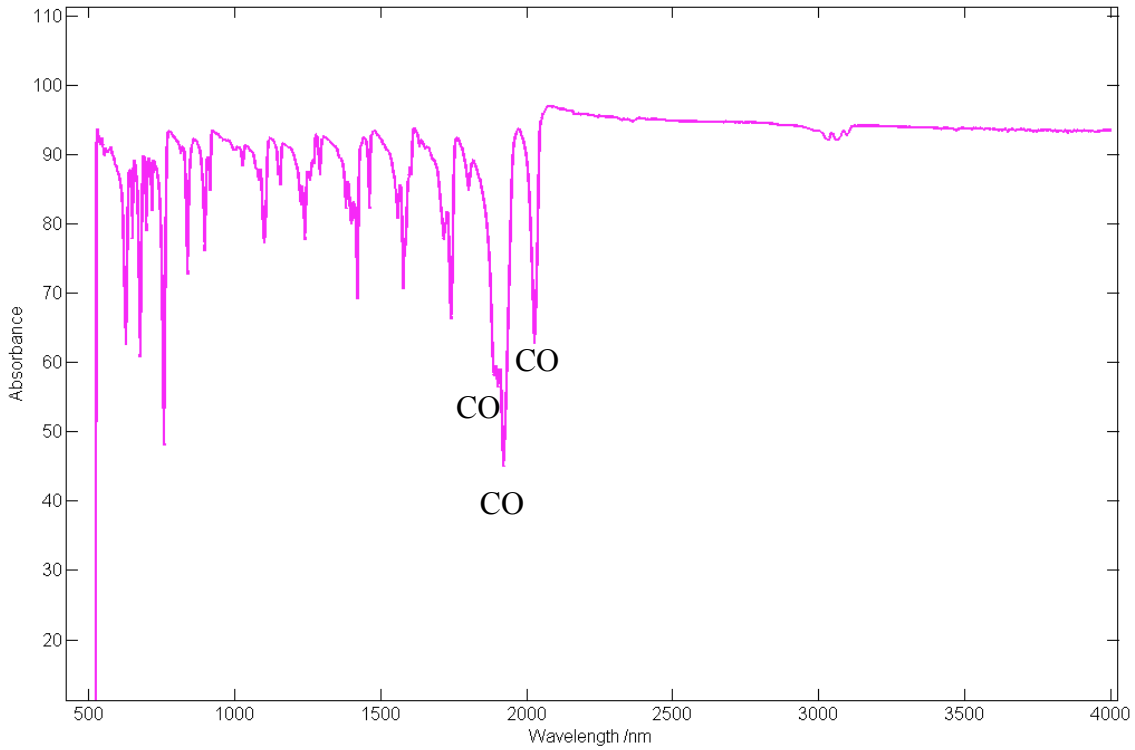

Figure 3.3: FTIR Spectra for $Mn^{I}(CO)_3$ L Br (**4**).

3.3.3 X-ray Crystallography

Crystals were grown in saturated solvent through gas-phase diffusion method to give good crystals of compounds (**3** and **4)**. Cell parameters and other collection data for compounds (**3** and **4)** are provided in Table 3.1. The structure of compounds **(3** and **4)** can be seen in Figure 3.4 and 3.5, which confirm the *fac*-tricarbonyl configuration of the complexes and the bidentate coordination mode to the 4,5-diazafluoren-9-one to the metal center. Crystals suitable for x-ray analysis were unable to be collected from compound (**2)** due to the small size of the crystals.

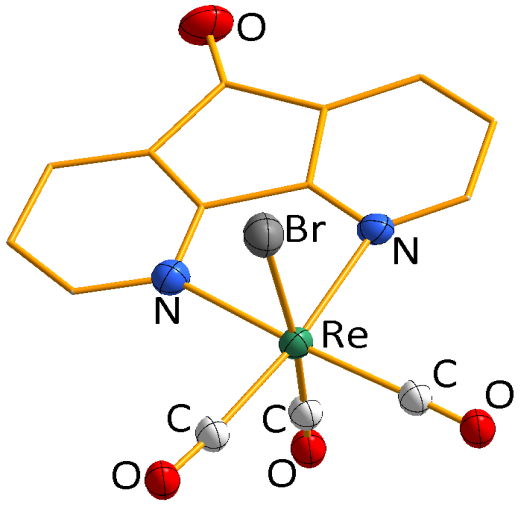

Figure 3.4: X-ray structure derived representation of compound $Re(CO)_3LBr$ **(3).** Hydrogen atoms and thermal ellipsoids of the ligand carbon atoms are omitted for clarity.

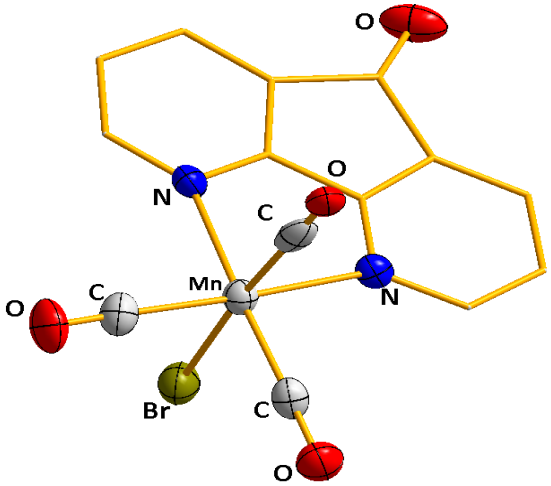

Figure 3.5: X-ray structure derived representation of compound $Mn(CO)_3LBr$ **(4).** Hydrogen atoms and thermal ellipsoids of the ligand carbon atoms are omitted for clarity.

Table 3.1: Crystal data and structure refinement for compounds (**3** & **4)**

Compound	**3**	**4**
Empirical formula	$C_{14}H_6BrN_2O_4Re$	$C_{14}H_6BrMnN_2O_4$
Formula weight (g/mol)	532.32	401.06
Temperature (K)	200	200
Wavelength (A)	0.71073	0.71073
Crystal System	Monoclinic	Monoclinic
Space group	P 21/n	P 21/n
a (A)	6.5492	6.5301
b (A)	16.772	16.5697
c (A)	13.327	13.2126
α (deg)	90	90
β (deg)	100.752	100.868
γ (deg)	90	90
Volume (A3)	1438.2	1404.0
Absorption coefficient (mm-1)	11.245	3.805
Absorption correction		
Final R indices[I≥ 2σ(I)]	R1= 0.0923	R1= 0.0624
	wR2= 0.1828	wR2= 0.1618

Both (**3** & **4**)present the metal center in a pseudooctahedral geometry that is supported by a bidentate. planar 4,5-diazafluoren-9-one ligand. Complexes (**3** & **4)** have three carbonyl groups in facial coordination to the metal center. Two of these CO groups are in the plane of the ligand and *trans* to the N centers. The third is perpendicular to that plane and *trans* to the halo ligand. Selected bond lengths, bond angles are listed in Table 3.2 and 3.3 for complex (**3** & **4)**.

Table 3.2: Selected Angles, Distances and Torsion angles for (**3)**

Angle	Experimental Degrees (°)
C(14)-Re(1)-C(12)	89.3(10)
C(14)-Re(1)-C(13)	93.0(11)
C(12)-Re(1)-C(13)	89.3(10)
C(14)-Re(1)-N(2)	85.7(9)
C(12)-Re(1)-N(2)	94.8(9)
C(13)-Re(1)-N(2)	175.6(9)
C(14)-Re(1)-N(1)	92.5(8)
C(12)-Re(1)-N(1)	173.1(8)
C(13)-Re(1)-N(1)	97.2(8)
N(2)-Re(1)-Br(2)	86.6(5)
C(10)-N(2)-Re(1)	135.6(16)

Bond	Experimental Distance Å
Re(1)-C(14)	1.87(2)
Re(1)-C(12)	1.977(19)
Re(1)-C(13)	1.99(2)
Re(1)-N(2)	2.212(19)
Re(1)-N(1)	2.269(18)
Re(1)-Br(2)	2.604(3)
O(4)-C(12)	1.070(18)
O(5)-C(13)	1.070(19)
O(6)-C(14)	1.006(19)

Torsion	Experimental Degrees (°)
O(4)-C(12)-Re(1)	176(2)
O(5)-C(13)-Re(1)	178(2)
O(6)-C(14)-Re(1)	178(2)

Table 3.3: Selected Angles, Distances and Torsion angles for (**4)**

Angle	Experimental Degrees (°)
C(12)-Mn(1)-C(13)	90.5(4)
C(12)-Mn(1)-C(14)	90.0(4)
C(13)-Mn(1)-C(14)	92.3(4)
C(12)-Mn(1)-N(2)	92.5(3)
C(13)-Mn(1)-N(2)	177.0(4)
C(12)-Mn(1)-N(1)	173.2(3)
C(13)-Mn(1)-N(1)	94.7(4)
C(14)-Mn(1)-N(1)	94.1(3)
N(2)-Mn(1)-N(1)	82.3(3)
C(12)-Mn(1)-Br(1)	88.1(3)
C(13)-Mn(1)-Br(1)	92.1(3)
C(14)-Mn(1)-Br(1)	175.3(3)
N(2)-Mn(1)-Br(1)	88.35(18)
N(1)-Mn(1)-Br(1)	87.29(19)

Bond	Experimental Distance Å
Mn(1)-C(12)	1.806(9)
Mn(1)-C(13)	1.845(9)
Mn(1)-C(14)	1.848(12)
Mn(1)-N(2)	2.089(7)
Mn(1)-N(1)	2.141(7)
Mn(1)-Br(1)	2.5092(17)
O(2)-C(12)	1.112(9)
O(3)-C(13)	1.090(9)
O(4)-C(14)	0.964(10)

Torsion	Experimental Degrees (°)
Mn(1)-N(1)-C(1)-C(2)	-178.9(7)
C(5)-N(1)-C(1)-C(6)	-179.3(8)
N(1)-C(1)-C(2)-C(3)	-3.2(13)
N(1)-C(1)-C(2)-C(11)	177.4(8)

3.3.4 UV-Vis spectroscopy

The compounds (**2** & **3)** were completely soluble in dichloromethane with approximate concentration 0.1mM. As expected, the spectra showed two strong absorption bands; the first absorption band in the UV region is at 280 nm which attributed to intra-ligand (IL) transitions ($\pi - \pi^*$) in 4,5-diazafluoren-9-one ligand Figure 3.6. The second absorption band is in the visible region at 402 nm, which could be attributed to a metal-to ligand charge transfer MLCT (d - π^*) transition [1]. In addition, these transitions are responsible for the color change observed.

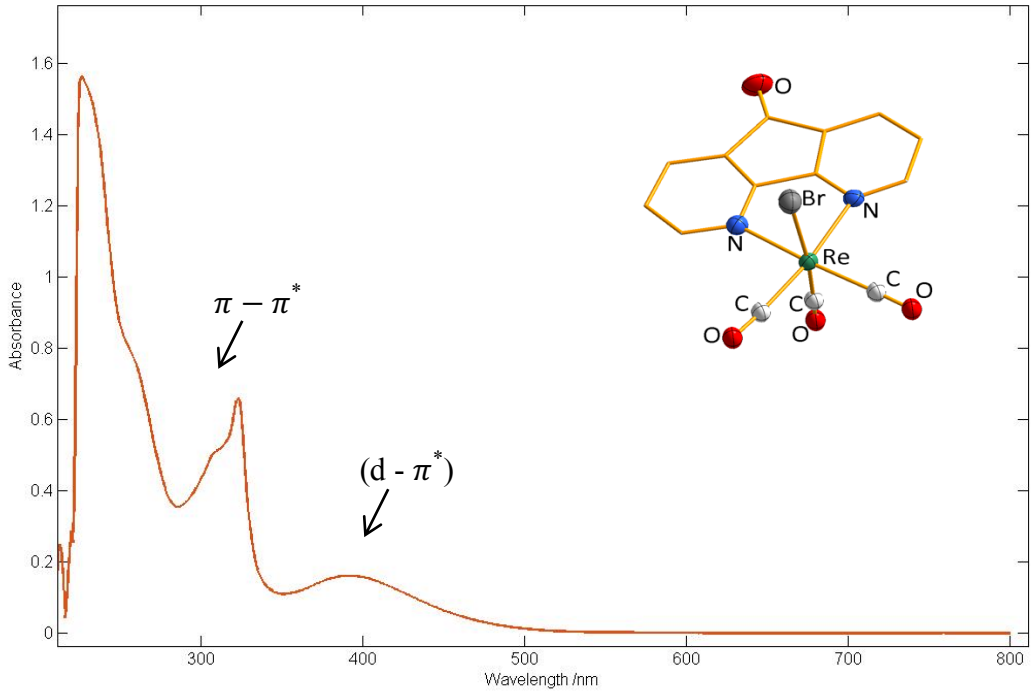

Figure 3.6: UV-Vis spectra for compound (**3)**

3.4 Examining the ability of the complexes for the photocatalytic reduction of CO_2

Attempts to photocatalytically reduce CO_2 were carried out under what has been called the "Strasbourg Conditions" after the original reaction conditions employed for CO_2 reduction using bipyRe$(CO)_3$X.[2-4] These conditions employ 15 ml of dimethylformamide (DMF) as a solvent and triethanol amine (TEOA), as a sacrificial reductant. The DMF/TEOA volume ratio is 4:1 and the catalyst concentration is 0.1 mM. It is important to note that Re^I complexes (**2** & **3)** can be classified as Type II systems, that means these complexes can act to both harvest light and catalyze the reduction reaction. However, Mn^I complex (**4)** does not have the ability to absorb the light; thus, use of a photosensitizer would be required in order to achieve CO_2 reduction.

3.4.1 The Photocatalytic Reduction of CO_2 for Re$(CO)_3$LCl (2)

Under these reaction conditions, compound (**2)** displayed a great activitiy for CO_2 reduction using a mercury lamp (500 W) as the light source. The reaction products were analyzed using gas chromatography. There are few metal complexes can act as Type II catalyst and these include as Re(bipy)CO_3X,[2,4,7,8] and Ir terpyridine (terpy) 2-phenyl pyridine (ppy) Cl.[30] As a benchmark for these results I choose Re$(CO)_3$bpyCl as a reference due to the similarity to compound (**2** & **3)**. Re$(CO)_3$bpyCl was prepared in the lab exactly as in literature.[3] Under the same reaction conditions, both (**2)** and Re(CO)3bpyCl were irradiated under an atmosphere of CO_2. After 24 hours, 94 $\mu\, mol$ of CO was obtained from Re(CO)2bpyCl while 92 $\mu\, mol$ of CO were generated from (**2).**

Having established the ability of (**2)** to reduce CO_2 to CO, changes to the general reaction conditions were explored using different sacrifical reductants such as ascorbic acid and 1-benzyl-1,4-dihydronictinamide (BNAH). These reductants failed to reduce CO_2 to CO or other products. Furthermore, replacing DMF with acetontrile as solvent resulted in no observed CO formation. Finally, the impact on water on the reduction reaction was explored by the addition of small amount of water (2 μl) to the reaction mixture (15 ml). This resulted in lower formation of CO. Table 3.4 illustrates the different irradation times, sacrificial reductants, solvents and CO yield.

Table 3.4: The amount of CO generated by (**2)** under varied conditions

Irradition time	**Solvent**	**Sacrificial Reductant**	**Amount of CO produced** μl
2 h	DMF	TEOA	20
24 h	DMF	TEOA	92
24 h	DMF+ 2μl H_2O	TEOA	4
24 h	DMF	0.1 mM of BNAH	0
24 h	DMF	0.1 mM of Ascorbic acid	0
24 h	Acetonitrile	TEOA	0
24 h	Acetonitrile	0.1 mM of BNAH	0

I also explored the effect of the yield of CO using different sources of the light. Using three different light sources but maintaining the same concentration of (**2)** and

same irradiation time resulted in three different yields of CO. The mercury lamp produced the highest conversion compared to LED 365 nm and a tungsten lamp. The lowest yields of CO was obtained by using LED 365, which did appropriate with the UV-Visble spectroscopy when the MLCT band of compound (**2)** has shown at 401 nm Table 3.5.

Table 3.5: Different yields of CO for compound (**2)** with different sources of light under "Strasbourg condition" after 24 hours of irradition.

The Source of Light	The Amount of CO μl
Mercury lamp	50
LED 365	3
Tungsten lamp	8

Finally, it has been considered that compound (**2)** has three carbonyl groups which could release CO; thus, it is important to ensure that the amount of CO was originating from CO_2 reduction only. The easiest ways to reveal whether CO comes form CO_2 reduction or decomposition the compound is to perform all the reactions under N_2 environment as a blank. Under the same condition, irradition time, the source of light and under N_2 environment, gas chromotography does not detect any signal peak for CO. This strongly suggests that the observatoin of CO is the result of CO_2 reduction.

3.4.2 The Photocatalytic Reduction of CO_2 using $Mn(CO)_3LBr$ (4)

In contrast with rhenium compounds (**2** & **3)**, manganese compound (**4)** required a photosensitizer to reduce CO_2 to CO under analogous photocatalysis reaction

conditions. As a first selection of photosensitizer, I chose to use tris(bipyridine)ruthenium(II) chloride. This species is perhaps the most well established photosensitizer and is thus a good benchmark for these studies. Attempted reduction of CO_2 using compound (**4)** were carried out under similar photochemical conditions employed for compounds (**2** and **3)** with the addition 0.1 mM $(bipy)_3Ru(II)Cl_2$ as sensitizer and this mixture yields 18 $\mu\, mol$ of CO. Variation of the reaction conditions were also explored through changes in sacrificial reductants and reaction solvent. The Mn compounds have shown some activity for CO_2 reduction as illustrated in Table 3.6.

Table 3.6: The amount of CO after 24 h of irradition and using different agent reductants for Mn compound (**4)** as catalyst and Ru(II) as a photosenitizer.

Solvent	**Agent Reductant**	**Amount of CO produced** $\boldsymbol{\mu\, mol}$
15 ml of DMF	0.1 mM of BNAH	20
15 ml of DMF	0.1 mM of Ascorbic Acid	33
15 ml Acetontrile	0.1 mM of BNAH	0
12 ml of Acetontrile	3 ml of TEOA	0

Under the "Strasbourg Conditions" and in the absence of a photosensitizer, the Mn compound (**2)** yielded 33 $\mu\, mol$ of CO. It would seem that the Mn compound (**2)** yields CO as result of decompostion of the three carbonyl in the compound rather than CO_2 reduction reaction. There are two possible explanations for this unexpected situation;

first, Mn compound may not be stable enough and decompose as result of that, 33 $\mu\, mol$ of CO was yielded, or Mn compound **(2)** may have reacted with DMF to release the CO ligands. Two samples of compound **(4)** were examined under different conditions. In the first, the sample was dissolved in DMF under a N_2 atmoshpere while the second sample, also in DMF was exposed to CO_2 under ambient light. Surprisingly both samples displayed a color change after an hour. The sample under N_2 turned from yellow to green and the sample under CO_2 became gray (Figure 3.7). It clearly seems that compound **(4)** has reacted with the DMF solvent and yielded CO.

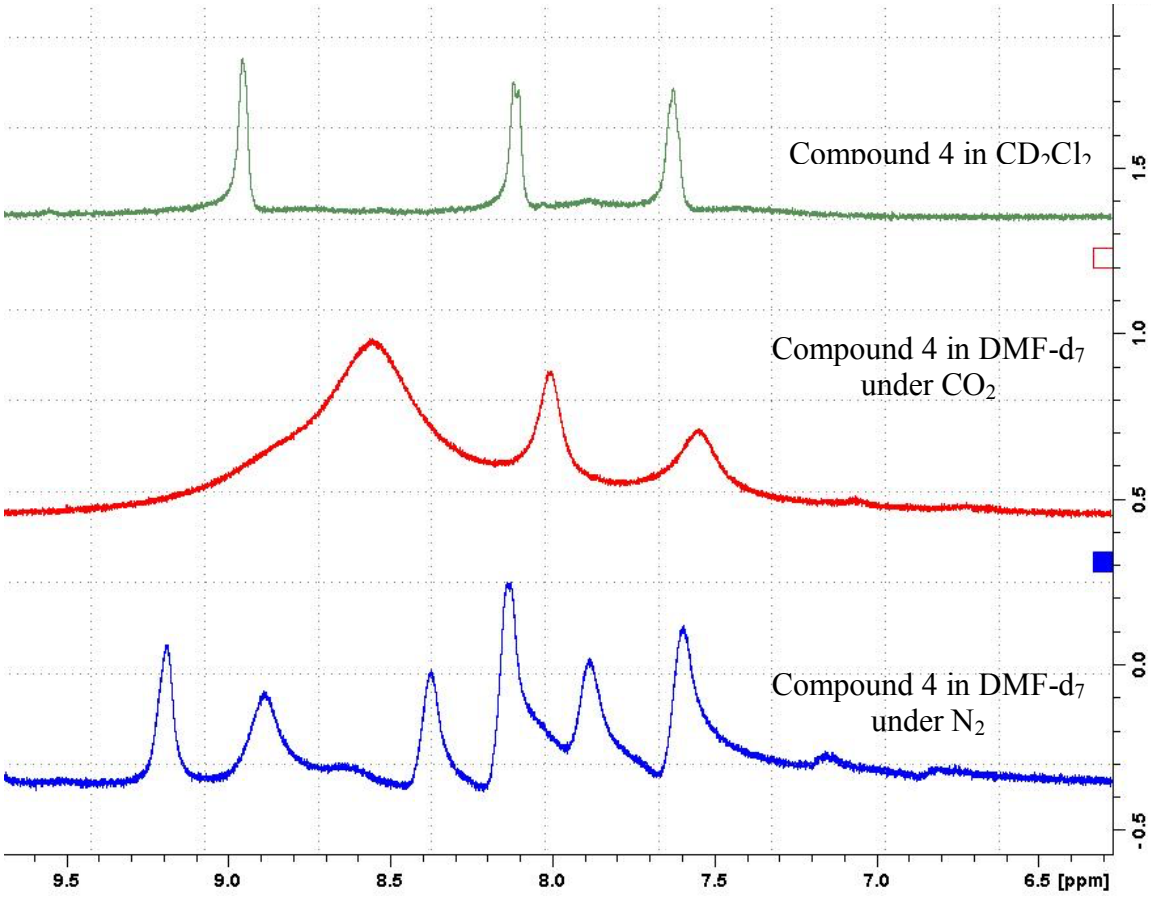

Figure 3.7: NMR shift peaks of compound **(4)** under different atmospheres and solvents.

3.5 Examining the ability of the complexes 2 and 4 for the electrocatalytic reduction of CO_2

While the two Re compounds (**2** & **3)** were able to successfully reduce CO_2 to CO with a good yield under photochemical conditions, I was unsuccessful in determining conditions that would be successful for compound (**4).** In addition to photochemical routes, the group 7 α-diimine complexes are known to electrocatalytically reduce CO_2.[9-30] Therefore the ability of these compounds to carry out this reduction electrocatalytically was also investigated

In a typical run dry acetontrile was used as solvent the catalyst concentration was set at 0.1 mM with 0.1M of tetrabutylammonium hexafluorophosphate ($TBAPF_6$) as supporting electrolyte. The electrochemical behavior of (**2)** under an N_2 environment is shown in Figure 3.8 and the potential scale has been adjusted with ferrocene/ferrocenium (Fc/Fc^+) couple as a reference at 0 V. A first reversible reduction wave appeared at -1.1 V vs. Fc/Fc^+, the difference between cathodic and anodic peak was found to be 61 mV. This reduction can be ascribed, based on comparison with the literature, to reducing Re(I) to Re(0).[31] The second reversible reduction wave was observed at -1.7 V vs. Fc/Fc^+ with 63 mV difference between cathodic and anodic peak . Again, based on comparison with analogous complexes in the literature, this reduction can be assigned to a ligand localized reduction.[32]

When these measurements are carried out under an atmosphere of CO_2, there is no a significant change in the behavior the two reduction events (Figure 3.9). It is known in the literature that in most cases for electrochemical reduction, the addition of water as a source of protons, can lead to electrocatalytic reduction.[33] Thus, a small amount of water

(0.25 μ mol) as source of proton was added to the solution of (**2**). This modification lead to an enhancement (30 μÅ) in the current in the second reduction wave as shown in Figure 3.10. The enhancement of the current could refer to CO_2 reduction to CO or to H_2O reduction to H_2. In order to determine the identity of the reduction product in this reaction, bulk electrolysis and analysis of the evolved gases was investigated. A solution of 0.1mM of compound (**2**) and 0.1M of $TBAPF_6$ in 20 ml acetonitrile and 2.5 ml of water was saturated with CO_2, the bulk electrolysis has shown after an hour to produce H_2 only which is approved that compound (**2**) does reduce H_2O to H_2. After (2) hours, the amount of H_2 had reached a plateau with no other observed gas phase products.

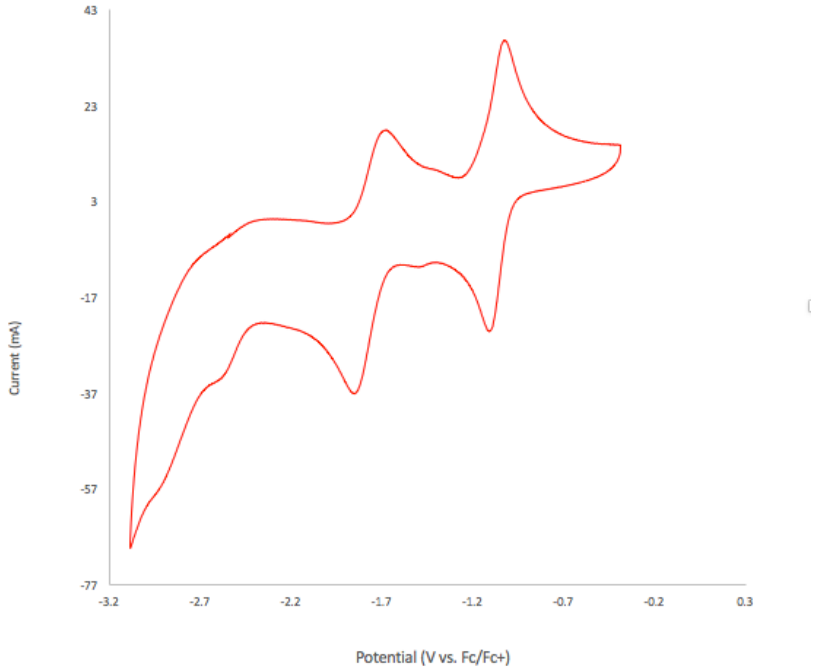

Figure 3.8: Cyclic Voltammogram at 100 mV s^{-1} of compound (**2**) **(0.1mM)** in acetonitrile with 0.1 M $TBAPF_6$, under N_2 atmosphere.

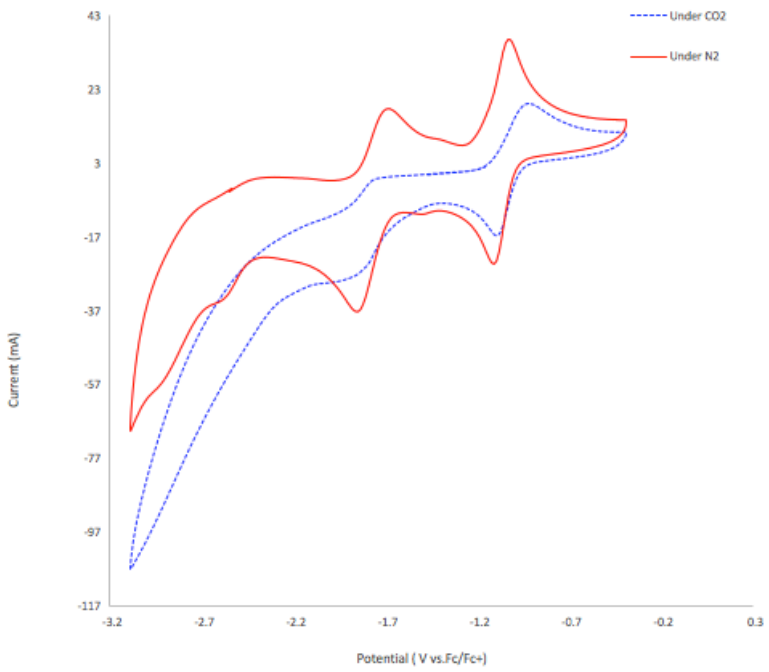

Figure 3.9: Cyclic Voltammogram at 100 mV s^{-1} of compound (**2**) in 0.1 M $TBAPF_6$, under N_2 and CO_2 atmosphere.

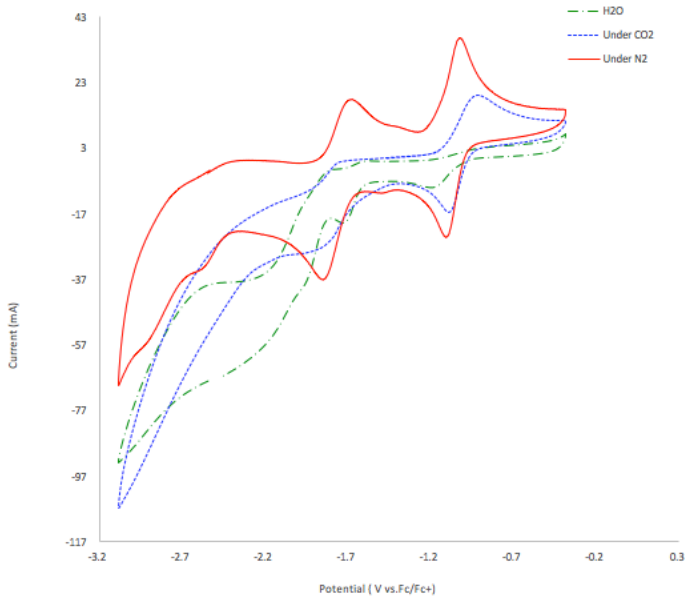

Figure 3.10: Cyclic Voltammogram at 100 mV s^{-1} of compound (**2**) in 0.1 M $TBAPF_6$, under N_2, CO_2 and CO_2 (5%water) atmosphere.

In terms of electrocatalytic reduction, Mn bipy complexes are active at lower electrochemical potentials than their Re analogues. As a result there has been an increasing attention given to Mn complexes for electrocatalytic reduction of of CO_2. Recently Mn bipy complexes have shown a great activity to reduce CO_2 to CO and formate [17-28]

The electrochemical behavior of Mn compound (**4**) (0.1mM) in acetontrile with 0.1M of $TBAPF_6$ was measured under a saturated N_2 atmosphere as shown in Figure 3.11. This species displayed two reduction waves with the first being a reversible redox event at -1.48 V vs. Fc/Fc^+ ($\Delta E = 61$ mV). This peak is a one electron transfer attributed to reducing Mn^1 to Mn^0.[23] The second reduction wave is irreversible and is at -2.4 V vs. Fc/Fc^+ . This reduction is ascribed to 4,5-diazafluoren-9-one reduction .[23]

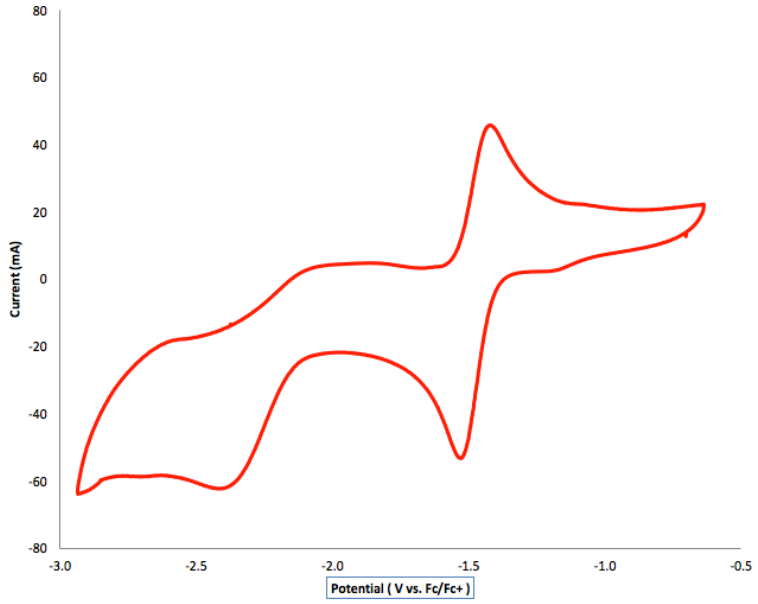

Figure 3.11: Cyclic Voltammogram at 100 mV s^{-1} of compound (**4**) in 0.1 M $TBAPF_6$, under N_2 atmosphere.

When a similar cyclic voltammetry experiment was carried out with Mn compound (**4**) under a CO_2 atmosphere, there was a slight shift of the reduction peaks. second reduction wave has positively shifted to -2.3 V vs. Fc/Fc^+ as shown in Figure 3.12.

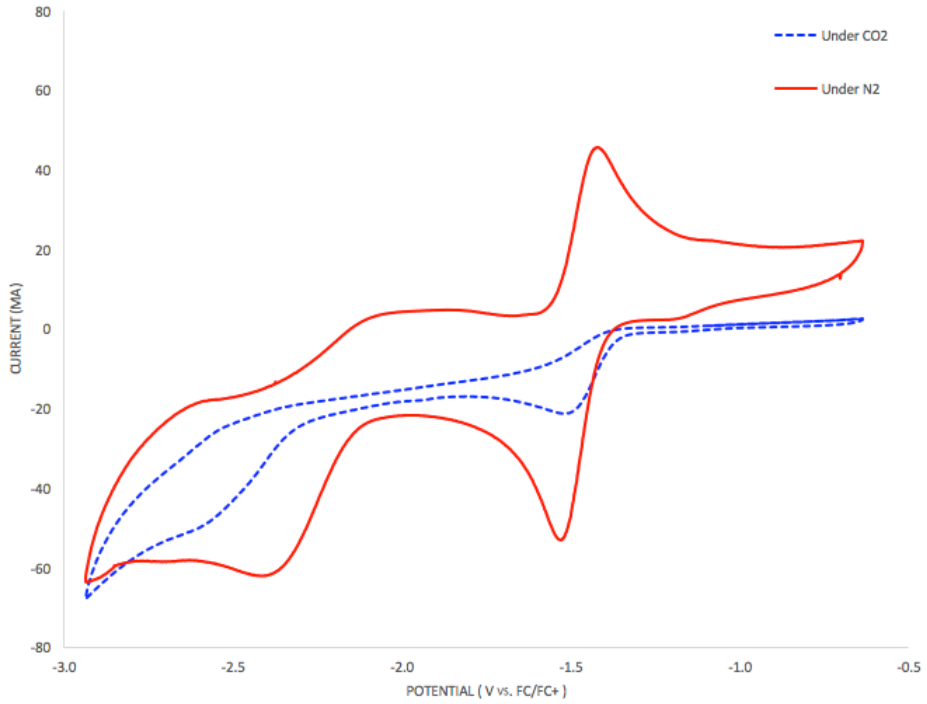

Figure 3.12: Cyclic Voltammogram at 100 mV s^{-1} of compound (**4**) in 0.1 M $TBAPF_6$, under N_2 and CO_2 atmosphere.

These observations changed in the presence of a small amount of water (5%). Under these conditions, an enhancement of the current (25μÅ) is observed Figure 3.13. Through bulk electrolysis and measurement of evolved gases, the enhancement of the current after adding a small amount of H_2O could be attributed to CO_2 reduction to CO. Table 3.7 and Figure 3.14. has summarized the result form bulk electrolysis and GC after varied time. In contrast with Re compounds (**2** & **3**), Mn compound (**4**) has successfully reducing CO_2 to CO in the presence of H_2O as source of proton.

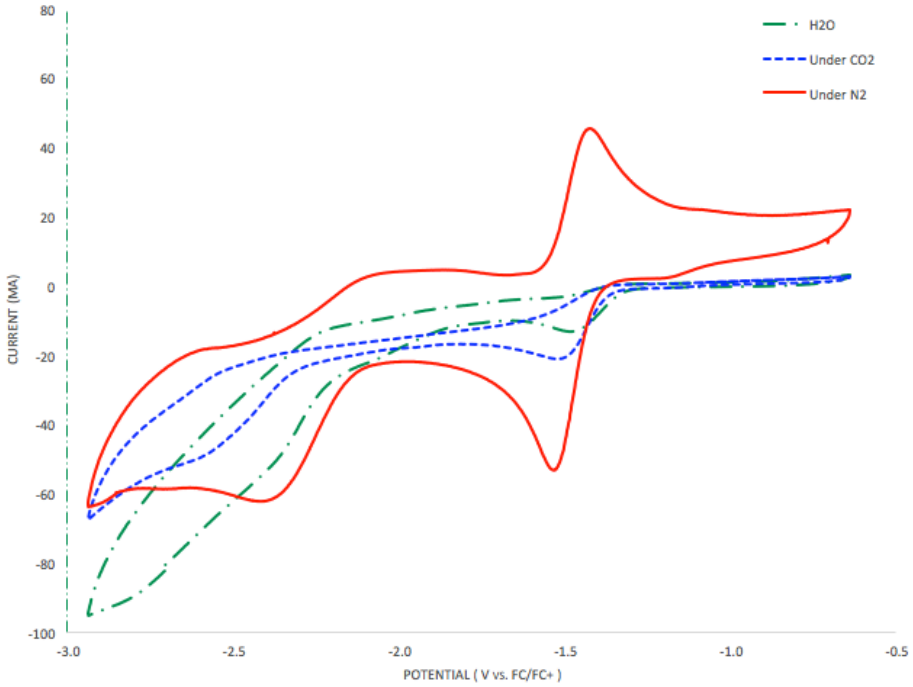

Figure 3.13: Cyclic Voltammogram at 100 mV s^{-1} of compound (**4**) in 0.1 M $TBAPF_6$, under N_2, CO_2 and CO_2 (5%water) atmosphere.

Table 3.7: The amount of CO that obtained from bulk electrolysis versus time.

Time (s)	**µmol of CO**
2000	18
3600	20
7700	22
9800	26

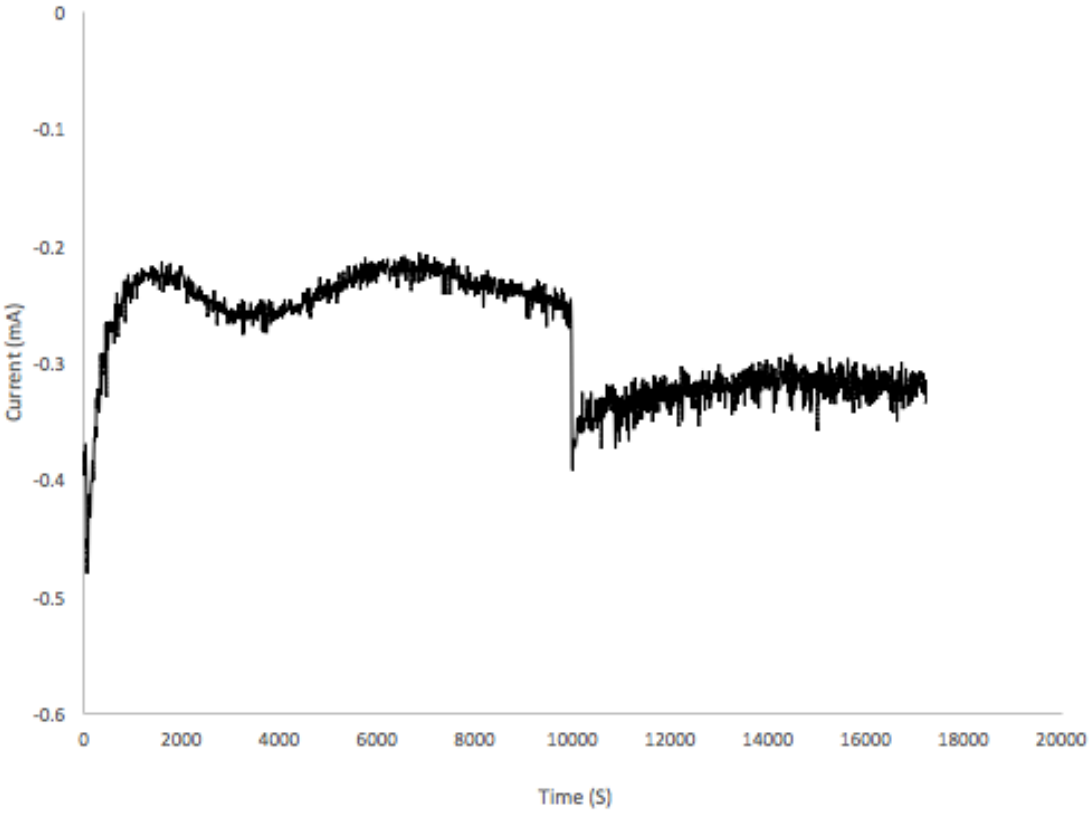

Figure 3.14: Bulk electrolysis experiments in presence of 2 mL H_2O at the second reduction -2.4

3.6 Conclusion

This chapter has described the successful synthesis of diimine rhenium and manganese compounds, characterized and tested for both photocatalytic and electrocatalytic CO_2 reduction. Re^I compounds (**2** & **3)** have shown a great activity for photocatalytic CO_2 reduction to CO; however, Mn^1 compound (**4)** has decomposed under "Strasbourg Condition" On the other hand, only the Mn^1 compound (**4)** has shown the ability for CO_2 reduction to CO under electrocatalytic conditions. The analogous Re^1 compounds (**2** & **3)** did not reduce CO_2 but rather reduced water to hydrogen. The second goal here was to modifying these compounds by modification of the diimine ligand to allow for incorporation of a photosensitizer. These efforts will be presented in Chapter 4.

Experimental section

All reactions were carried out in a glovebox under a nitrogen atmosphere. Solvents were dried by passage through a column of activated alumina using an apparatus purchased from Anhydrous Engineering. $M(CO)_5Cl$ and $M(CO)_5Br$ (M = Mn, Re) were purchased from Aldrich and used as received. Deuterated dichloromethane was dried using activated molecular sieves. NMR spectra were run on Bruker Avance 400MHz spectrometers with CD_2Cl_2 as solvent and internal standard. Infrared spectra were collected using an Agilent Technologies Cary FT-IR spectrome-Experimental Procedures using a diamond ATR attachment. UV-Vis spectra were collected using a Agilent Technologies Cary 5000 UV-Vis spectrometer.

Synthesis of Ligand: 4,5-Diazafluoren-9-one (1)

Potassium permanganate (20 g, 128 mmol) was added to (300 ml) of water and heated to dissolve. A hot solution of 1,10-phenanthroline (8g, 44 mmol) and potassium hydroxide (8 g, 144 mmol) in (500) ml water were slowly added to the KMnO4 mixturewhich was heated during the course of addition. The reaction mixture was heated to reflux under nitrogen for 3 hours. The reaction mixture was filtered when it is hot and the cool filtrate was extracted with chloroform and dried over anhydrous $MgSO_4$. The product was re-crystallization twice from acetone. After the solution was evaporated the product was purified by column chromatography on silica gel (EtOAc). Total yield: (3.1 g, 38.7%) as light yellow. ^{1}H NMR ($CDCl_3$, 400 MHz) δ 8.1, (dd, 2H), 7.57 (dd, 2H), 8.90 (dd, 2H). ^{13}C NMR ($CDCl_3$) δ 188.7, 162.7, 154.6, 131.0, 128.9, 124.3.

4,5-Diazafluoren-9-one Re(I) $(CO)_3Cl$ (2)

In a glovebox**, (**91.09 mg, 0.5 mmol) of 4,5-Diazafluorene-9-one was dissolved in (50 ml) of dry toluene. $Re(CO)_5Cl$ (180.85 mg, 0.5 mmol) was added to the solution. The mixture was stirred with a magnetic stir bar until the solution became a yellow in color. The flask was sealed with a stopper and removed from the glove box. The reaction mixture was heated to reflux under nitrogen for 2 hours. A bright-orange solid was removed by suction filtration and washed with hexane then dissolved dichloromethane. The mixture was dried through rotary evaporation under a reduced pressure. Total yield (180 mg, 66.1%). ^1H NMR (CD_2Cl_2, 400 MHz) δ 8.83, (d, J= 4.6, 2H), 8.20 (d, J= 7.6 2H), 7.66 (m, 2H). ^{13}C NMR (CD_2Cl_2) δ 189.0, 165.4, 154.7, 134.4, 129.6, 128.90

4,5-Diazafluoren-9-one Re(I) $(CO)_3Br$ (3)

A similar procedure as for the synthesis of (**2)** was used with**, (**91.09 mg, 0.5 mmol) of 4,5-Diazafluorene-9-one dissolved in (50 ml) of dry toluene. $Re(CO)_5Br$ (202.92 mg, 0.5 mmol) was added to the solution. The mixture was stirred with a magnetic stir bar until the solution became a yellow in color. The flask was sealed with a stopper and removed from the glove box. The reaction mixture was heated to reflux under nitrogen for 2 hours. A bright-orange solid was removed by suction filtration and washed with hexane then dissolved in dichloromethane. The mixture was dried through rotary evaporation under a reduced pressure. Total yield (231.6 mg, 94.9%). ^1H NMR (CD_2Cl_2, 400 MHz) δ 8.95, (b, s , 2H), 8.10 (b, s, 2H), 7.66 (t, J=5 , 2H). ^{13}C NMR (CD_2Cl_2) δ 195.2, 163.5, 155.0, 134.4, 131.2, 128.9, 124.7

4,5-Diazafluoren-9-one Mn(I) $(CO)_3Br$ (4)

A similar procedure as for the synthesis of (**2)** was used with**, (**91.09 mg, 0.5 mmol) of 4,5-Diazafluorene-9-one dissolved in (50 ml) of dry toluene. $Mn(CO)_5Br$ (123.9 mg, 0.5 mmol) was added to the solution. The mixture was stirred with a magnetic stir bar until the solution became an orange in color. The flask was sealed with a stopper and removed from the glove box. The reaction mixture was heated to reflux under nitrogen for 2 hours. A bright-orange solid was removed by suction filtration and washed with hexane and then dissolved in dichloromethane. The mixture was dried through rotary evaporation under a reduced pressure. Total yield (139.6 mg, 69.9%). ^1H NMR (CD_2Cl_2, 400 MHz) δ 8.95, (br s, 2H), 8.10 (br s, 2H), 7.63 (br s, 2H). ^{13}C NMR (CD_2Cl_2) δ 185.2, 168.2, 154.4, 134.4, 132.7, 129.6, 128.9

References

1. Hawecker J.; Lehn, J.; Ziessel, R. *Helv. Chim. Acta.,* **1986**, *69,* 1990–2012.
2. Hawecker, J.; Lehn, J. M.; Ziessel, R. J. Chem. Soc., *Chem. Commun.* **1984,** 328–330.
3. Hawecker J.; Lehn, J.; Ziessel, R. ***J. Chem. Soc., Chem. Commun.***, **1983**, 536-538.
4. Gibson, D. H.; Yin, X. *J. Am. Chem. Soc.,* **1998**, *120*, 11200–11201.
5. Hayashi, Y.; Kita, S.; Brunschwig, B. S.; Fujita, E. *J. Am. Chem., Soc*., **2003**, *125*, 11976–11987.
6. Hori, H.; Johnson, P. AS.; Koike, K.; Ishitani, O.; Ibusuki. T. *J. Photochem. Photobiol. A: Chem*., **1996**, *96,* 171–174.
7. Kurz, P.; Probst, B.; Spingler, B.; Albertp, R. *Eur. J. Inorg. Chem*., **2006**, 2966–2974.
8. Chabolla, S. A.; Dellamary, E. A.; Machan, C. W.; Tezcan, F. A.; Kubiak, C. P. *Inorg. Chim. Acta.,* **2014**, *422*, 109−113.
9. Wong, K.-Y.; Chung, W.-H.; Lau, C.-P. *J. Electroanal. Chem.,* **1998**, *453*, 161−169.
10. Benson, E. E.; Grice, K. A.; Smieja, J. M.; Kubiak, C. P. *Polyhedron.,* **2013**, *58,* 229−234.
11. Benson, E. E.; Kubiak, C. P. *Chem. Commun*., **2012**, *48*, 7374−7376.
12. Machan, C. W.; Chabolla, S. A.; Yin, J.; Gilson, M. K.; Tezcan,F. A.; Kubiak, C. P. *J. Am. Chem. Soc*., **2014**, *136*, 14598−14607.

13. Sampson, M. D.; Froehlich, J. D.; Smieja, J. M.; Benson, E. E.; Sharp, I. D.; Kubiak, C. P. *Energy Environ. Sci*., **2013**, *6*, 3748−3755.

14. Smieja, J. M.; Benson, E. E.; Kumar, B.; Grice, K. A.; Seu, C. S.; Miller, A. J. M.; Mayer, J. M.; Kubiak, C. P. *Proc. Natl. Acad. Sci. U. S. A.*, **2012**, *109*, 15646−15650.

15. Smieja, J. M.; Kubiak, C. P. *Inorg. Chem.,* **2010**, *49*, 9283−9289.

16. Sullivan, B. P.; Bolinger, C. M.; Conrad, D.; Vining, W. J.;Meyer, T. J. *Chem. Commun.,* **1985**, 1414−1416.

17. Bourrez, M.; Molton, F.; Chardon-Noblat, S.; Deronzier, A. *Angew. Chem., Int. Ed.* **2011**, *50,* 9903−9906.

18. Bourrez, M.; Orio, M.; Molton, F.; Vezin, H.; Duboc, C.; Deronzier, A.; Chardon-Noblat, S. *Angew. Chem., Int. Ed*. **2014**, *53,* 240−243.

19. Grice, K. A.; Kubiak, C. P. *Adv. Inorg. Chem,*. **2014**, *66*, 163−188.

20. Smieja, J. M.; Sampson, M. D.; Grice, K. A.; Benson, E. E.; Froehlich, J. D.; Kubiak, C. P. *Inorg. Chem.,* **2013**, *52,* 2484−2491.

21. Sampson, M. D.; Nguyen, A. D.; Grice, K. A.; Moore, C. E.; Rheingold, A. L.; Kubiak, C. P. *J. Am. Chem. Soc.,* **2014**, *136,* 5460−5471.

22. Takeda, H.; Koizumi, H.; Okamoto, K.; Ishitani, O. *Chem. Commun*., **2014**, *50*, 1491−1493.

23. Fei, H.; Sampson, M. D.; Lee, Y.; Kubiak, C. P.; Cohen, S. M. *Inorg. Chem.,* **2015**, *54,* 6821−6828.

24. Sampson, M. D.; Nguyen, A. D.; Grice, K. A.; Moore, C. E.; Rheingold, A. L.; Kubiak, C. P. *J. Am. Chem. Soc.,* **2015**, *137*, 3718–3718.

25. Benson, E. E.; Sampson, M. D.; Grice, K. A.; Smieja, J. M .; Froehlich, J. D.; Friebel, D.; Keith, J. A.; Carter, E. A.; Nilsson, A.;Kubiak, C. P. *Angew. Chem., Int. Ed.* **2013**, *52,* 4841−4844.

26. Johnson, F. P. A.; George, M. W.; Hartl, F.; Turner, J. *J.Organometallics* **1996**, *15*, 3374−3387.

27. Machan, C. W.; Sampson, M. D.; Chabolla, S. A.; Dang, T.; Kubiak, C. P. *j. Organometallics* **2014**, *33*, 4550−4559.

28. Keith, J. A.; Grice, K. A.; Kubiak, C. P.; Carter, E. A. *J. Am. Chem. Soc*. 2**013**, *135,* 15823−15829.

29. Sato, S.; Morikawa, T.; Kajino, T.; Ishitani, O. *Angew. Chem., Int. Ed.* **2013**, *52*, 988.

30. F. Paolucci, M. Marcaccio, C. Paradisi, S. Roffia, C. A. Bignozzi, C. Amatore, *J. Phys. Chem. B* **1998**.

31. Chiericato, G., C. r Arana, C. Casado, I. Cuadrado, and H. d Abruña. *Inorg. Chim. Acta*., **2000**, 300-302: 32–42.

32. Jhong, H.-R. M.; Ma, S.; Kenis, P. J. *Curr. Opin. Chem. Eng.,* **2013**, *2* (2), 191–199.

Chapter 4

Exploring The Modification of the 4,5-diazafluoren-9-one Ligand with Mn^{1} Complexes for The Photocatalytic Reduction of CO_2

4.1 Introduction

In Chapter 3, the target was focused on synthesizing diimine rhenium and manganese compounds that might be used as catalysts for CO_2 reduction. This effort led to a successful Re compound for the photocatalytic reduction of CO_2 as well as a Mn complex for the electrocatalytic reduction of CO_2. With these results, I now wanted to utilize the ketone function of the 4,5-diazafluoren-9-one ligand as a means to attach a photosensitizer unit to the group 7 metal complex. The idea was to increase the life-time of catalyst systems and increase the efficiency and the selectivity of CO_2 reduction in general.[1]

In this chapter, the first avenue of exploration was to modify the diimine ligand through a Schiff base reaction by reacting 4,5-diazafluoren-9-one with NH_2R to yield a modified ligand (**2)**. Later, the modified ligand could be reacted directly with $M(CO)_5X$, (M= Re^{1} or Mn^{I} and X= Cl^{-} or Br^{-}) to form $M(CO)_3LX$, where L is the new modified ligand. An additional focus was the synthesis of a new light-harvesting complex of Os(II) that might be used as a photosensitizer to replace the more well-studied tris(bipyridine)ruthenium (II) chloride, which I used in the previous chapter.[2]

4.2 Modification of the 4,5-diazafluoren-9-one ligand

As a first approach to modification of the diazafluorenone, the direct reaction of this compound with 4-aminoazobenzene was carried out to yield compound (**2)** in Scheme

4.1. The advantage of using 4-aminoazobenzene is increasing the conjugated π system of the ligand which should result in a longer wavelength of the light absorbed due to the energy gap for $\pi - \pi^*$ transition becomes more narrow. The synthesis of the modified ligand (**2)** was confirmed by using ^{1}H NMR and the mass spectrometry. The mass spectrometry (electron impact) supports the formulation of the modified ligand and proton NMR spectrum definitively indicates a *cis* arrangement of ligand **(2).** Comparing the modified ligand (**2)** with the free ligand revealed an increase of NMR peaks due to a loss of ligand symmetry after the Schiff base reaction.[3] The electron ionization technique has used to confirm the formulation of the modified ligand (**2)**: ^{12}C 23, ^{1}H 15, ^{14}N 5 and ^{16}O 0, this result perfectly matched with the calculated formulation.

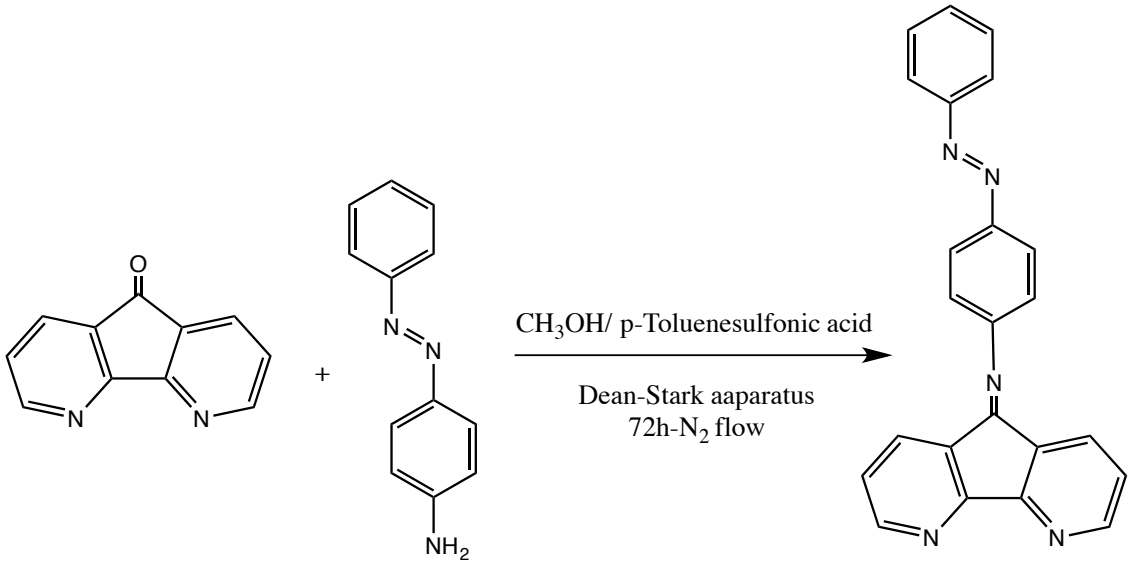

4,5-Diazafluoren-9-one 4-aminoazobenzen Compound **2**

Scheme 4.1: The modification of 4,5-diazafluoren-9-one reaction

The modified ligand was allowed to react with $Mn^{I}(CO)_5Br$ in refluxing solvent to formed the potential catalyst $Mn(CO)_3LBr$ with a good yield of 85% (see Scheme 4.2).[1] The reasons behind choosing manganese have been previously discussed in the Introduction and in Chapter 3. The catalyst constitution was confirmed by ^1H NMR and Fourier Transforming Infrared (FTIR) Spectroscopy. On the Agilent Cary 630 FTIR spectrometer a small amount of the catalysts (powder) was set with a 2 cm^{-1} resolution. Figure 4.1 shows at 2050 cm^{-1} a large absorption refers to CO strength for compound **(3).** Other two absorption peaks have appeared around 1850 nm refer to other carbonyl stretching in the compound **(3).** Also, the peak of carbonyl in ketone site that appeared at 1720 cm^{-1} has been shifted to 1622 cm^{-1} which refers to C=N absorption peak which confirmed the structure of compound **(3)**.[4]

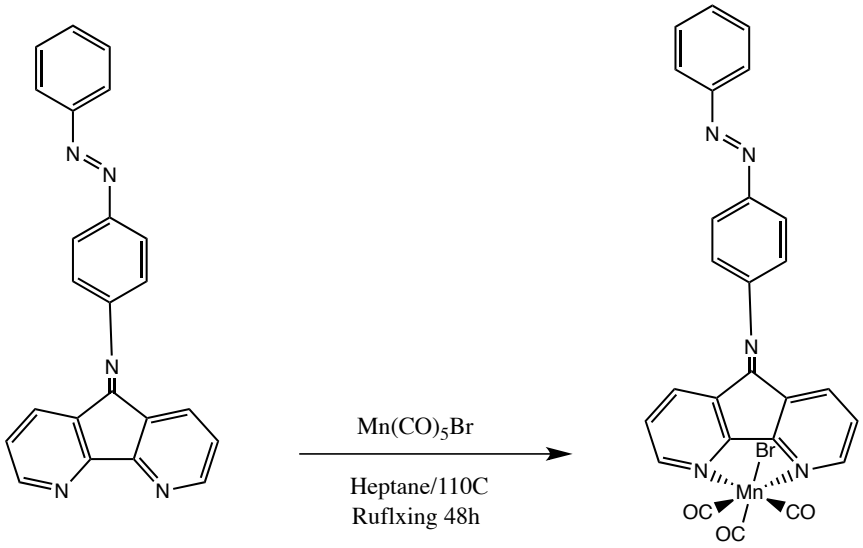

Compound **2** Compound **3**

Scheme 4.2: Direct reaction of compound (**2)** with $Mn(CO)_5Br$ to form compound (**3)** $Mn(CO)_3LBr$, L= compound (**2**).

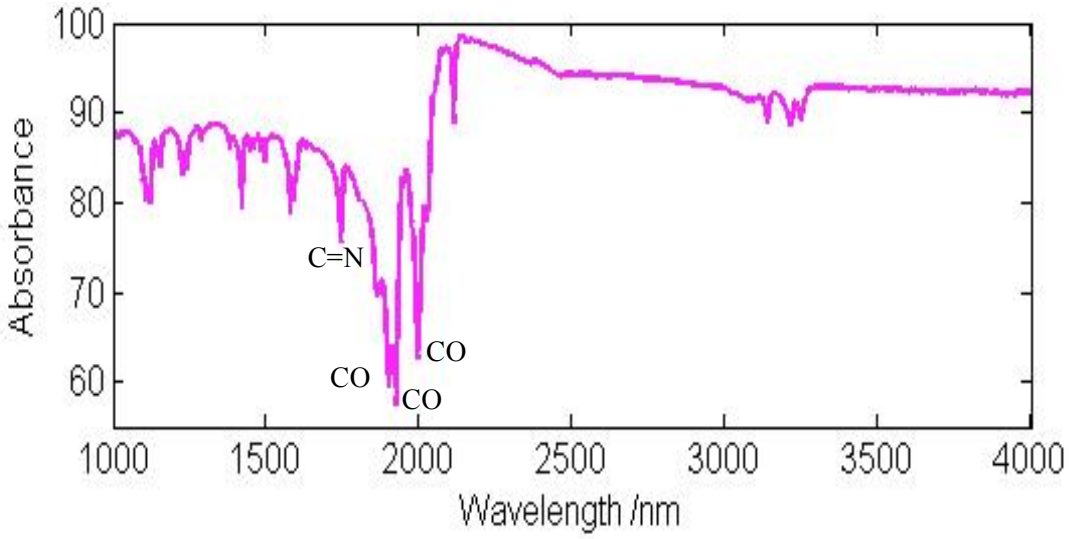

Figure 4.1 The IR spectrum of compound (**3)**

4.3 Synthesis of an Osmium Photosensitizer

Tris(bipyridine)ruthenium(II)chloride is perhaps the most investigated light-harvesting compound in the photocatalytic reduction of CO_2 and it has already been well documented in several comprehensive reviews.[5-6] Other photosensitizers have received only scant attention. For example, Os(II) polypyridine complexes have similarities in chemical properties to Ru(II) because both are located in group VIII. The comparison between Os and Ru cannot be clearly illustrated as points but it can be said that the energies of d-d excited states in Os are higher than in Ru due to the large value of 10*Dq* for Os. Also, Os has a lower ionization energy that may causes a lower redox potential and higher stabilization of higher oxidation state. Lastly, the metal-d orbitals have a great extension that can strengthen the metal- ligand back-bonding.[8] For these reasons, the potential of Os(II) complexes as a light-harvesting compounds and an exploration of the

differences in the efficiency of the photocatalytic reduction of CO_2 for Os(II) comparing to Ru(II). The target compound **(4),** cis-bis(5,5'-dimethyle-2,2'-dipyridine) dichloro osmium(II) was prepared based on a method reported by Buckingham *el al* which gives a 70% yield of Os(II) Scheme 4.3.[10] Compound (**4)** has confirmed by using the elemental analysis as shown in Table 4.1 that perfectly matched with calculated formulation.

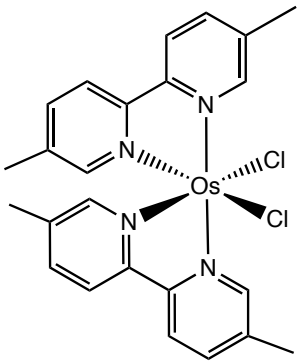

Scheme 4.3: The structure cis-bis(5,5'-dimethyle-2,2'-dipyridine) dichloro Osmium(II) (**4**)

Table 4.1: Elemental analysis data for compound cis-bis(5,5'-dimethyle-2,2'-dipyridine) dichloro Osmium(II) **(4)**

Compound 4	Calculated			Found		
$C_{24}H_{24}C_{l2}N_4Os(CH_2Cl_2)0.5$	C	H	N	C	H	N
	43.79	3.75	8.34	43.46	3.66	8.33

4.4 X-ray Crystallography

Crystals were grown in saturated solvent of dichloromethane through gas-phase diffusion method to give good crystals of compounds (**4**). Cell parameters and other collection data for compound (**4**) are illustrated in Table 4.2. and Selected Angles, and Distances in Table 4.3. The structure of compounds **(4)** can be seen in Figure 4.2 that confirms the cis-arrangement.

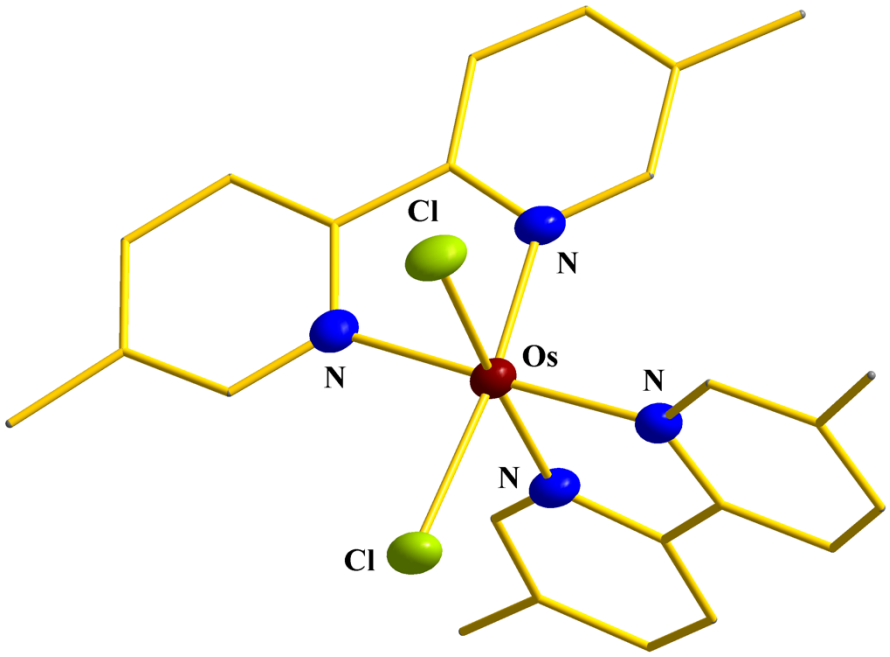

Figure 4.2: X-ray structure derived representation of cis-bis(5,5'-dimethyle-2,2'-dipyridine) dichloro Osmium(II) **(4).** Hydrogen atoms and thermal ellipsoids of the ligand carbon atoms are omitted for clarity.

Table 4.2: Crystal data and structure refinement for compounds (**4)**

Compound	**4**
Empirical formula	$C_{26}H_{28}C_{l6}N_4Os$
Formula weight (g/mol)	799.42
Temperature (K)	200
Wavelength (A)	0.71073 Å
Crystal System	Monoclinic
Space group	P 21/n
a (A)	16.108(4)
b (A)	10.7555(15)
c (A)	17.628(2)
α (deg)	90
β (deg)	93.47
γ (deg)	90
Volume Å^3	3048.4
Absorption coefficient (mm^{-1})	4.732 mm^{-1}
Absorption correction	
Final R indices[I$\geq 2\sigma$(I)]	R1= = 0.0341
	wR2= 0.0734

Table 4.3: Selected Angles, and Distances for (**4)**

Angle	Experimental Degrees (°)
N(12)#1-Os(1)-N(12)	94.22(18)
N(12)#1-Os(1)-N(1)#1	78.78(13)
N(12)-Os(1)-N(1)#1	98.03(13)
N(12)#1-Os(1)-N(1)	98.03(13)
N(12)-Os(1)-N(1)	78.78(13)
N(1)#1-Os(1)-N(1)	175.38(18)
N(12)-Os(1)-Cl(1)#1	88.81(10)
N(1)#1-Os(1)-Cl(1)#1	95.27(10)
N(1)-Os(1)-Cl(1)#1	88.04(9)

Bond	Experimental Distance Å
Os(1)-N(12)#1	2.023(3)
Os(1)-N(12)	2.023(3)
Os(1)-N(1)#1	2.050(3)
Os(1)-N(1)	2.050(3)
Os(1)-Cl(1)#1	2.4159(10)
Os(1)-Cl(1)	2.4159(10)
N(1)-C(2)	1.360(5)
N(1)-C(6)	1.364(5)
N(12)-C(11)	1.349(5)

Torsion	Experimental Degrees (°)
C(6)-N(1)-C(2)-C(3)	-1.4(6)
Os(1)-N(1)-C(2)-C(3)	176.1(3)
N(1)-C(2)-C(3)-C(4)	0.6(7)
N(1)-C(2)-C(3)-C(13)	179.5(4)
C(2)-C(3)-C(4)-C(5)	0.4(7)
C(13)-C(3)-C(4)-C(5)	-178.5(4)

4.5 UV-Visible Spectroscopy

A light-harvesting compound **(4)** cis-bis(5,5'-dimethyle-2,2'-dipyridine) dichloro osmium(II) can absorb the light which is in contrast with compound **(3)** $Mn(CO)_3LBr$. Compound **(4)** was completely dissolved in dichloromethane with 0.1 mM concentration. The spectra of compound **(4)** has shown two absorption bands refer to intra-ligand (IL) and metal to ligand-charge transfer (MLCT). The first band was observed in UV region

310 nm and the second band was at 560 nm which is higher than tris(bipyridine) ruthenium (II) that strongly absorbs at 452 nm corresponding to (MLCT) Figure 4.3).[2,6] (Also, around 820 nm, there is a small absorption peak refers to d-d transitions.

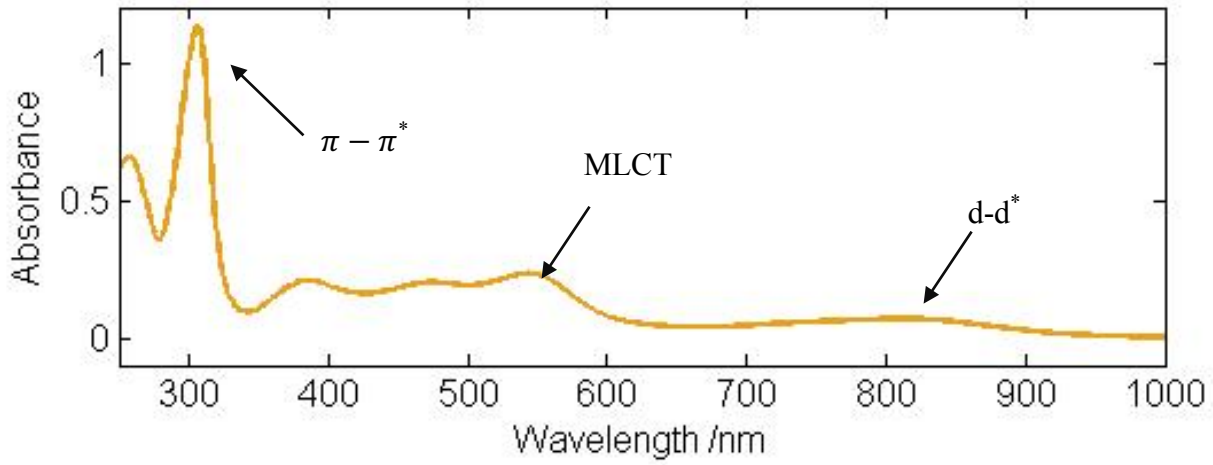

Figure 4.3: The UV-Vis spectrum of compound cis-bis(5,5'-dimethyle-2,2'-dipyridine) dichloro Osmium(II) (**4)**

4.6 Examining the ability of the complex (3) for the photocatalytic reduction of CO_2

In the investigation of the ability of compound (**3)** to perform photocatalytic reduction of CO_2, two light-harvesting compounds were examined, the cis-bis(5,5'-dimethyle-2,2'-dipyridine)dichloro osmium(II) (**4)** and tris(bipyridine) ruthenium(II) chloride. The conditions examined for this reaction were a mixture of dimethylformamide (DMF) and triehanolamine (TEOA) 4:1 and 0.1 mM of the catalyst. These are the

classical “Strasbourg Conditions” employed for Re bpy complexes. The reaction mixture was sealed and the atmosphere was exchanged with CO_2. A mercury lamp (500 watts) was used as source of the light.

Under these conditions, the reaction mixture was irradiated for 24 hours with the Hg lamp. Unfortunately, GC analysis did not show any signal peak for CO or other products. Similarly, using the Ru(II) compound as a photosensitizer also did not show any CO product. Furthermore, changing the reaction conditions by using acetonitrile as the reaction solvent or by changing the reducing agents to either ascorbic acid or 1-benzyl-1,4-dihydronicotinamide (BNAH) did not produce any gas phase products. It is possible that these reactions did not produce gas phase reduction products. Potential alternative reduction products are species that could remain in solution.

4.7 Conclusion

This chapter has established that simple functionalization of 4,5-diazafluoren-9-one by a direct reaction with NH_2R can be carried out and that such species can be incorporated into the coordination sphere of Mn(I) complexes by the synthesis of compound (**3).** These results suggest that additional modification of the diazafluorenone ligand to incorporate extended π systems of a photosensitizer should be possible.

The concept of adding a photosensitizer to this new Mn complex in order to prepare a system for CO_2 photoreduction was explored. In addition to investigating the more common ruthenium (II) photosensitizer a new Os(II) photosensitizer was synthesized and fully characterized. The preliminary photophysical characterization suggested that this species has higher absorbance of visible light compared to Ru(II). Unfortunately, under

the conditions investigated, neither of these photosensitizer/Mn complex systems was capable of photoreduction of CO_2. However, due the lack of time, I would have tried to functionalize the ketone site to get different modified ligands as 9,9-di-(4-ethoxyphenyl)-9-H-4,5-diazafluorene) or similar and using different metal instead of manganese. Moreover, the supramolecular complexes have shown an increase in the efficiency and the selectivity of CO_2 reduction (see the Introduction), but synthesizing this type of complexes would take a lot of time and it is not easy to attach the photosensitizer unit to the catalyst through a bridge ligand. This step could be in the future planes.

Experimental Section

All reactions were carried out in a glovebox under a nitrogen atmosphere. Solvents were dried by passage through a column of activated alumina using an apparatus purchased from Anhydrous Engineering. $Mn(CO)_5Br$ and ammonium hexachloroosmate (IV) and were purchased from Aldrich and used as received. Deuterated dichloromethane was dried using activated molecular sieves. NMR spectra were run on Bruker Avance 400MHz spectrometers with CD_2Cl_2 as solvent and internal standard. Infrared spectra were collected using an Agilent Technologies Cary FT-IR spectrome-Experimental Procedures using a diamond ATR attachment. UV-Vis spectra were collected using a Agilent Technologies Cary 5000 UV-Vis spectrometer.

Compound 2

(91.09 mg, 0.5 mmol) of 4,5-Diazafluorene-9-one was dissolved in (50 ml) of methanol. 4-aminoazobenzen (98.5 mg, 0.5 mmol) was added to the solution and p-toulenesulfonic acid. The Dean-Stark apparatus was used in the reaction to remove the

excess water from the mixture. The reaction mixture was heated to reflux under nitrogen for 72 hours. A bright-orange solid was removed by suction filtration and washed with hexane. The mixture was dried through rotary evaporation under a reduced pressure. Total yield (140 mg, 66%).

^{1}H NMR (CD_2Cl_2, 400 MHz) δ 8.7(dd, J= 5, 1.6, 2H), 7.98 (dd, J= 7.6, 1.6, 2H), 7.82 (d, J = 7.8, 2H), 7.7 (d, J = 9, 2H), 7.48 (m, 2H), 7.41 (m, 1H), 7.35 (d, J = 7, 2H), 6,75 (d, J = 8.7, 2H). Also, compound (**2)** was confirmed by using mass spectral analysis (electron-ionization) to give 23 ^{12}C, 15 ^{1}H, 5 ^{14}N and 0 ^{16}O.

- **Compound (3)**

In a glovebox**, (**0.541 g, 0.75 mmol) of compound (**2)** was dissolved in (50 ml) of dry heptane. $Mn(CO)_5Br$ (0.206 g, 0.75 mmol) was added to the solution. The mixture was stirred with a magnetic stir bar until the solution. The flask was sealed with a stopper and removed from the glove box. The reaction mixture was heated to reflux under nitrogen for 48 hours. A bright-orange solid was removed by suction filtration and washed with hexane then dissolved dichloromethane. The mixture was dried through rotary evaporation under a reduced pressure. Total yield 85%.^{1}H NMR (CD_2Cl_2, 400 MHz) δ 8.83 (dd, J= 5.6, 1.2, 2H), 8.20 (dd, J=7.6, 1.2, 2H), 7.99(d, 8.4, 2H), 7.78 (d, J=8.2, 1H), 7.66(dd, J=7.4, 2, 2H), 7.52 (m, 2H), 7.32(d, J= 8.7, 2H), 6.76(d, J=8.6, 2H).

- **Compound (4)**

219 mg of ammonium hexachloroosmate(IV) was dissolved in dry ethylene glycol (50 ml) with 185 mg of 5,5'-dimethyl-2.2'dipyridyl and then heated at reflux for 6 hours under an atmosphere of N_2. 30 ml of a saturated aqueous sodium dithionite was added after the mixture was cooled to reduce Os(III) to Os(II). The dark precipitate was washed with water and ether to give a 70% yield of cis-bis(5,5'-dimethyle-2,2'-dipyridine) dichloro Osmium(II).

References

1. Li, X.; Zhang, D.; Li, W.; Chu, B.; Han, L.; Li, T.; Su, Z.; Zhu, J.; Wu, S.; Chen, Y.; Lei, P.; Hu, Z.; Zhang, Z. *Synth. Meta.* **2009**, *159*, 1340–1344.
2. Tamaki, Y.; Koike, K.; Morimoto, T.; Yamazaki, Y.; Ishitani, O. *Inorg. Chem.* **2013**, *52* (20), 11902–11909.
3. 4-AMINOAZOBENZENE(60-09-3)^{1}HNMR http://www.chemicalbook.com/spectrumen_60-09-3_1hnmr.htm (accessed 2015).
4. Kanumfre, F.; Lima, E. M. D.; Scheidt, G.; Carneiro, P. I. B.; Rosso, N. D. *J. Braz. Chem. Soc.* **2010**, *21* (5), 800–805.
5. Endicott, J. F.; Schlegel, H.; Uddin, M.; Seniveratne, D. S. *Coord. Chem. Rev*. **2002**, *229* (1-2), 95–106.
6. Kalyanasundaram, K. *Coord. Chem. Rev.* **1982**, *46*, 159–244.
7. Juris, A.; Balzani, V.; Barigelletti, F.; Campagna, S.; Belser, P.; Zelewsky, A. V. *Coord. Chem. Rev.***1988**, *84*, 85–277.
8. Meyer, T. J. *Pure. App. Chem.* **1986**, *58*, 9.

9. Kober, E. M.; Caspar, J. V.; Sullivan, B. P.; Meyer, T. J. *Inorg. Chem.* **1988**, *27*, 4587–4598.

10. Buckingham, D. A,; Dwyer, F. P.; Goodwin, H. A,; Sargeson, A. M . *Aust. J. Chem*. **1964**, *17,* 325.

Conclusion

The first goal of the thesis was successfully achieved through synthesizing new elusive pincer geometry of rhenium(I) by using an unconventional reaction that required high temperature. I was also able to fully characterize both the bidentate and tridentate bis(imino)pyridine complexes and exam the ability of these complexes as homogenous catalysts for photo/ electrocatalytic reduction of CO_2. Under the so-called "Strasburg conditions" the tridentate complexes failed to convert CO_2 to CO.

Given these negative results, the direction of the thesis changed to an investigation of α-diimine ligands due to the similarity in the structure 2,2′-bipyridine) (bipy) and 4,5- diazafluorene-9-one. The presence of a ketone function in the diazafluorenone ligand provided a site for potential introduction of photoactive species and the preparation of a supramolecular species with photosensitizer linked to the catalysts site. Before decorating the ligand, the priority was to first examine the ability of the diazafluorenone ligand with Re(I) and Mn(I) for photo/ electrocatalytic reduction of CO2 under different conditions. These complexes have shown the ability to reduce CO_2 to CO as have been described in chapter 3. Lastly, I explored means of covalent linkage of a photosensitizer to the diazafluorenone complexes. This was first examined by attaching the ligand to 4-aminoazobenzene and later reacting with $Mn(CO)_5Br$. The ability of an Os(II) complex as a photosensitizer was also tested and showed higher absorbance for the light than tris(bipyridine)ruthenium(II) chloride but under "Strasbourg Condition" with the modified Mn(I) complex, did not reduce CO_2 to CO.